

Effect of Processing Conditions on Properties of Fly ash-Epoxy Composite

Ashutosh Pattanaik



**Department of Metallurgical & Materials Engineering
National Institute of Technology, Rourkela**

Effect of Processing Conditions on Properties of Fly Ash-Epoxy Composite

*Dissertation submitted to the
National Institute of Technology Rourkela
In partial fulfilment of the requirements
Of the degree of*

*Doctor of Philosophy
In
Metallurgical & Materials Engineering*

*By
Ashutosh Pattanaik
(Roll Number-512MM1004)
Under the Supervision of
Prof. Subash Chandra Mishra*



Jan, 2017

Department of Metallurgical & Materials Engineering
National Institute of Technology Rourkela



Department of Metallurgical & Materials Engineering
National Institute of Technology Rourkela

Jan 18, 2017

Certificate of Examination

Roll Number: 512MM1004

Name: Ashutosh Pattanaik

Title of Dissertation: Effect of Processing Conditions on Properties of Fly ash-Epoxy Composite

We the below signed, after checking the dissertation mentioned above and the official record books of the student, hereby state our approval of the dissertation submitted in partial fulfillment of the requirements of the degree of Doctor of Philosophy in Metallurgical & Materials Engineering at National Institute of Technology Rourkela. We are satisfied with the volume, quality, correctness and originality of the work.

Prof. Subash Chandra Mishra
Supervisor

Prof. Suhrit Mula
External Examiner

Prof. Sudipta Sen
Member (DSC)

Prof. Jopesh Bera
Member (DSC)

Prof. Abanti Sahoo
Member (DSC)

Prof. Mithilesh Kumar
Chairman (DSC)

Prof. Smarajit Sarkar
HOD, MM



Department of Metallurgical & Materials Engineering
National Institute of Technology Rourkela

Dr Subash Chandra Mishra
Professor

Jan 18, 2017

Supervisor's Certificate

This is to certify that, the work presented in this dissertation entitled “ **Effect of Processing Conditions on Properties of Fly ash-Epoxy Composite**” by “**Ashutosh Pattanaik**”, Roll Number **512mm1004**, is a record of original research carried out by him under my supervision and guidance in partial fulfillment of the requirements of the degree of ***Doctor of Philosophy in Metallurgical & Materials Engineering***. Neither this dissertation nor any part of it has been submitted to any institute or university in India or abroad for the award of any degree or diploma.

Subash Chandra Mishra
Professor

DEDICATED TO

MY

“MOTHER”

Ashutosh Pattanaik

Declaration of Originality

I, *Ashutosh Pattanaik*, Roll Number *512MM1004* hereby declare that this dissertation entitled "*Effect of Processing Conditions on Properties of Fly ash-Epoxy Composite*" represents my original work carried out as a doctoral student of NIT Rourkela and, to the best of my knowledge, it contains no material previously published or written by another person, nor any material presented for the award of any other degree or diploma of NIT Rourkela or any other institution. Any contribution made to this research by others, with whom I have worked at NIT Rourkela or elsewhere, is explicitly acknowledged in the dissertation. Works of other authors cited in this dissertation have been duly acknowledged under the section "Bibliography". I have also submitted my original research records to the scrutiny committee for evaluation of my dissertation.

I am fully aware that in case of any non-compliance detected in future, the Senate of NIT Rourkela may withdraw the degree awarded to me on the basis of the present dissertation.

Jan 18, 2017

NIT, Rourkela

Ashutosh Pattanaik

Acknowledgement

The journey of reaching any milestone is never easy without a determined ambition, sincere dedication and a perfect person who can torch your path of ignorance. I am obliged to Prof. Subash Chandra Mishra for being an embodiment of the constant source of inspiration and knowledge. Under his guidance, I have learnt the art of doing research and the true value of life.

I am thankful to my previous director Prof. Sunil Kumar Sarangi, for his motivational speeches during his tenure. Also, I am conveying my gratitude to our Director Prof. Animesh Biswas as an embodiment of knowledge. At the same time, I am thankful to Prof. Mithilesh Kumar, Prof Sudipta Sen, Prof. Japesh Bera and Prof. Abanti Sahoo whose valuable suggestions at the right time helped me reach the goal. At the same time, I am grateful to Prof S Sarkar (HOD, MM) for his kind support and advice.

I sincerely acknowledge the helping hand of Mr Rajesh Ku. Pattanaik, Mr.Uday Kumar Sahu and Mr Subrat Pradhan for their timely help and support. My friends, whose consolation during the bad days and encouraging words, helped me maintain the equilibrium while fulfilling my ambition.

After all, the love of family and relatives whose blessings are like the rays of sunshine help me seeing my inner strength and step towards the goal.

Lastly, I must thank the invisible force which we define as the almighty God for giving me patience and driving me towards a never ending process of learning.

Jan 18, 2017
NIT, Rourkela

Ashutosh Pattanaik
512MM1004

CONTENTS

| | |
|---|-----|
| Supervisor's Certificate | iv |
| Dedication | v |
| Declaration of Originality | vi |
| Acknowledgement | vii |
| List of Figures | xi |
| List of Tables | xiv |
| Abstract | xv |
| | |
| Chapter 1 | 1 |
| Introduction..... | 1 |
| 1.1. Background and Motivation | 1 |
| 1.2. Thesis Outline | 4 |
| Chapter 2..... | 6 |
| Literature Survey | 6 |
| 2.1. Particulate Filled Polymer Composite | 6 |
| 2.2. Mechanical Properties of Polymer Composites | 7 |
| 2.3. Dielectric Characteristics of Composites..... | 10 |
| 2.4. Thermal Characteristics of Polymer Composite | 12 |
| 2.5. Wear Behaviour of Composite..... | 14 |
| 2.6. Durability of Polymer Composite | 21 |
| 2.7. Knowledge Gap | 25 |
| 2.8. Objective and Work Plan | 26 |
| Chapter 3 | 27 |
| Materials and Methods..... | 27 |
| 3.1 Composite Materials | 27 |
| 3.1.1 Matrix material | 27 |
| 3.1.2 Reinforcement | 29 |
| 3.2 Composite Fabrication | 31 |
| 3.2.1 For tensile/flexural/impact testing..... | 31 |

| | | |
|------------------------------|--|----|
| 3.2.2 | For wear test | 32 |
| 3.2.3 | For dielectric study | 33 |
| 3.3 | Post-Treatment of Composite | 34 |
| 3.3.1 | Conventional oven..... | 34 |
| 3.3.2 | Microwave oven..... | 34 |
| 3.4 | TOPSIS method | 35 |
| 3.5 | TAGUCHI Method | 36 |
| Chapter 4..... | | 38 |
| Results and Discussion | | 38 |
| 4.1 | Physicomechanical Properties | 38 |
| 4.1.1 | Density Measurement..... | 38 |
| 4.1.2 | Tensile properties | 39 |
| 4.1.3 | Flexural properties..... | 42 |
| 4.1.4 | Impact properties..... | 46 |
| 4.1.5 | Microstructural aspect | 48 |
| 4.1.6 | Differential scanning calorimetry..... | 51 |
| 4.1.7 | Spectroscopic analysis..... | 52 |
| 4.2 | Electrical Properties | 56 |
| 4.2.1 | Dielectric constant..... | 56 |
| 4.2.2 | Effect of frequency on impedance | 59 |
| 4.2.3 | Effect of frequency on loss factor | 60 |
| 4.2.4 | Effect of frequency on resistance | 62 |
| 4.2.5 | Effect of frequency on capacitance | 64 |
| 4.3 | Corrosion Behaviour | 67 |
| 4.3.1 | Variation of weight..... | 68 |
| 4.3.2 | Change in surface morphology | 69 |

| | | |
|-------------------------------|--|-----|
| 4.3.3 | Tensile properties of different environmentally treated samples | 71 |
| 4.3.4 | Flexural properties of different environmentally treated samples | 74 |
| 4.3.5 | Impact properties of different environmentally treated samples..... | 77 |
| 4.3.6 | Microstructural analysis | 78 |
| 4.3.7 | Thermal analysis | 80 |
| 4.3.8 | Spectroscopic analysis..... | 82 |
| 4.3.9 | XRD analysis..... | 84 |
| 4.4 | Wear Behaviour | 86 |
| 4.4.1 | Statistical Analysis | 86 |
| 4.4.2 | Morphology of worn surfaces: | 95 |
| Chapter 5 | | 98 |
| Discussion | | 98 |
| 5.1 | Effect of ultrasonic mixing | 98 |
| 5.2 | Effect of post curing treatment | 98 |
| 5.3 | Effect of viscosity on composite fabrication | 99 |
| 5.4 | Effect of Tg on mechanical properties..... | 100 |
| 5.5 | Overview..... | 101 |
| Chapter 6..... | | 103 |
| Summary and Conclusions | | 103 |
| 6.1 | Summary | 103 |
| 6.2 | Conclusions..... | 104 |
| 6.3 | Scope of future work..... | 104 |
| References..... | | 106 |
| Annexure-I | | i |
| Annexure-II..... | | iii |
| Dissemination | | vii |

LIST OF FIGURES

| | |
|--|----|
| Figure 2.1: Schematic diagram of adhesive wear. | 14 |
| Figure 2.2: Schematic diagram of abrasive wear. | 15 |
| Figure 2.3: Schematic diagram of erosion wear. | 16 |
| Figure 2.4: Schematic diagram of fatigue wear. | 16 |
| Figure 2.5: Schematic diagram of corrosion wear. | 17 |
| Figure 3.1: Structure of epoxy resin & hardener. | 28 |
| Figure 3.2: SEM micrographs of fly ash. | 30 |
| Figure 3.3: Particle size analysis of fly ash. | 31 |
| Figure 3.4: Patterns ready for sample preparation. | 32 |
| Figure 3.5: Samples after solidification. | 32 |
| Figure 4.1: Variation of (a) density and (b) void fraction of the composites. | 38 |
| Figure 4.2: Variation of tensile strength with mixing time for different percentage of fly ash reinforcement. | 39 |
| Figure 4.3: Variation of tensile strength with percentage of fly ash reinforcement at different curing conditions and mixing times. | 40 |
| Figure 4.4: Variation of percentage elongation with different fly ash percentage at different mixing times. | 41 |
| Figure 4.5: Variation of flexural strength with mixing time for different fly ash percentage. | 42 |
| Figure 4.6: Variation of flexural strength with percentage fly ash addition at different curing condition and mixing time. | 43 |
| Figure 4.7: Variation of strain with different percentage of fly ash at different curing conditions and mixing time. | 44 |
| Figure 4.8: Variation of maximum deflection with different fly ash reinforcement for different mixing time and curing conditions. | 45 |
| Figure 4.9: Variation of impact strength with mixing time at different curing conditions and percentage reinforcement of fly ash. | 46 |
| Figure 4.10: Variation of impact energy with percentage of fly ash for different curing conditions and mixing time. | 47 |
| Figure 4.11: Micrographs are showing proper mixing of fly ash and epoxy resin (10%FA+90%EP). | 48 |

| | |
|--|----|
| Figure 4.12: SEM micrograph showing initiation and propagation of crack at the breaking point (10%FA+90%EP in microwave curing condition)..... | 48 |
| Figure 4.13: SEM micrograph showing protruded a portion of the tensile test specimen (10%FA+90%EP in microwave curing condition). | 49 |
| Figure 4.14: SEM micrographs of flexural test samples (10%FA+90%EP in microwave curing condition). | 50 |
| Figure 4.15: SEM micrograph of impact test sample showing the direction of energy flow (20%FA+80%EP in microwave curing condition). | 50 |
| Figure 4.16: SEM micrograph of impact test specimen showing crater (20%FA+80%EP in microwave curing condition). | 51 |
| Figure 4.17: Variation of the amount of heat absorbed with temperature for different curing conditions. | 52 |
| Figure 4.18: FTIR plot between wave number and percentage transmittance for atmospherically cured samples. | 53 |
| Figure 4.19: FTIR plot between wave number and percentage transmittance for the oven and micro oven cured samples. | 54 |
| Figure 4.20: Variation of dielectric constant with frequency for different percentage of fly ash reinforcement. | 56 |
| Figure 4.21: Variation of dielectric constant with percentage of fly ash for different curing conditions. | 58 |
| Figure 4.22: Variation of impedance with frequency at different percentage of fly ash reinforcement. | 59 |
| Figure 4.23: Variation of impedance with frequency at different curing conditions. | 60 |
| Figure 4.24: Variation of loss factor with frequency for various percentage reinforcement of fly ash. | 61 |
| Figure 4.25: Variation of loss factor with frequency at different curing conditions. | 62 |
| Figure 4.26: Variation of resistance with frequency for different fly ash percentage. | 63 |
| Figure 4.27: Variation of resistance with frequency at different curing conditions. | 64 |
| Figure 4.28: Variation of capacitance with frequency for different percentage reinforcement of fly ash. | 65 |
| Figure 4.29: Variation of capacitance with frequency at various curing conditions. | 66 |
| Figure 4.30: Variation of weight with different fly ash percentage, treated in different environmental condition. | 68 |

| | |
|---|----|
| Figure 4.31: SEM micrographs showing deposition of materials in sea water (40%FA+60%EP). | 69 |
| Figure 4.32: SEM micrographs showing crater and etching of surface in the acid solution treated specimen (40%FA+60%EP). | 70 |
| Figure 4.33: SEM micrographs showing swelling of the sample in sea water (40%FA+60%EP). | 70 |
| Figure 4.34: Variation of tensile strength with duration time (A) for 10% fly ash (B) for 20% fly ash (C) for 30% fly ash (D) for 40% fly ash reinforcement. | 72 |
| Figure 4.35: Variation of the percentage elongation with different amount of fly ash reinforcement for different durations. | 73 |
| Figure 4.36: Variation of flexural strength with treatment duration periods(A)for 10% fly ash (B) for 20% fly ash (C) for 30% fly ash (D) for 40% fly ash reinforcement. | 74 |
| Figure 4.37: Variation of strain with different percentage of fly ash reinforcement for different duration of immersion. | 75 |
| Figure 4.38: Variation of maximum deflection with different percentage of fly ash reinforcement for different duration of immersion. | 77 |
| Figure 4.39: Variation of impact strength with duration time (A) for 10% fly ash (B) for 20% fly ash (C) for 30% fly ash (D) for 40% fly ash reinforcement. | 78 |
| Figure 4.40: SEM micrograph of the fractured surface of tensile test specimen (for 10% fly ash treated in basic solution after 28 days). | 79 |
| Figure 4.41: SEM micrograph of the fractured surface in flexural test specimen (for 10% fly ash treated in basic solution after 28 days). | 79 |
| Figure 4.42: SEM micrograph of the fractured surface in impact test specimen (for 10% fly ash treated in basic solution after 28 days). | 80 |
| Figure 4.43: Variation of the amount of heat absorbed with temperature treated in different ways (10%FA after 28 days & 40%FA after 28 days). | 81 |
| Figure 4.44: Variation of glass transition temperature with different treatment conditions (10% fly ash after 28days). | 81 |
| Figure 4.45: IR spectra of 10% fly ash reinforced specimens after 28 days of treatment. | 82 |
| Figure 4.46: IR spectra of 40% fly ash reinforced specimens after 28 days immersion. | 83 |
| Figure 4.47: XRD analysis of various samples treated in different environmental conditions (after 28 days). | 84 |
| Figure 4.48: S/N ratio plot (atmospheric condition). | 91 |
| Figure 4.49: S/N ratio plot (oven treated the condition). | 91 |

| | |
|---|----|
| Figure 4.50: S/N ratio plot (micro oven treated the condition)..... | 92 |
| Figure 4.51: SEM micrographs of worn surfaces (for 10% fly ash reinforced, microwave cured specimen). | 96 |

LIST OF TABLES

| | |
|--|----|
| Table 3.1: Properties of neat epoxy resin..... | 29 |
| Table 3.2: Properties of fly ash. | 30 |
| Table 4.1: Wave numbers showing possible bonding in atmospheric curing samples..... | 53 |
| Table 4.2: Wave numbers showing possible bonding in oven & micro oven curing samples..... | 55 |
| Table 4.3: Wave numbers are showing possible bonding in oven & microwave curing samples..... | 83 |
| Table 4.4: % Crystallinity of fly ash reinforced composite | 85 |
| Table 4.5: L32 Orthogonal array with results for atmospheric curing condition | 86 |
| Table 4.6: L32 Orthogonal array with results for oven curing condition | 87 |
| Table 4.7: L32 Orthogonal array with results for micro oven curing condition..... | 88 |
| Table 4.8: Mean response table for relative closeness coefficient for atmospheric curing condition | 89 |
| Table 4.9: Mean response table for relative closeness coefficient for oven curing condition..... | 89 |
| Table 4.10: Mean response table for relative closeness coefficient for micro oven curing condition | 90 |
| Table 4.11: ANOVA table with adjusted sum of square for tests (atmospheric treatment) | 92 |
| Table 4.12: ANOVA table with adjusted sum of square for tests (oven treatment)..... | 93 |
| Table 4.13: ANOVA table with adjusted sum of square for tests (micro oven treatment)..... | 93 |
| Table 4.14: Confirmatory test results (atmospheric condition) | 94 |
| Table 4.15: Confirmatory test results (oven treatment condition)..... | 94 |
| Table 4.16: Confirmatory test results (micro oven condition)..... | 95 |

Abstract

Fly ash being generated in massive scale has minimum utilisation as compared to its rate of production. It is the waste generated from thermal power plants, which find its primary usage in road embankment, cement making, making of fly ash bricks, etc. This current research focuses on finding out the ways of utilising fly ash as reinforcement to fabricate polymer composite. Fly ash comprises of oxides of silicon, aluminum, iron and titanium along with some other minor constituents. Here investigation has been done for processing and characterization of fly ash reinforced epoxy composites. Fly ash being immiscible is mixed with the epoxy using an ultrasonic sonicator for varied time periods. Various mechanical tests viz. tensile, flexural, impact, dielectric properties and tribological analysis are carried out to find out its proper application according to its suitability. The composite is treated in different environments viz. acid, base, fuel and sea water to find its proper environmental/chemical degradation/stability.

The percentage of fly ash reinforcement is varied from 10 to 40%. For composite fabrication different mixing time i.e. 10, 20 and 30 minutes are chosen to check the effect of mixing time on the mechanical behaviour of the material. The prepared samples are cured at three different conditions i.e. standard atmosphere at room temperature, inside the oven and in the micro oven. Combinations of all these variables have been taken into consideration to analyse the effect on the mechanical properties of the material. The dielectric properties of the composites are evaluated. The sliding wear behaviour of the samples was studied with a pin on disc type sliding wear testing machine of DUCOM make; by varying the parameters, viz., time, RPM and applied load, etc. Optimisation techniques have been implemented to reduce the number of experiments and to find out the percentage contribution of each parameter. Simultaneously, a suitable combination of parameters has been given and the confirmatory test has been done to determine the percentage of error in the experiments. Finally, the samples are treated with an acid solution, basic solution, fuel (Petrol), sea water and acetone for 28 days; and change in mechanical properties has been recorded periodically.

From the above-detailed examinations, these fly ash reinforced epoxy composites found to be moderately suitable for the automobile industry, to be used as the dashboard, brake pads, seat assembly plates, bumpers and in the interior portion of aircraft, etc. due to its mechanical properties. Most suited for construction industry for making of floor and wall tiles partition wall etc. Out of the treatment conditions, these composites are found to be most

suitable for use in the petroleum industry for fuel carrying tanks and containers. Finally, it can also be used for making of beautiful decorative articles and household appliances.

Chapter 1

Introduction

1.1. Background and Motivation

Overgrowth of the population in the modern era demand more material for its day to day life. It consumes the natural resources and generates a significant amount of hazardous waste. With the use of these natural resources, we are putting a severe impact on the environment. We all know that there is no alternative to the natural resources, still trying to adjust and replace some newly developed material in that place. From the last one decade, all countries simultaneously adopted one single anthem i.e. “Recycle, Reuse & Remanufacture” which will reduce the impact on the environment and value addition to the wastes.

In the modern world, sufficient electrical energy is required out of which a major contribution from the thermal power plants. Thermal power plants depend on the use of coal as the raw material. Simultaneously, it is producing a hazardous waste named fly ash, which is a burden on the environment. This research work is only a step towards reuse of the waste material by using it as a reinforcement to fabricate polymer composite. Work is in progress for making low-cost composites with the aim of producing a suitable alternative at a reduced cost for various applications. The easy manufacturing process, low cost and high strength lead the composite materials to a higher dimension for users.

From the name itself, a composite is defined as the mixture of two or more distinct material/phases. One of which is continuous and the other is dispersed in it with their distinct identities [1]. The continuous phase is called matrix and the discontinuous phase is called reinforcement. The reinforcement material is harder and stronger than the matrix material. Nomenclature of the composite materials depends on the nature of the matrix material. In broad ways, there are three different types of matrix materials, i.e. metal, ceramic and polymer. When the matrix material is a polymer, it is called a Polymer Matrix Composite. The use of composite material started long back from the human civilisation for making of houses by using mud and bamboo. Composites differ from the alloy regarding its performance and strength and other properties. In alloys, the two constituents mix chemically to give an entirely structure/phases, etc. whereas, in the case of composite material, the two phases remains distinctly identifiable and independent in their nature.

Polymers and their composites are replacing many conventional materials like steel, aluminium etc. due to its low cost, high strength, low weight and durability. It is mainly because of its low cost and high production rate. Properties of polymers are usually modified by these reinforced materials and their influence impact heavily on the final properties. Fibres are reinforced in the polymer matrix where high tensile strength is required, but it is expensive and ease production is low. So, sometimes ceramic and metallic particles are reinforced in the polymer matrix to enhance the different property. Although the particles are reinforced in the matrix and retain their identity but help in providing a combined effect other than their properties. As the matrix is continuous, it helps in carrying and transferring the load to the reinforcing phase constituent [1]. Although the particle reinforcement doesn't contribute to its load transfer, it helps in decreasing the strain energy developed in the material. Polymers are of three types, thermosetting, thermoplastic and elastomers. All three types of polymers can be used as polymer matrix composite. As far as the reinforcement is concerned, fillers like aluminium, starch, silica are costlier. So in our investigation, to minimise the cost, industrial waste viz. fly ash is chosen as the reinforcement material. It is well known from the composition of fly ash that it is a ceramic (filler) which can help in increasing strength of the material.

Fly ash find its maximum utilisation in road embankment, making of Portland cement, making of fly ash bricks and other low scale applications like agriculture. All these consume only one-third of its production which leads to accumulation of that hazardous waste. So, many researchers have thought of using fly ash from a different angle. They have added fly ash as a filler material while making fibre composites. Typically hard ceramic particles, when combined with fibres, increase the strength and wear properties of the material. But to reduce the cost of the component, only fly ash has been chosen for making of polymer composite and verifying its potentiality is a major challenge. If only filler material can give the near equal result as compared to fibre with particle reinforced composite, there is no justification for using bio fibres and other low-grade fibres [2]. Natural and artificial fibres along with fly ash have been used earlier and good results have been obtained. But no work has been done taking the fly ash as the single filler material and as the only reinforcing material so far. This work is an effort of using fly ash as the single constituent and uses it in large scale efficiently. As matrix and reinforcement are the main components of the material, properties of reinforcement play a vital role in shaping the characteristics of the composite material.

In another aspect, the only use of particulate filler will increase the crystallinity and homogeneity of the material. As the polymer consists of crystalline and amorphous

simultaneously, its properties depend mainly on the crystalline part of the material. Crystalline relates to its glass transition temperature, mechanical strengths and wear characteristic of the material [3, 4]. The samples are prepared by changing the mixing time and curing condition so as to alter and increase its properties. Post curing in the oven and the micro oven has been done to modify its surface and internal properties. It has been discussed that oven curing helps in surface modification whereas micro oven curing helps in the bulk modification of the sample.

Wear is one of the major characteristic properties of any material as it is concerned with the loss of material. Wear is defined as the loss of material due to the continuous relative motion of two mating parts [5]. As it is a continuous loss of material, it is directly related to the cost of the component. So, before using any product in massive scale, its wear characteristics must be studied. Wear is also related to loss of energy. A lot of work is done externally to maintain the continuous flow of energy on a worn out surface. The complexity of wear phenomenon is visible in industries. So, extensive and scientific study has been carried out long before [6]. There are different types of wear like adhesive wear, abrasive wear; adhesion wear and fatigue wear [7]. Dry sliding wear is one type of abrasive wear which is mainly due to rubbing action of one material over the other [8]. The friction generated at the interface results in loss of material as well as the generation of heat. This test is usually carried out where there is the possibility of rubbing action at the time of operation. Various parameters like duration of operation, speed, loading condition and percentage of reinforcement of filler material affect the wear. Usually, composites are used in non-lubricated and high-temperature tribo-engineering purposes. So a detailed study is required for the practical implication of the material in the field of wear [9]. As there are lots of parametric conditions influencing the wear, frictional force and coefficient of friction, so it is quite difficult to find wear in all the combination of parameters. Statistical analysis plays a major role in reducing the number of experiments and getting the suitable combination of parameters where all the desired outputs will be minimum. It also gives the ranking of parameters in which they affect the output. Moving one step further, it also gives the percentage contribution of each parameter and the amount of error involved in the experiment. In short, a statistical analysis gives a systematic way of finding the influence of parameters.

Finally, to get the practical implication of material in different mediums, the developed polymer composite is treated in various mediums like an acid solution, basic solution, sea water and fuel for a long period. The samples were taken out periodically and its

mechanical properties, thermal properties as well as the change in weight are measured to find out the field of environment for application of the material. After one month of treatment, the samples inside acetone degrades completely and samples inside fuel (petrol) show the highest resistance to the environmental condition.

The present research work thus characterises the fly ash epoxy composite with the aim of finding suitable application in industry. It shows the mechanical properties at different curing conditions, different mixing time and different treatment conditions. Dielectric properties and corrosion behaviour of the composites are also evaluated. Tribological behaviour has been studied and the best suitable combination is found out for minimum wear.

1.2. Thesis Outline

The remaining portion of the thesis is outlined as follows-

Chapter 2: This describes the literature survey in the area of polymer composite and finds out the areas where one can proceed further. This chapter helps in determining the knowledge gap in which a particular research can be carried out and gives an idea of a specific field of research.

Chapter 3: This describes the selection and collection of raw materials. It also includes fabrication of composites according to ASTM standards, different testing methodologies and procedures to evaluate and improve the mechanical as well as other properties. It also includes the application of statistical analysis.

Chapter 4:

Part: I

It presents the mechanical, thermal and microstructural analysis results. Mechanical properties include measurement of density, void fraction, tensile strength, flexural strength and impact strength of the material. Glass transition temperature and chemical bonding has been determined using DSC and FTIR respectively.

Part: II

This section describes the electrical behaviour of the developed composite. Variation of dielectric strength, loss factor, impedance, capacitance and resistance has been evaluated at different frequency ranges. Effect of different curing conditions has also been mentioned in this section.

Part: III

This part describes the change in mechanical properties and other analysis of the composite after treated with the different chemical environment.

Part: IV

This chapter describes the study and evaluation of wear properties. Using the statistical approach (i.e. Taguchi method, to minimise the number of experiments), the analytical results obtained conducting sliding wear test. It helps in finding out the contribution of parameters, a ranking of parameters and influence of parameters on the output result.

Chapter 5: This chapter discusses the results obtained in the present piece of research work.

Chapter 6: It summarises the present research findings and conclusions of the work. It also suggests the future scope for improvement in this field.

Chapter 2

Literature Survey

This chapter includes various findings of earlier researchers in the related field of work. Literature survey helps in determining the knowledge gap between the previous works and the present status of that area of research. It also gives us a vast knowledge which will enable to choose a particular area of research. This chapter includes the literature survey on the following topics-

1. Particulate-filled polymer composite
2. Mechanical characteristics of polymer composite
3. Dielectric characteristics of polymer composite
4. Thermal characteristics of polymer composites
5. Wear behaviour of polymer composites
6. Durability of composites

2.1. Particulate Filled Polymer Composite

It is thought that addition of filler materials decrease the cost of the component. At the time of achieving lower cost, it simultaneously changes all the characteristics of the polymer. It is, therefore, the term functional filler is used for any filler addition to the material resulting some advantages and disadvantages to the properties. Besides that, particulate filled composite gives the flexibility of giving any complicated shape to the material.

Researchers have described that the importance of taking volume percentage as the proportion of making the composite. They have explained that properties of the polymer composite depend on the volume percentage of filler material. It is always difficult to take weight percentage into consideration as it is related to the density of the material.

Fillers in polymer composites helps in increasing density, improving processability, mechanical strength, thermal strength, electrical properties and other properties. Polymer composites behave isotopically as the filler and the reinforcement is differently sensitive to the same condition [10, 11].

Metal particle reinforced polymer composites are used as heaters and electrodes in industries. Ceramic and metallic fillers are usually used to improve the performance of the composite [12, 13, 14]. Usually, silica particles are added to the polymers for better mechanical, electrical and thermal properties.

Njoku et al. [15] described the effect of particle size on the mechanical strength of the composite. She has concluded that Nanoscale particles help in increasing the mechanical strength than micro-scale particles. Smaller particle size helps in better fracture toughness [16, 17]. Thus, many researchers have reduced particle size and have focussed on how single particle size affects the mechanical properties of the polymer composite [18-24].

Nakamura et al. discussed the effect of size and shape of silica particle on the strength and fracture toughness based on particle matrix adhesion and increased mechanical properties of the composite. The strength of any composite material depends on the particle and matrix reinforcement [25-27].

The effect of particle size of the reinforced material on the properties of the composite material have also been investigated by Pattanaik et al. [28] and have concluded that the properties of the composite are greatly influenced by the particle size. The random size of filler material helps in compromising in the inter-particulate gap which helps in increasing the strength. In some cases, random particle size helps in proper adhesive bonding between matrix and the reinforcement which results in excellent mechanical properties.

Moreover, when cost plays a significant role in product development, particulate filled polymer composite are preferred over fibre reinforcement in making a composite material. Powder density, particle size and shape also play a significant role in fabrication and strengthening behaviour of any material. Considering the above aspects, developed composite depend on the property of the filler material, adhesion between reinforcement and the filler, particle size, particle shape and volume percentage of the filler material [29, 30, 31].

2.2. Mechanical Properties of Polymer Composites

Mechanical properties of any material include its hardness, tensile strength, flexural strength and impact strength of that material. In case of polymeric materials, fibres and/or particulates are reinforced / dispersed in the polymer matrix to increase its mechanical properties. Many researchers have investigated on the fibrous and particulate reinforced composites and concluded that fibrous polymer composites have higher (unidirectional) mechanical strength than particulate filled polymer composites. Polymers and polymer matrix composites are widely desired in industries for applications like heaters, electrodes and positive temperature coefficient. These materials find their application due to their low density, high corrosion resistance, low cost and easy fabrication process [32-35].

The variation of the hardness of the polymer composites has been investigated by many researchers. Zhanwei et al. [36] measured the microhardness by micro-indentation technique. The micro-indentation measurement was done at various loads and loading speeds. Under the same test conditions, Young's modulus and microhardness decline with increasing loading speed. They also showed that the indentation hardness decreases with increasing the indentation depth.

Mehan et al. [37] studied the micromechanical behaviour of short fibre reinforced polymer composites and the maximum strain transfer rate did not depend on the angle of orientation. They also explained the mechanism of load transfer at the fibre-matrix interface.

Gungor [38] studied the mechanical properties by incorporating metallic filler into the polymer. He has studied the influence of metallic filler in the polymer composite. There is a sudden decrease in impact strength due to the addition of filler but the tensile strength and flexural modulus decrease gradually. It may be attributable to improper bonding between high-density polyethylene and iron powder.

In a composite material, fibre/fibre interaction and the resulting stress concentration due to a fibre failure is crucial in determining the composite fracture behaviour. Susumu and Nikkeshi studied the effect of stress concentration and stress factor in epoxy-graphite composite [39]. Stress concentration plays a major role in reducing the strength of the composite as the stress flow direction changes in the presence of voids that are present during the fabrication of polymer composites. They have concluded that stress concentration factor is much less in the case of tension as compared to that in compression and the difference in stress concentration is due to interfacial bonding between the polymer matrix and the filler material [40-44].

As polymer composites have gained popularity in structural applications, there is need of designing the polymer composite by multiple loading conditions [45-47]. The effect of type/fibre size is a factor also. In this regard, the investigation of Behrouz et al. [48] is worth noting. They have studied the effect of low weight fraction of the filler material, orientation and length to diameter ratio of the filler with bi-axial or multi-axial loading conditions.

Hinton and Kaddour [49] and others [50] have evaluated the tensile strength of glass epoxy composites with random microstructures and found a nonlinear decreasing trend of the tensile strength with increasing the randomness of the dispersed fibres in the matrix.

Fu SY and Lauke B [51] studied about the flexural behaviour of the epoxy hybrid composite. They have validated the experimental result with FEA analysis. They have shown that the flexural strength increases with increase in span to depth ratio. They have also mentioned

that, with hybridization, the flexural strength increases. In earlier studies, tensile, flexural, compressive strength and tensile modulus showed no effect of hybridization while flexural modulus only showed a positive effect [52]. In a 3 point bend test, when the load is applied, the bottom side of the specimen is subjected to tension and the upper side is subjected to compression. Shear strength plays an important role at the mid-span of the sample. So, the failure of the sample may be due to tensile, flexural, shear or combination of these forces.

Sung et al. have studied the fracture toughness and failure mechanisms in silica filled epoxy composite on temperature and loading rate [53]. Various researchers have explained that particle size and shape also plays a significant role in determining the mechanical strength especially fracture strength. The fracture is initiated from the particles where surface flaws and defects are present. It can be due to stress concentration or irregular stress due to the non-homogenous distribution of reinforcement material. They have also concluded that strength and stiffness are reduced above ambient temperatures. Finally, they have summarised that, particle fracture itself also contributes to the fracture toughness of the composite since the failure mechanism is caused mainly by inherent defects present in the particles. In conclusion, the primary failure mechanisms are matrix shear yielding between the particulate matter and crack tip deflection which generates a large fracture surface area [54].

Bowen et al. [55] described the results of an experimental and numerical investigation of the impact behaviour of short carbon fibre reinforced polyether-ether-ketone. They have mentioned that in all impact energies, short carbon fibre reinforced PEEK composites showed a brittle fracture and the energy absorption capability decreases in comparison with unfilled fibre reinforced composite.

Kotoul and Vrbka [56] have found that, there are two primary mechanisms to increase the fracture toughness of the polymer composite; i.e. intrinsic toughening and extrinsic toughening. The toughness of any material is defined as the amount of energy to crack the sample. Intrinsic toughening includes shear yielding that acts at crack tip against its ignition or propagation. Extrinsic toughening is the crack tip shielding which acts to inhibit the damage.

Hei-lam Ma et al.[57] studied the impact response of glass fibre reinforced epoxy composite at different temperatures.

From findings mentioned above, it can be concluded that the mechanical properties of the virgin polymer increase with reinforcement. Fibre reinforced polymers show higher toughness and mechanical strength than particulate filled polymer composites. Sometimes it is better to fabricate hybrid composite with the help of both particulate and fibres. It is also

concluded that mechanical strength of polymer composites mainly depend on the interface adhesion, particulate size, shape and nature of the surface.

2.3. Dielectric Characteristics of Composites

Electrical properties of any material include its dielectric strength, resistivity, conductivity and its capacitance. Dielectric strength is the measurement of the maximum electric field that a pure material can withstand under ideal conditions without experiencing failure of its insulating properties. So, dielectric strength plays a significant role in describing the role of any material to be used in electrical and electronics industries.

Polymers and polymer matrix composites are excellent insulating materials. So, various researchers have thought of using these materials in electrical and electronics appliances. Materials having high dielectric strength find its primary application in storing of energy, electric stress control devices and thin film resistors.

Yanyan [58] fabricated Nanocomposites by using no biodegradable polymers as matrix material. They have concluded that composites having Nanoparticles at the core show better dielectric strength than conventional composites.

Shaohui [59] modified the surface of filler material to increase the dispersion stability of the filler. With the modification of the surface, there is three times higher dielectric strength which helps in storing a large amount of potential energy. They have mentioned that the interface between the filler and the polymer matrix composite plays a major role in determining the dielectric strength of the material. They have concluded that surface fluorination improves the energy storage density of the Nanocomposite [60].

Hristiyanand et al. [61] described that dielectric elastomer actuators had found numerous promising applications such as soft motors, soft robots, energy harvesting, optics, Braille displays, adaptive optics and biomedical devices. They described the effect of loading condition on the dielectric properties of the material [62, 63].

Betts et al. [64] developed a new soft dielectric elastomer from dopamine-coated barium titanate particles and silicon rubber. They have shown that dopamine, in addition to coating the barium titanate (BaTiO_3 , BT), the coated particles (DP-BT) were highly compatible with silicone rubber. They have again concluded that the electromechanical properties were significantly improved regarding voltage induced deformation [65].

Chang et al. have developed a polymer composite with $(\text{Pb}(\text{Zr}_{0.52}\text{Ti}_{0.48})\text{O}_3)$ (Lead Zirconate Titanate) (PZT) Nanofibres with diameters of 150–200 nm [66]. The orientation of PZT

Nanofibres perpendicular to the external electric field gives rise to improved dielectric breakdown strength. A subsequent uniaxial stretching of the composite films leads to higher crystallinity and breakdown strength of the polymer composites, which is favourable for the polarisation of the Nanocomposites at higher electric fields.

Dang et al. [67] have observed that single composition materials couldn't meet high dielectric constant. So, there is a need for developing a composite with high dielectric constant. They have mentioned the effect of fillers, fabrication processes and nature of the interface between fillers and interface. They emphasised the use of Nanofillers as it will increase the area of interface and will consequently increase the polarisation effect.

Liang et al. introduced Ag nanoparticles in core-shell and used it as an oxidative agent and dopamine as a reducing agent to produce a composite material having high dielectric properties. Both the AgNO_3 /dopamine ratio and the pH value of the dopamine solution had an impact on the dielectric properties of the composite. They have achieved dielectricity of 53 when the pH ratio is 1:0.5 [68-70].

Observations of Wenying et.al. [71] show with metal powder reinforced polymer composites have relatively high permittivity, high thermal conductivity and low dissipation factor of the composite. They indicated that the aluminium particles decrease the degree of crystallinity of PVDF. They again mentioned that particle size and shape of the filler affect the thermal conductivity and dielectric properties of the material.

Yuan et al. [72] have used carbon nanotubes which have unique dielectric properties and large specific areas as Nanoscale filler material. They have used carbon nanotubes as they have high aspect ratio, large specific surface area and excellent mechanical properties. They have proposed the use of the developed material in high performance embedded capacitors.

Wang et al. [73] have used ultra-fine fly ash particles for the preparation of carbon fibre mixed composite. They have investigated the effect of ultra-fine fly ash on the dielectric properties of Carbon fibre sulphoaluminate cement composite (CFSC). They have found that ultra-fine fly ash particles help in producing micro-capacitors, with excellent mechanical properties and simultaneously weaken the ionic polarisation. The sensitivity, accuracy and reversibility of the change in dielectric constant under stress condition are improved due to the addition of ultra-fine fly ash particles.

Sakonwan et al. [74] measured the electrical conductivity and dielectric of the fly ash geopolymers in a frequency range of 100Hz to 10MHz. They have analysed the effect of liquid alkali solution to ash ratio. They have mentioned that water molecules present in

geopolymers are responsible for electrical conductivity and dielectric of the material at room temperature.

Jumrat et al. [75] investigated the dielectric properties and temperature profile of fly ash geopolymers. They have discussed the importance of microwave for the drying of the geopolymer. They have related the dielectric properties with the absorbability of microwave energy. They have concluded that the dielectric properties of mortar tend to decrease continuously with increasing time after mixing. For the mortars with more water and liquid, the dielectric constant and dielectric loss factors are also higher.

Sergy et al. [76] introduced natural graphite into linear low-density polyethylene to improve the thermal conductivity of the material. And produce a low cost thermally dissipative material. They have not any mentioned any dielectric results but, they have developed a suitable sink which can dissipate the energy at a quick rate.

Navin and Nidhi [77] measured the dielectric properties of fly ash filled polypropylene at different frequencies and different temperatures. They have found that the dissipation factor of pure polypropylene decreases with increasing frequency and the dielectric constant increases with increase in fly ash content.

From the research works mentioned above, it can be concluded that nanoparticles result in higher dielectric strength due to strong polarisation effect. Surface modification helps in increasing the dielectric strength due to strong polarisation effect. Sometimes, the orientation of the fibres also helps in increasing the dielectric strength of the composite. pH value of the solution also plays a significant role in determining the dielectric strength of the material. The most important thing is that the contribution of ionic polarisation towards dielectric behaviour with the use of fly ash particles helps in increasing the dielectric strength of the composite.

2.4. Thermal Characteristics of Polymer Composite

Polymer and polymer composites have low melting point and low coefficient of thermal expansion. They deform plastically at the glass transition temperature which is at about 0.5-0.7 T_m (i.e. melting temperature). So, while fabricating any polymer matrix composite, it is important to enhance the glass transition temperature to a larger extent so as to enhance/favour the interface bonding of polymer chains on reinforcement particles/fibres, etc. Xing et al. [78] mentioned that the melting temperature range is one of the most important parameters for phase change of material and also dependent on the heating rate.

Zvetkov et al. [79] studied the reaction kinetics and observed that, both the mass and dielectric characteristics of cured epoxy could alter the temperature evolution during the curing process. Thermal energy storages (TES) based on solid-liquid phase change materials (PCM) use the latent heat of the phase transition. Christoph [80] mentioned that TES allows the decoupling between supply and demand of heat or cold, thereby increasing the energy efficiency and the utilisation of renewable energies.

Akihiko & Misuzu [81] in their investigation have confirmed that, the thermal lags are comprised of the effective thermal resistance and the temperature gradient in the sample.

Ruiz et al.. [82] characterised the HCN polymers by various thermoanalytical methods. The Tg curves reveal that the thermal stability is not influenced by the reaction time used in their synthesis.

Mihai et al. [83] studied the mechanical and thermal properties of zinc powder filled high-density polyethylene composites. Results reveal that the thermal stability of HDPE(High-Density Poly Ethylene) charged with zinc powder is better than of the unfilled polymer. They have mentioned that the incorporation of zinc powder in HDPE increases the thermal diffusivity and thermal conductivity and decreases the specific heat.

Tavman [84] studied the thermal and mechanical properties of Cu powder filled polyethylene composites. Mechanical properties found to be increasing with increase in Cu concentration [85].

Akihiko [86] et al. used fast scan DSC to examine the melting behaviour of crystals in a broad range. For the melting of polyethylene (PE), the power law behaviour has been confirmed.

Mike et al. [87] measured the crystallinity in polymers using modulated temperature DSC. The essence of the technique is that it attempts to estimate the contribution from the vibrational heat capacity to the total enthalpy absorbed by the sample over the temperature range where crystallisation rearrangement and melting occur. They have also mentioned that the difference between the total enthalpy and the estimate of the vibrational heat capacity contribution must then be a measure of the enthalpy of melting of any initial crystallinity.

Nearingburg and Elias [88] investigated the formulation and optimisation of stimulus-responsive composites consisting of gold nanoparticles in polyethylene glycol diacrylate. They have found that, the magnitude and the rate of energy transduction can be tuned by varying both nanoparticles concentration and dispersion.

Roger [89] provides a rapid method for determining polymer crystallinity based on heat required to melt the polymer. He has reported the heat as percent crystallinity by normalising the observed heat of fusion to that of a 100% crystalline sample of the same polymer.

From the above references, it is clear that glass transition temperature is dependent on the heating rate of the material. DSC is helpful in determining the crystallinity of the material and also associated with deformation behaviour/mechanical behaviour and quality of the composite. Hence curing condition plays an important role in fabrication and properties of the composite.

2.5. Wear Behaviour of Composite

Materials are subjected to wear during its course of application. Wear can be classified into five different categories. They are-

- Adhesive wear
- Abrasive wear
- Fatigue wear
- Corrosion wear
- Erosion wear

Adhesive wear

Adhesive wear is a mechanism which occurs between two contact surfaces with sufficient force to cause the removal of material. Engineering surface is never perfectly flat. The surface of most highly polished design component shows irregularities or asperities.

When two such surfaces are brought into contact, the real contact occurs only at some high asperities which are a small fraction, e.g. 1/100 of the visible contacting area. As a result, plastic deformation and intermetallic adhesion will occur, forming cold weld junctions between the contacting asperities. Adhesive wear is dominated by material transfer and removal of the transferred material. The former is determined by the material properties and the strength of adhesion junction.

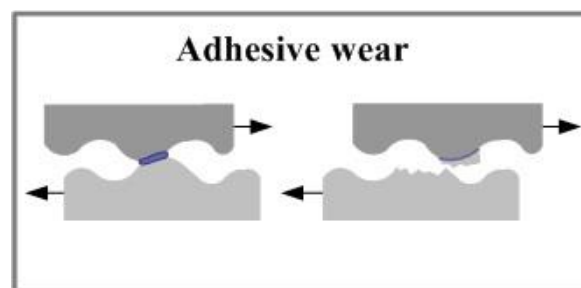


Figure 2.1: Schematic diagram of adhesive wear.

Abrasive wear

Abrasive wear occurs when a hard surface slides across a softer surface. It is also defined as the loss of material due to hard particles or hard protuberance that is formed against and moves along a solid surface.

The way the grates pass over the worn surface determines the nature of abrasive wear. There are two basic modes of abrasive wear-

- a. Two-body abrasion
- b. Three-body abrasion

Two-body wear occurs when the grits or hard particles remove material from the opposite surface. The common analogy is that of material being removed or displaced by cutting or ploughing operation.

Three-body wear occurs when the particles are not constrained and are free to roll and slide down a surface. The contact environment determines whether the wear is classified as open or closed. An open contact occurs when the surfaces are sufficiently displaced to be independent of one another.

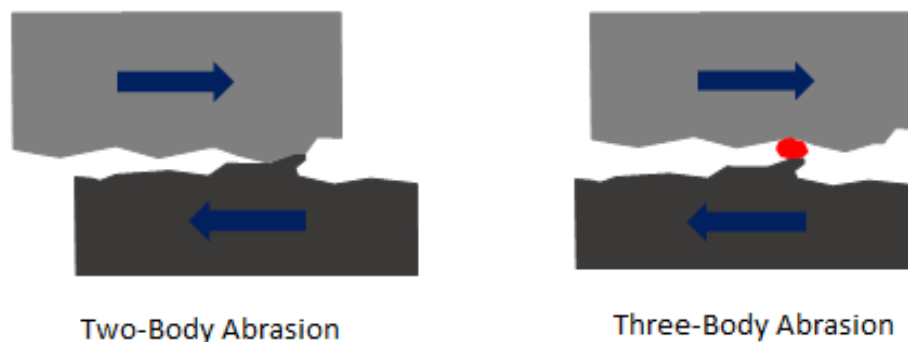


Figure 2.2: Schematic diagram of abrasive wear.

Erosion wear

Wear which is caused by the impact of particles of solid or liquid against the surface of an object. The impacting particles gradually remove materials from the surface through repeated deformations and cutting actions. The rate of erosion wear is dependent on some factors viz. shape, size, hardness and impact velocity and impingement angle.

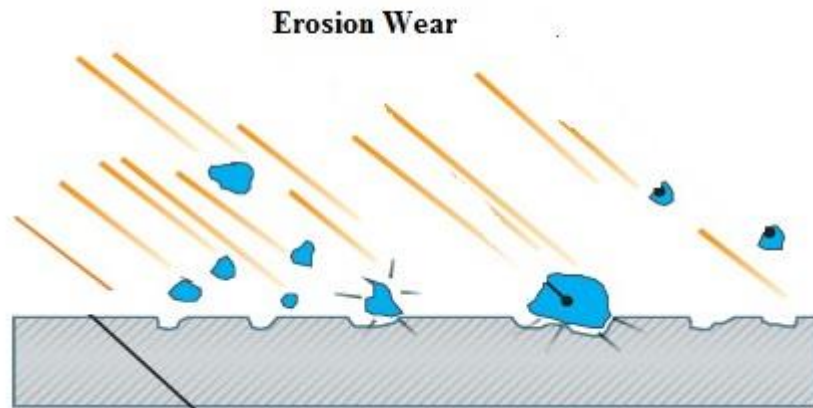


Figure 2.3: Schematic diagram of erosion wear.

Fatigue wear

Fatigue wear of material is caused by a cyclic loading during friction. It is the progressive and localised structural damage that occurs when a material is subjected to cyclic loading. Fatigue happens if the applied load is higher than the fatigue strength of the material.

Fatigue wear is caused by contact between asperities with very high local stress and is repeated during sliding or rolling with or without lubrication. The result of fatigue wear is severe plastic deformation. Repeated or cyclic loading leads to the formation and propagation of cracks under the stressed surface, which is thus destroyed.

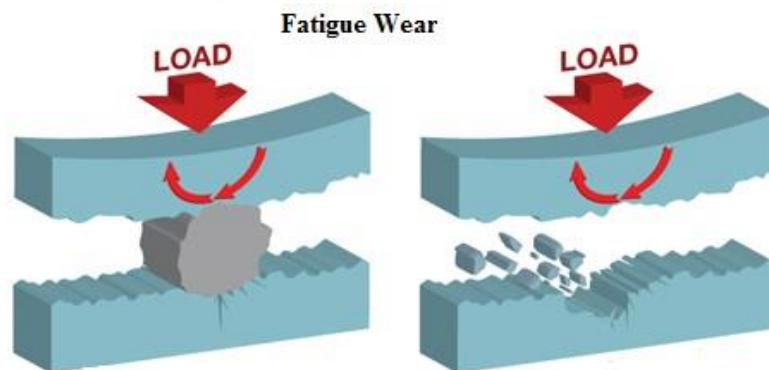


Figure 2.4: Schematic diagram of fatigue wear.

Corrosion wear

Corrosive wear is material degradation wherein both wear and corrosion wear mechanisms are present. The effects of both wear and corrosion can result in intense damage or material losses. The effects can be more severe than when encountering either of these two mechanisms alone. Typically, surface failure such as erosion and abrasion results from the

dynamic interaction between two surfaces. It is the kind of damage caused by the synergetic attack of both wear and corrosion when it takes place within a corrosive setting.



Figure 2.5: Schematic diagram of corrosion wear.

Type of wear is related to the field of implementation of the material. So, it is necessary to study the characteristics of any newly developed material and predict the life of the component and its suitability for any particular application.

Malhotra et al. have explained the effects of fly ash and bottom ash on the frictional behaviour of the polymer composite [90]. They have studied the frictional behaviour with a friction assessment and screening test (FAST). They have confirmed that the fly ash has abrasive characteristics and a higher μ value. Results show that, composites having more than 20% fly ash reinforcement have high wear rate and can't be used for automobile applications. In fly ash some particles are solid and some are hollow in nature. Most of the fly ash particles are solid particles whereas Cenospheres are hollow particles. Chauhan and Thakur have described the effect of particle size, particle loading and sliding distance on the friction and wear properties [91]. They have examined the mechanical properties of cenospheres filled vinyl ester composite. It was observed that in the steady state region, the specific wear rate of vinyl ester composites varies marginally.

Srivastava and Pawar have studied the erosive behaviour of hybrid composite made out of glass fibre, fly ash and epoxy resin [92]. They have varied the fly ash percentage, impingement angle and particle velocity for analysing wear behaviour. They found that, fly ash filler resists the formation of crack growth, which improves the resistance to erosive wear.

Jinfeng et al. have studied the effect of graphite particle reinforcement on dry sliding wear of Si/Gr/Al composite [93]. Results show that friction coefficient decreases and the wear resistance increase with an increase in of graphite percentage. They have also mentioned that

with an increase in graphite particle size, wear resistance increases. It may be due to the enhancement of integrity of lubrication in tribo-layer.

Srinivas et.al. [94], have described the Tribological behaviour of epoxy composites with different types of particulate fillers viz. graphite, silicon carbide. They have mentioned that addition of metallic filler improves the wear resistance of the material. They have concluded that graphite filled epoxy and hybrid fillers filled epoxy containing a higher fraction of graphite exhibits lower friction coefficient.

Automobile brake pads or clutches require high coefficient of friction coupled with little wear. So, the main aim of developing a polymer composite is to have the criteria mentioned above. Chandra et al. [95] described that, the work is done in overcoming friction in bearing and other mechanical components are dissipated as heat and its reduction will lead to an increase in the overall efficiency. They have also mentioned that, incorporation of fillers in polymers could provide a synergism regarding improving mechanical properties and wear performance.

Esteves et al. [96] studied the tribological and mechanical behaviour of epoxy/ nano clay composites. They have considered the tribological tests in dry and lubricated conditions. For epoxy resins, the wear resistance and friction coefficient improve when up to 2% of the volume of nano silica is added. However, this behaviour isn't constant because an excess of filler material usually leads to particle agglomeration and a decrease in composite properties. Fly ash particles possess certain characteristics that make them suitable for use in friction composites as a filler material. Mohanty and Chugh [97] attempted to incorporate more than 50% fly ash in automotive brake lining friction composites. They have also added phenolic resin, aramid pulp, glass fibre, potassium titanate, graphite, aluminium fibre and Cu powder during the composite fabrication. They developed brake lining which exhibits a higher coefficient of friction with low wear rate.

Kurahatti et al. [98], studied the dry sliding wear behaviour of epoxy reinforced with Nano ZrO_2 particles. Their experimental results show that the frictional force and wear rate of epoxy can be reduced at low concentration of nano- ZrO_2 particles. They have concluded that wear performance of the composite doesn't correlate with the static mechanical properties.

Erosive characteristics of $CaCO_3$ filled unsaturated polyester/glass fibre composite is evaluated by Yelmaz [99] et al. $CaCO_3$ gives high strength as a reinforced material. They have again revealed that strength and erosive resistance of the developed polymer composite increase with a smaller particle size of $CaCO_3$. It is also mentioned that brittle failure occurs during the erosion wear of the material.

Supeethet et al. [100] discussed the influence of fibre length on the tribological behaviour of short pineapple leaf fibre (PALF). The investigation shows that specific wear rate and coefficient of friction decreases with increase in normal load. Strength and adhesion between fibres and matrix increase up to a maximum length of 8mm, then it decreases. They have mentioned that coefficient of friction for all the different fibre length composites decreases with increase in normal load due to self-lubrication. More material is removed and the removed material is held at the mating surface of the composite which results in self-lubrication.

Glass fibre acts as a conventional filler material in various polymer matrix composites. Raju et al. [101] investigated the mechanical and tribological behaviour of particulate filled glass fibre reinforced epoxy composites. From the experimental investigation, it is found that the presence of Al_2O_3 filler improves the tensile strength but reduce the specific wear rate.

Chauhan et al. [102] studied the effect of fly ash on friction and dry sliding wears behaviour of glass fibre reinforced polymer composite with optimisation technique. They have found that incorporation of fly ash particulate as a secondary phase in the vinyl ester matrix improves the tribological characteristics. It is also observed that the coefficient of friction decreases with the addition of 10-20% fly ash but wear resistance increases [103].

Kumar et al. [104] reviewed the mechanical and tribological behaviour of particulate filled aluminium metal matrix composite. They have mentioned that surface finish, load, speed, temperature and properties of the opposing surface are the parameters which influence the wear. Metallographic observations show that there is less chemical interaction of the composite due to less contact area. They have mentioned that, at higher sliding velocity, wear rate is lower for metal matrix composites; which is due to the formation of a transfer layer at the region of the worn surface. Particles removed from the counter-body forms a protective layer which reduces the wear rate. They have also mentioned that higher surface roughness leads to higher wear rate.

Sudhakar et al. [105] found rice husk as a suitable filler material in the epoxy matrix. They have found that abrasive wear rate decreases with the addition of rice husk. High wear rate at a higher percentage of rice husks may be due to agglomeration of fibres and reduced adhesion between fibre and matrix. They have further noticed that wear resistance is further increased by treating the surface of the fibres.

Temesgen et al. [106] thought of using the natural jute fibre reinforced with polypropylene. Jute fibre is widely used for its good mechanical strength and has replaced the traditional

fibres. Results indicate that friction coefficient decreases with the addition of jute fibre. In normal cases, wear rate is higher at higher loading condition, but the developed composite show considerable improvement in wear rate higher loading condition.

Thermal conductivity and wear resistance are critical parameters for a good service performance and durability. Metallic fillers improve the thermal conductivity of the material. Vasconcelos et al. [107] studied the tribological behaviour of aluminium filled resin and tri-phase composites made out of epoxy, aluminium and milled glass made out of epoxy, aluminium, milled glass and carbon fibres. They have concluded that, due to geometric relations and surface chemistry, the fibres tend to adhere more strongly to the resin matrix than aluminium particles. At higher loading condition, particles are eroded while fibres stay longer. In hybrid composites, the load carrying capacity increases reducing the friction coefficient and increasing the composite wear rate.

Hanumantharya et.al. [108] compared the dry sliding wear behaviour of the glass-epoxy composite with granite fly ash filled epoxy composite under constant load and sliding condition. They have concluded that granite fly ash filled composites show a better result than glass epoxy composite.

Mohan et al. [109] studied the erosive wear behaviour of tungsten-reinforced carbide glass epoxy composites. The effect of different impact velocities and impact angles on the performance of the wear resistance of the composites were measured. As the hardness of tungsten is more than glass fibre, wear is negligible for tungsten filled composite. From this investigation, they show that hardness plays a major role in wear characteristics of any material.

From the above references, it is clear that, particulate filled composites show better wear resistance than conventional unfilled materials. Wear of any composite material is independent of other mechanical properties like tensile strength, flexural strength, etc. The hardness of the material is directly proportional to the wear resistance of the material. The total amount of frictional force results in wear and heat generated at the interface between the matrix and the reinforcement material. Hence, reinforcement of hard phase/particles helps in providing high friction coefficient and lower wear rate.

2.6. Durability of Polymer Composite

Durability describes the resistance of the material to sustain for a longer lifetime at different operating environmental conditions. Here are some references which describe the durability of various types of polymer composites.

Fujan et al. [110] described the durability of epoxy resin coating under different relative humidity conditions. They have conducted the peel strength to measure the adhesive property of the surface. They found that, moisture may penetrate through diffusion, transport along the interface, capillary action through cracks and crazes in the coating. They have concluded that, mechanical strength decreases very slowly at the initial stage and gradually decrease at a rapid pace. Once the surface is saturated with water, diffusion of water drops and remain stable and deteriorates the polymer.

Durability and environmental degradation of glass-vinyl ester are also studied by Hammami and Ghuilani [111]. They have emphasised on the cost-effectiveness and large scale application of the vinyl ester matrix polymer composite. Their work can be summarised as follows-

- A higher percentage of fibre inhibits the degradation of the matrix material.
- Degradation starts at the interface of matrix and reinforcement which propagate with time.
- Specimens under sea water degrade chemically leaving fibres with no protection which ultimately results in poor interlaminar shear strength.

Kishore et al. [112] studied about the variation in the compressive strength of saline water exposed to fly ash epoxy composite. They have found that, fly ash reinforced composite absorb more amount of water than the virgin epoxy specimen. Reinforced specimens show better mechanical properties than normal epoxy samples without any environmental conditioning, but it reverses once it is exposed to the sea water. Such action i.e. reversal in properties may be due to interface debonding and ingress of moisture by the fly ash particles.

Ribeiro et al. analysed chemical resistance of epoxy and polyester concrete to acid and salts [113]. They have compared the bending strength and variation of mass on time. They have correlated the amount of water uptake and the decrease in strength and concluded that matrix permeability is the sole reason for the decrease in flexural strength.

Glass fibres and glass fibre reinforced thermosetting resins are widely used for their high aspect ratio. So, Bledzki et al. [114] summarised the effect of corrosion phenomena in the

above-said materials. They have mentioned that corrosive environments act primarily to reduce through the matrix and by penetration of the chemically aggressive substance into the material interior through cracks. They have concluded that the degree of damage depends on several factors viz. glass content, test temperature and the aggressiveness of the chemical environments.

Glass-polyester pipes are heavily used in chemical industries. So, Stamenovic et al. [115] studied the influence of liquids on the state of stresses and tensile strengths in longitudinal and circumferential direction. They have immersed the samples in four different mediums like-strong alkaline, weak alkaline, weak acid and a strong acid. The following conclusions are drawn from the research-

- There is a decrease in the tensile property when immersed in the alkaline solution and it is higher with increasing the alkalinity.
- During treatment conditions, the solutions flow inside through microcracks which are the result of faulty fabrication and shrinkage of the material.
- The influence of solution is maximum at the interface between matrix and reinforcement which directly weaken the load carrying capacity.
- The amount of water absorbed is directly proportional to structure, the degree of crystallinity and polarity of the molecules.

Amaro et al. [116] studied the effects of alkaline and acid solutions on glass epoxy composite as it is widely used in automobile, aerospace and marine applications. They have considered HCl and NaOH solutions to determine the degradation in flexural and impact properties of the material. They have concluded that alkaline solution promotes a higher decrease in flexural and impact properties than the acidic solution.

Banna et al. [117] found out the effects of two aqueous acidic solutions on polyester and epoxy vinyl ester resin. They have conducted various mechanical testing after treating it in the solution and found that, bending test and microhardness are the most sensitive to solution effects. Polyester resin is affected more by exposure time than an epoxy vinyl ester. They have also mentioned that duration the average hardness increased up to two weeks and then decreases. Microhardness of plastic materials builds a relation with the depth of indentation which is the indication of how deep the exposure has affected regarding hardness.

Long before in 1984 Norwood & Hogg [118] studied the durability of glass reinforced polymers in acidic environments. They have mentioned that a tensile load transverse to the unidirectional glass fibre direction. Hence, gradual breakdown of glass in the chopped fibre

layers results in almost total loss of axial strength. The cause of inbuilt stresses is not clear but the result of resin shrinkage at the cure and post cure stages of production.

Pai et al. [119] studied the effect of H_2SO_4 concentration and the sequential lay up glass fibre reinforcement on the diffusion behaviour of glass epoxy composite laminates. Results indicate that isophthalic polyester resin exhibited maximum resistance to H_2SO_4 than other polyester resins. The degradation effects can be directly linked to the levels of moisture and chemicals, diffusing into the composite materials during their exposure to different mediums. Sindhu et al. [120] studied the degradation of coir fibre polyester and glass fibre/polyester composites under different conditions. They have suggested the application of short fibre reinforced polymer composites for their easy processing and low cost. Biofibres can be widely used as these are inexpensive, renewable, easy processing and bio-degradable.

The main disadvantage of bio-fibre is its hydrophilic nature, poor wettability, lower resistance to moisture and reduced weathering behaviour. The tensile strength and modulus of alkaline and saline water aged samples show an anomalous behaviour upon ageing. These properties increase with increased ageing.

As polymeric materials try to replace other structural materials, it is necessary to study the durability of concrete structures. The major durability problems are an alkali-aggregate reaction. Concrete structures are not durable to marine environments and continuous mechanical loading as described by Tang et al. [121].

Gkikas et al. [122] fabricated CNT modified epoxy systems to manufacture carbon fibre reinforced laminates and subjected those to thermal shock and hygrothermal exposure. They have concluded that ILSS remain unaffected after exposure to thermal shock.

Jones et al. [123] discussed the stress corrosion cracking and its implications for the long-term durability of E-glass fibre composites. They have considered the bending stress and tensile loading. They have concluded that the polyester resin protects the glass fibres more efficiently than the epoxy resin. The epoxy glass fibre composite is susceptible to rapid stress concentration in aqueous sulphuric acid because of the loss of the integrity of fibre/resin interface.

Glass fibre reinforced polyester polymer concrete is used for the making of utility hole and drainage components in SouthAfrica. So, Griffiths and Ball [124] studied about the modulus of rupture and fracture toughness of the polymer concrete. Various conclusions are mentioned as follow-

- The addition of glass fibre reduces the brittleness of the material, simultaneously increasing the toughness. The increase in toughness by increasing the energy required for crack propagation.
- The use of silane coupling agent in GFR polymer enhances the modulus of rupture.
- GFR polyester polymer concrete is susceptible to degradation by UV rays. The deterioration in properties is due to photo-oxidation of groupings on the polymer chains.
- The strength of the polymer concrete decreases when exposed to acids and alkalis.
- Saline water reduces the strength more than the usual water of GRP polymer concrete.

The main reason for degradation in mechanical properties is due to the chemical erosion of the matrix-reinforcement interface. Voids help in the diffusion of chemical to the core which ultimately attacks the bulk of the specimen.

Kawada and Srivastava [125] presented the direct effect of an acidic stress environment on the stress intensity factor of woven E-glass fibre reinforced bisphenol-vinyl ester resin and other resins. The constant tensile loading tests determined the rate of crack propagation and stress intensity factors for stress-corrosion cracking. Results reveal that crack propagation behaviour depends on the concentration of acid, temperature, stress intensity factor and time. Epoxy resin is widely used as coating material due to its high sustainability to environmental conditions. Saccani and Magnaghi [126] used epoxy resin to repair the damaged concrete structure and tested its durability. They have concluded that-

- Mechanical stresses induced don't compromise the efficiency of the repair system.
- Carbonation doesn't alter the properties of all the investigated system.
- Epoxy modified primer is more durable than epoxy modified mortar due to its more homogenous microstructure.

Maslehuddin et al. [127] evaluated the mechanical properties and durability characteristics of different types of polymers and cement based mortars. Durability regarding chloride permeability, electrical resistivity and carbonation depth is measured. They have found that the elastic modulus of the polymer based repair mortar is less than that of cement based mortar.

Barbero [128] submitted their conclusive points on a comparative study of effects on characteristics properties of FRP composites when exposed to distilled water, NaCl water solution and sea water separately. Following are the conclusions drawn from their experimental work-

- GFRC when exposed to different mediums, there is a decrease in their mechanical properties.
- Diffusivity is maximum in 3.2% NaCl solution and minimum in sea water.
- SEM micrographs show greater debonding and fibre pull outs in the affected areas and matrix cracking seems to be the primary cause.
- Heating after curing helps in regaining some amount of ILSS probably due to the rearrangement of molecular structure.

From the references mentioned above, it is concluded that there is a change in mechanical, electrical, thermal property of the polymer matrix composites due to exposure to different environmental conditions. Basic solutions influence the most than any other type of solution. SEM micrographs of the references mentioned above show that flow of solution take place through micro cracks and decrease the interface bonding between matrix and reinforcement.

2.7. Knowledge Gap

In the present time, polymers and polymer matrix composites have become the centre of attraction for developing new materials. Following knowledge gaps have been revealed from the reviewed literature-

That;

- i. Researchers have thought of developing new and better polymer matrix composites without looking at the cost-effectiveness of the product. Various researchers have used bio-fibres to reduce the cost to some extent, but very few have thought of using the industrial waste materials as a suitable reinforcing material.
- ii. Some researchers have used waste materials viz. blue dust, poultry feather, etc., but only a few has discussed fly ash as a filler material.
- iii. Some researchers have used fly ash as the filler material for making bricks and hybrid composite as in received condition, but no one has used it for reinforcement to develop a polymer matrix composite.
- iv. Some researchers have given emphasis on pre-processing of fly ash and curing at the time of hardening. But, no one has tried to modify the property with post curing processing. So, in our study post-curing has given emphasis for the structural modification of the composite.
- v. Effect of magnetic and ultrasonic mixing process on the composite properties has not

been emphasised in the earlier investigations.

- vi. Some researchers have tried to evaluate the mechanical properties viz. tensile strength and impact strength of the fly ash composite, but wear and durability of the composite haven't been studied yet.

In view of the above, the current research work is undertaken to investigate the (a) use of raw fly ash (i.e. as received) as the reinforcing material (b) to process with ultrasonic stirring method and (c) to find out the effect of post curing on the mechanical, dielectric and tribological behaviour of the composite. The investigation is further extended to determine the effect of different environmental conditions on the mechanical and thermal properties of the material to assess its durability and suitability for various applications.

2.8. Objective and Work Plan

Objective of the present research work is as follows-

- i. Development of a low-cost polymer matrix composite utilising fly ash as the reinforcement. The main aim of this step is to use the maximum amount of fly ash as the filler material.
- ii. To increase the strength by adapting appropriate processing route. Post curing of the composites to be carried out to improve the mechanical properties further.
- iii. Study of wear characteristics of the composite with the help of optimisation process (to reduce the number of experiments) and to find the effect of operating parameters on the wear behaviour of the material, with an aim to find suitability for household applications viz. as floor tile, etc. is carried out.
- iv. To find out the effect of different environmental conditions on the properties of these composite for remending its suitability and durability for use.

Chapter 3

Materials and Methods

This chapter elaborates about the raw materials; the methodology used for the fabrication of composite material. Specimens are prepared as per ASTM standards for different testing. Mechanical characterization, electrical characterization and thermal characterization have been done to evaluate the properties of the material. The details of machine specification, test conditions/limits and influencing parameters have also been discussed. TOPSIS method is used to convert the multi-objective optimisation into a single objective optimisation problem. A statistical analytical method viz. Taguchi method is also implemented to support the influence of various parameters responsible for wear behaviour of the material.

3.1 Composite Materials

Composite is a mixture of two or more physically distinct, mechanically different and chemically non-interacting materials/phases and constituents which exhibit better properties than the individual constituents. In the composite material, one is called reinforcing phase, consist of fibres, sheets or particles and embedded in the other material called the matrix phase. The matrix phase can be metal, ceramic or polymer. Concentration, size, shape, distribution and orientation of the filler material mainly determine the final property of the composite material. Advanced composite materials are developed and used in aerospace industries consisting of high-performance fibres as reinforcing material and polymer/metals as the matrix material.

3.1.1 Matrix material

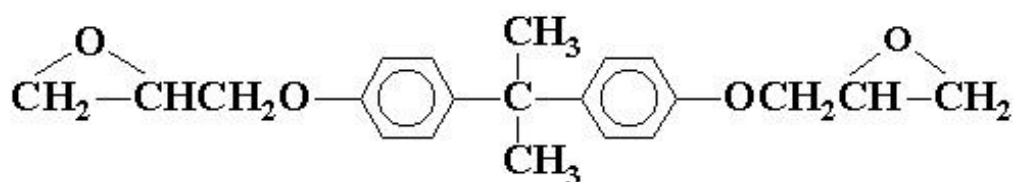
Matrix is a continuous phase of the material. It may be of metal or ceramic or polymer. Depending on the use of matrix material, the composite is named accordingly. There are three different types of composites viz.-

- Metal matrix composite
- Ceramic matrix composite
- Polymer matrix composite

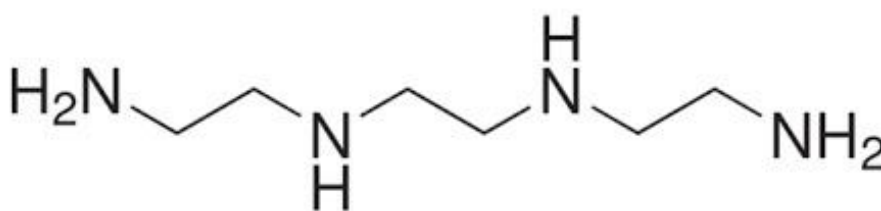
Out of these composites, polymer matrix composite is massively used due to its low cost, high production rate, high aspect ratio and high durability. It is easier to fabricate a

polymer matrix composite and give it a near net shape. So, polymer matrix composite is somewhat replacing the other two types of composite materials. Polymer matrix composite is of two types, thermosetting and thermoplastic polymer. The thermosetting polymer is the result of amorphous cross-linking of bonds. Thermosetting polymers can't undergo a reversible process to initial monomeric stage once it is hardened. Due to its high cross-linking of bonds, it has high thermal and electrical stability which make them suitable for the electrical industries [129].

Epoxy, vinyl ester, phenolic and polyester are the major types of resin which are used commercially. Out of these epoxy resin is most suitable due to its high adhesive property, good mechanical and thermal properties. It is also plentifully available at low cost. So epoxy resin is chosen as the matrix material in this research work. Epoxy resin (LY 556), supplied by ATUL Industries Ltd. is used as the matrix material. It is a high viscous semi-solid material having a density of 1120kg/m^3 and its chemical name is "Bisphenol-A-Diglycidyl-ether". Figure 3.1 shows the structure of the epoxy resin and the hardener.



Epoxy Resin(Bisphenol-A-Diglycidyl-ether)



Hardener (N,N'-Bis (2-aminoethyl) ethane-1,2-diamine)

Figure 3.1: Structure of epoxy resin & hardener.

An amino group hardener (HY 951) chemically named as triethylene-tetraamine is used as a hardener. In general, thermosetting resins have good mechanical, thermal properties along with high corrosion resistance.

Some of the properties of the neat uncured epoxy resin are mentioned in Table 3.1 below.

Table 3.1: Properties of neat epoxy resin.

| Characteristic Property | Inferences |
|----------------------------------|----------------------------|
| Density | 1.1-1.2gm/cm ³ |
| Compressive strength | 110-120MPa |
| Tensile strength | 55-70MPa |
| Flexural strength | 120-140MPa |
| Impact Strength | 17-20MPa |
| Coefficient of thermal expansion | 64-68 10 ⁻⁶ /°C |
| Dielectric constant | 4.1 |

3.1.2 Reinforcement

The reinforcement material is always made with the matrix material to enhance its properties and is two different types; fibre reinforcement and particle reinforcement. In some cases where both are simultaneously used are called hybrid composites. In this experiment, the only particulate filler material is used. The use of particulate composite is just like using mortars with the cement to increase the strength.

The selection of particulate composite varies according to its final mode of use. Use of industrial waste like fly ash, red mud, bauxite ore powder, etc. can be a novel idea of giving extra property at very low cost. Fly ash is industrial by-product which is generated in massive scale from thermal power plants and it put a significant effect on the environment. It is accumulated at the electrostatic precipitator or other particulate filtration equipment before the flue gases reach the chimney.

According to ASTM C 618, there are two classes of fly ash present i.e. Class C and Class F. The classification depends on the amount of Silica, Alumina and Calcium present in the ash. The chemical composition of fly ash mainly depends on the chemical content of coal used. The class C fly ash used here is collected from CPP-2 of Rourkela Steel Plant (SAIL), India. The detail chemical composition revealed the following elements as shown in Table 3.2.

Table 3.2: Properties of fly ash.

| Constituents | Vol % |
|--------------------------------|-------|
| Fe ₂ O ₃ | 8.1 |
| MgO | 1.14 |
| Al ₂ O ₃ | 24.98 |
| SiO ₂ | 55.85 |
| P ₂ O ₅ | 0.15 |
| SO ₃ | 1.16 |
| K ₂ O | 0.85 |
| CaO | 2.54 |
| Na ₂ O | 0.2 |
| TiO ₂ | 1.75 |
| LOI | 3.28 |

From Table 3.2, it is visible that silicon and aluminium consist more than 70% of volume. As the ceramic are harder than polymer and can have better interface bonding gives the idea that, fly ash as filler, will increase the mechanical properties of the composite.

Scanning electron microscopy has been carried out on the fly ash and shown in figure 3.2 which reveals that the particles are spherical in nature and of random in size. Spherical particles when agglomerate leaves a gap in between them which can be filled with epoxy resin. At the same time, the smaller particles will adjust in the spherical gaps which will lead to increase in strength.

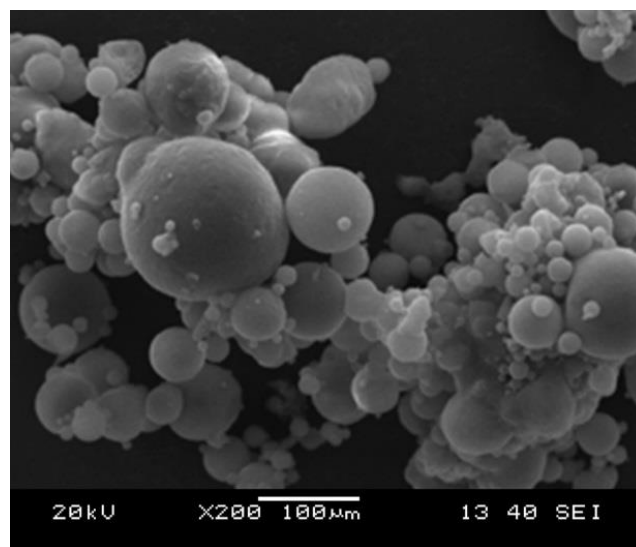


Figure 3.2: SEM micrographs of fly ash.

Particle size has been determined by MALVERN (Masterizer) particle size analyser, shown in figure 3.3. From the figure 3.3, the mean particle size diameter is found to be 27.26 μ m.

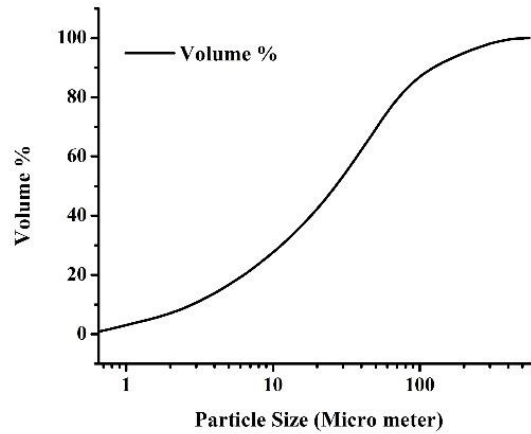


Figure 3.3: Particle size analysis of fly ash.

3.2 Composite Fabrication

Initially, epoxy resin with fly ash is mixed with proper weight percentages (10%, 20%, 30% and 40%) by stirring the mixture with the help of an ultrasonic stirrer with a pulse rate of 5 sec. Once the mixture lowers its viscosity, are cast in required sample dimensions as per ASTM standards. Increasing stirring speed results in agglomeration of fly ash particles and also air entrapment/bubble formation.

3.2.1 For tensile/flexural/impact testing

Tensile strength is measured using INSTRON 1195 with a crosshead speed of 1mm/min following ASTM D 638 specification. Samples of ASTM D 790 specification is used for the flexural test. The flexural test was carried out with a crosshead speed of 1mm/min at a span length of 40mm, in INSTRON 1195. Flat rectangular Izod type samples with dimension according to ASTM D 256 is made initially. The impact test was carried out in a VEEKAY TLVS4 impact tester. The pendulum when released from an angle 150 degrees, can provide a maximum energy of 21.4 J. This amount of energy absorbed is monitored and noted as the impact energy.

Split patterns as shown in figure 3.4 are made out of ABS (Acrylonitrile butadiene styrene) plastic in rapid prototyping machine. These ABS plastics can sustain high temperature than the temperature generated during polymerization.



Figure 3.4: Patterns ready for sample preparation.

These patterns are easy to manufacture, durable and flexible for some operations. Pre-weighed fly ash is mixed with epoxy resin in an ultrasonic sonicator for a maximum duration of 30 minutes. Once the mixture is ready with a lower viscosity, the hardener is then added and stirred gently; samples are allowed to cure for 24 hours. After it is hardened completely, these are removed from the mould carefully and put in air tight polythene packets for further use. The solidified samples are shown in Figure 3.5.

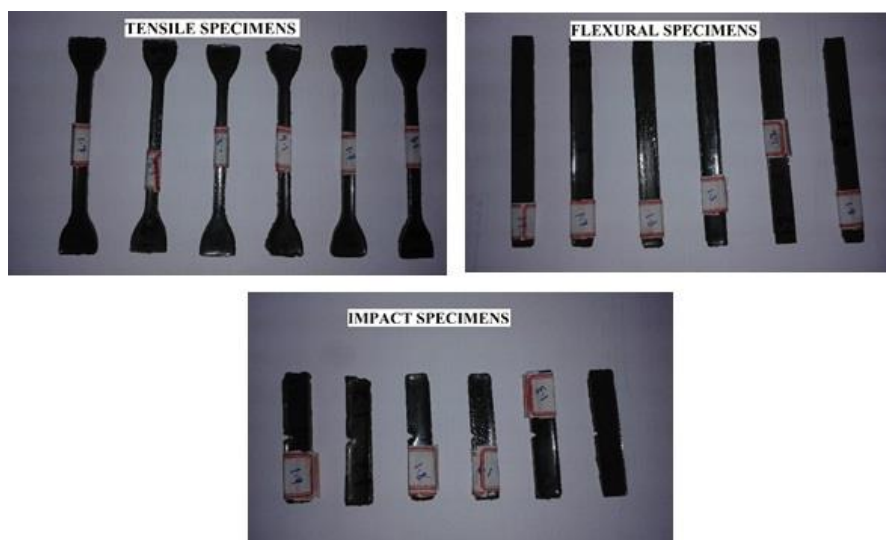


Figure 3.5: Samples after solidification.

3.2.2 For wear test

Specimens for sliding wear test are made following ASTM G99 standard. The DUCOM sliding wear test rig has been used, for the wear test. Plastic pipes available for gardening

purposes in the market having a diameter of 10mm is cut into small pieces of 1-inch height to be used as a mould. Samples of four different reinforcement percentages are mixed using an ultrasonic sonication machine and poured gently and allowed to cure for 24 hours in normal atmospheric condition. Various operating parameters viz. temperature, pressure, strain rate and even the environmental conditions play an important role in influencing the mechanical response of polymers [130-134]. So, the controlled atmosphere (room temperature) is maintained while making of samples for uniformity. Total 32 samples of each treatment condition are made and stored in poly packs for further use.

3.2.3 For dielectric study

For the dielectric test, cylindrical coins like specimens are made. So, once the complete mixture is ready, it is poured into a predesigned mould cavity of 15mm diameter and 1-inch height. Once it is completely hardened, these are cut into slices of 2mm thickness to produce some specimens for the dielectric test. Before that, these samples are treated in the normal atmospheric condition, oven and micro oven to enhance its properties and for comparison. As discussed earlier, the controlled atmosphere (room temperature) is maintained to maintain uniformity of samples.

Solartron 1296 Dielectric Interface Instrument is utilised to evaluate the dielectric properties at room temperature, between the frequency ranges of 100Hz to 1 MHz. The specimen is put between two parallel plate electrodes. Silver paint is applied on both sides of the tablet samples to make the sample surface electrically conductive.

Capacitance is calculated using the following equation,

$$C = \text{capacitance} = \epsilon_0 [A/d] \dots \dots \dots (3.1)$$

Where C_p = Measured capacitance

$\epsilon_0 = 8.8562 \times 10^{-12} \text{ F/m}$ = Dielectric constant of vacuum

ϵ_r = Relative permittivity

A = Surface area of the specimen

D = specimen diameter

Dielectric constant = $K = C_p / C$

3.3 Post-Treatment of Composite

3.3.1 Conventional oven

Conventional ovens are appliances with enclosed space with metallic elements at the top and bottom. Electric current heats up the metallic element and in turn the enclosed space. The thermostat in the oven measures the temperature and controls the current flow to maintain the temperature. Sometimes, the oven is provided with fans that help in maintaining the heat. These ovens with fans are much more efficient than conventional ovens as they uniformly distribute the heat and thus can help in reducing the thermostat temperature. A typical Oven is between 1000 and 2000 watts, but it does not consume all of it during its complete operation. In a conventional oven, the heat has to migrate by conduction from the outside of the material to the middle. In a conventional oven, the material is placed on a metal rack inside the chamber and a heating element heats the air inside of the chamber which causes a hot layer of air to build up around the material.

3.3.2 Microwave oven

Microwaves are radio waves (2500MHz-2.5GHz). These waves can be absorbed by water, fats and sugar. They are not absorbed by plastics, glass or ceramics. Metals reflect microwaves, so causes a spark.

Molecules consist of positive charge on one side and negative charge on another side. When the molecules are exposed to the electromagnetic field, all molecules are rearranged i.e. + charge is to – charge and vice versa. During this process, molecular heat is produced by friction. As the frequency of micro oven is 2500MHz, it changes the direction of electromagnetic fields 2.5×10^9 times/sec. In the micro oven, the whole heating process is different because of exciting atoms rather than conduction of heat. In the micro oven, the air in the oven is at room temperature, so there is no way to form a crust. That is because it heats up materials by microwaves instead of heat conduction. The way in which a material heated by a microwave depend on its-

- Shape
- Size
- Dielectric constant
- Nature of equipment

When a dielectric is placed in a microwave field, energy is dissipated in the material; usually, the power decays with increasing depth of penetration into the dielectric. Without

surrounding insulation material, heat will be lost from the surface of the object, by convention and radiation. Through conduction, heat will be transferred towards the centre of the object. Shortly after the commencement of radiation, the maximum temperature reaches the surface. As time increases, the position of maximum temperature moves into the interior of the object. Microwaves ovens use electromagnetic energy and generate electromagnetic waves to heat up the material. Unlike a conventional oven, they do not heat up the whole space inside the appliance and just use the waves to heat the material kept in it.

Unlike conventional heating, it generates heat within the material and heats the entire volume at about the same rate. In a microwave, there is uniform temperature distribution, improved heating efficiencies and is pollution free environment since there are no products of combustion. In contrast to that in conventional drying, microwave drying gives higher temperature inside the drying samples while the surface temperature stays colder due to the cooling effect of ambient air.

The main aim of using the microwave is to reduce the curing time, but it increases the void fraction in the sample. The entrapment of voids is due to less curing time and low pressure. The efficiency is more when the microwave curing is applied to single phase materials rather than composite materials. More void fraction is induced in the microwave cured composite due to lower external applied pressure and shorter curing time.

3.4 TOPSIS method

To minimise the number of experiments and conclude the interrelationship of different experimental parameters and their dominance, statistical analysis is an important tool. In our study TOPIS and Taguchi methods are used for analysis purpose.

The traditional TOPSIS strategy takes into account that; the best option ought to have the most limited separation from the perfect positive arrangement and the best separation from the negative perfect arrangement. TOPSIS model shows the alternative ways of normalising the data and measuring the distances from the mean position. TOPSIS method has superior advantages concerning the adaptability of its evaluation method and the accuracy of the evaluation result. The TOPSIS method consists of the following steps:

- Normalising the decision matrix

$$r_{ij} = \frac{X_{ij}}{\sqrt{\sum_{k=1}^m X_{kj}^2}}, i = 1, \dots, m; j = 1, \dots, n \quad \dots \dots \dots (3.2)$$

Multiplying the columns of the normalised matrix with associated values. Here similar weights have been assigned to each parameter, i.e., .033.

$$V_{ij} = W_j \times r_{ij}, \dots\dots\dots (3.3)$$

- Determine the positive ideal and ideal negative solutions respectively,

$$A^+ = \{v_1^+, v_2^+, \dots, v_n^+\} = \left\{ \left(\max v_{ij} \mid j \in K_b \right) \left(\min v_{ij} \mid j \in K_c \right) \right\} \dots\dots\dots (3.4)$$

$$A^- = \{v_1^-, v_2^-, \dots, v_n^-\} = \left\{ \left(\min v_{ij} \mid j \in K_b \right) \left(\max v_{ij} \mid j \in K_c \right) \right\} \dots\dots\dots (3.5)$$

Where, K_b = Set of benefit criteria

K_c = Set of cost criteria

Obtaining the distances of the existing alternatives from the positive ideal and ideal negative solutions, two distances for each alternative are, respectively, calculated as follows:

$$S_i^+ = \sqrt{\sum_{j=1}^n (v_{ij} - v_j^+)^2}, i = 1, 2, \dots, m \dots\dots\dots (3.6)$$

$$S_i^- = \sqrt{\sum_{j=1}^n (v_{ij} - v_j^-)^2}, i = 1, 2, \dots, m \dots\dots\dots (3.7)$$

- Calculate the relative closeness to the ideal alternatives;

$$RC_i = \frac{S_i^-}{S_i^+ + S_i^-}, i=1, 2, \dots, m, 0 \leq RC_i \leq 1 \dots\dots\dots (3.8)$$

- Rank the alternatives according to their relative closeness to the ideal alternatives, the bigger RC_i , the better alternative A_i .

3.5 TAGUCHI Method

Being the most important statistical tools of total quality management Taguchi optimal design is used for designing high-quality systems at a reduced cost. Taguchi recommends a three-stage process to achieve a desirable quality product by system design, parameter design and tolerance design. System design helps in identifying the working levels of each parameter of the design parameters; parameter design seeks to determine levels of the parameter that provide the best performance of product or process. Orthogonal arrays, ANOVA, S/N ratio analysis and confirmation test, are the essential tools for parameter design. Main effects plots drawn indicate the general trend of influence of each parameter [135-141].

Parameter design involves selection of appropriate parameter with a high level of performance based characteristics with a minimal possible of variation [141]. It helps mainly during research to get high-quality results at low cost. It exposes the process to various levels of design parameters and requires the use of strategically designed experiments.

Design of the Orthogonal Array (OA)

Orthogonal array significantly reduces the number of experiments by selecting a certain number of combinations of experiments. It was designed and proposed by Taguchi which shows the effect of process parameters on the output result. Initially, the parameters affecting a process are chosen, then the levels at which these parameters affect is determined. Determining what levels of a variable to test requires an in-depth understanding of the process, including the minimum, maximum and current value of the parameter. If the difference between the minimum and maximum value of a parameter is large, the values being tested can be further apart, or more values can be tested. The difference between the minimum and maximum value determine whether to enlarge or reduce the range of parameters.

Analysis of S/N Ratio Based On Taguchi Method

Taguchi uses the signal to noise ratio to measure the quality characteristics deviating from the desired value. There are three types of signal to noise ratio depending on the characteristics-

1. Lower is better
2. Higher is better
3. Nominally is better

In our research work, Taguchi approach is used for calculating wear. In the experiment wear, frictional force and coefficient of friction should be minimum i.e. lower is the better criteria is considered in our experimentation.

The equation for calculating the signal to noise ratio is-

$$\eta = -10 \log_{10} [1/n \sum y_i^2] \text{ where } 1 \leq i \leq n \quad \dots\dots\dots (3.9)$$

n= no of experiments carried out

Results and Discussion

4.1 Physicomechanical Properties

Physicomechanical properties are the prime factors to recommend a material for any specific applications.

4.1.1 Density Measurement

Density is measured by Archimedes principle and there from void fraction is calculated. Polymeric materials are desirable as replacement of metals due to its low density but having desirable strength. Figure 4.1 (a) plotted between percentage reinforcement of fly ash and density. It is found to be decreasing with increasing percentage of fly ash reinforcement. Figure 4.1 (b) plotted between percentage reinforcement of fly ash and void fraction show an increasing trend with an increase in reinforcement. It may be due to the following reasons.

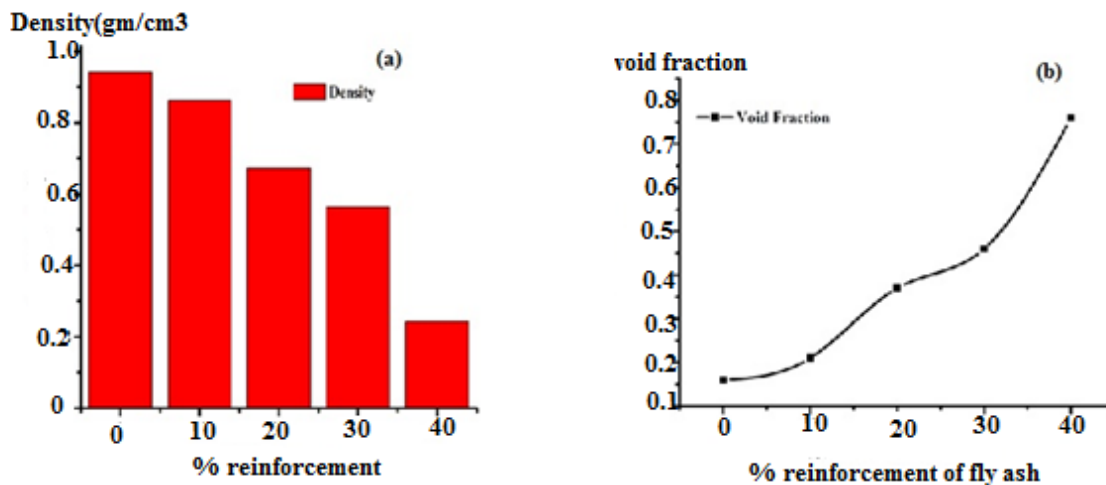


Figure 4.1: Variation of (a) density and (b) void fraction of the composites.

The density of epoxy is much higher than that of fly ash. Due to impregnation of fly ash and during processing, the voids/porosity regions are formed at the polymer chain and particle interface. Also, stress concentration increases at the voids which ultimately results in developing slip or twinning defect in the material. So, it is always desirable to reduce the void fraction in a material to increase the mechanical strength.

4.1.2 Tensile properties

The tensile tests were carried out with INSTRON 1195 following ASTM D 638 standard and the results are plotted in figure 4.2; shows the effect of mixing time on the tensile strength of the composite at various curing conditions. Each data point is an average of five test readings (with $\pm 5\%$ deviation). From the figures, it is observed that depending on mixing time during fabrication of the composite; the tensile strength has increased from 85.76 MPa to 90.07 MPa for normal atmospheric treatment, 95.48MPa to 101.32MPa for oven treatment and 106.05MPa to 113.57 MPa for microwave treatment; for composites with 10% fly ash reinforcement. Similarly, for 20% fly ash reinforcement, the tensile strength vary between 79.37 MPa to 104.47 MPa with a maximum value of 104.47 MPa in microwave curing. With 30% fly ash addition tensile strength ranges from 67.23 MPa to 92.88 MPa with a maximum value of 92.88 MPa at 30minutes of mixing time and microwave curing. For 40% fly ash addition, tensile strength varies between 54.51 MPa at the atmospheric condition to 80.53 MPa at microwave curing condition.

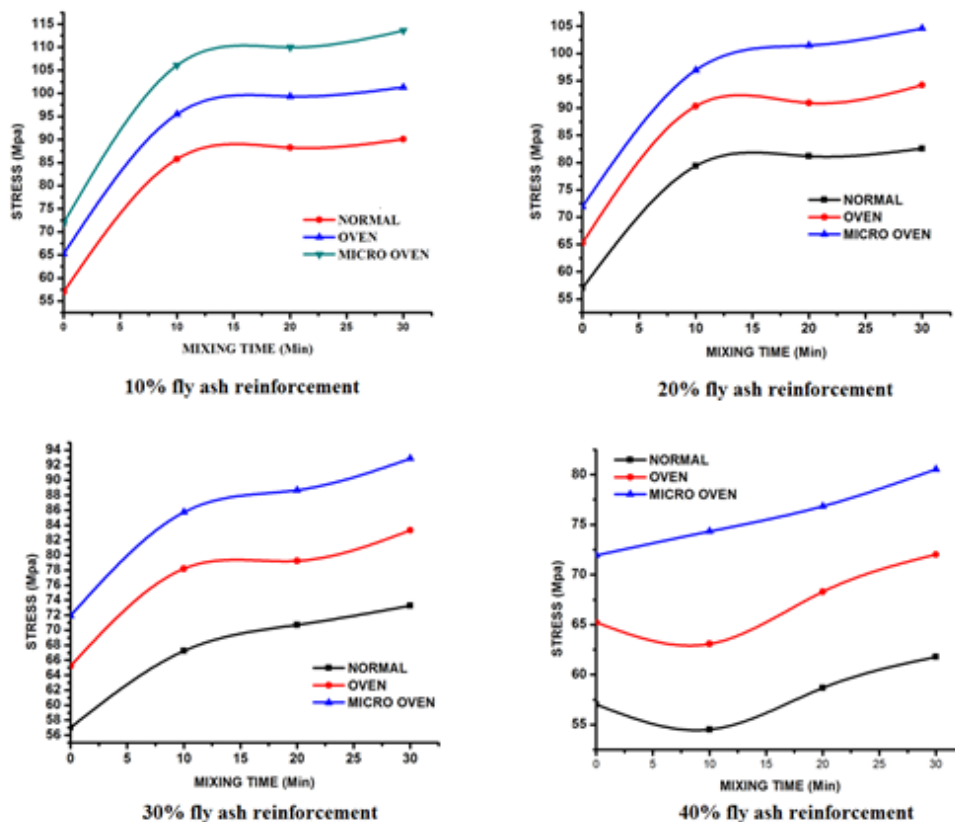


Figure 4.2: Variation of tensile strength with mixing time for different percentage of fly ash reinforcement.

When polymerization starts, there is a rise in temperature and hence a decrease in viscosity. So, it is easier for developing a uniform surface coating on each fly ash particle. The formation of continuous matrix network helps in increasing the tensile strength. Mixing time should be within the time scale (10-30) minutes before settling-solidification starts. Thirty minutes is found to be the suitable mixing time for casting of the samples into the mould.

The tensile strength of the neat epoxy material is found to be 60 MPa. Incorporation of ceramic filler i.e. fly ash increases the tensile strength of the polymer composite. From the experiment, it is clear that the tensile strength increases with the mixing time. The tensile strength is found to be maximum (of 90.07 MPa), at 30 minutes of mixing for 10% reinforcement of fly ash.

Post curing has been done in the oven and micro oven on atmospheric condition with the aim of increasing the tensile strength. The tensile strength is maximum (of 113.57MPa) at 30 minutes of mixing (for 10% fly ash reinforcement) for micro oven cured specimens which is much higher than the tensile strength of the neat epoxy at the uncured/untreated condition. Figure 4.3 shows the variation of tensile strength under different curing conditions. It is seen that irrespective of percentage of fly ash reinforcement, tensile strength varies with the type of curing conditions. In every case, tensile strength is maximum for microwave cured samples followed by oven curing and standard atmospheric curing.

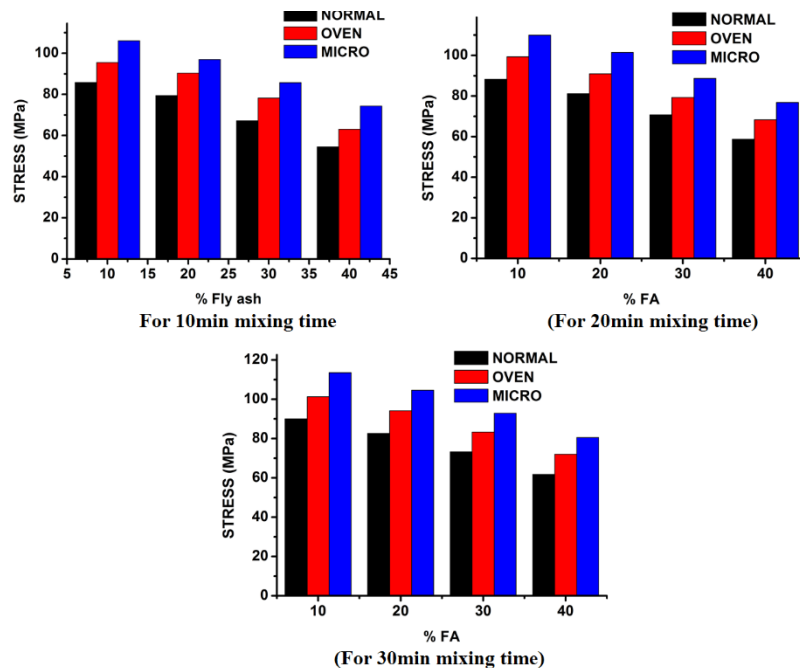


Figure 4.3: Variation of tensile strength with percentage of fly ash reinforcement at different curing conditions and mixing times.

Maximum tensile strength of 113.57 MPa is obtained at microwave curing condition for 10% fly ash reinforcement. Curing removes the internal stresses and also affect the quality of polymer bonds-blends which may be the possible reason for an increase in tensile strength of the material.

Figure 4.4 shows the variation of percentage elongation of the specimen (at maximum load) for a different amount of fly ash reinforcement. It is evident from the figure that percentage elongation of the samples decreases with increase in the percentage of fly ash irrespective of curing condition. A maximum value of 3.38% elongation is obtained in 10% fly ash at micro oven curing condition.

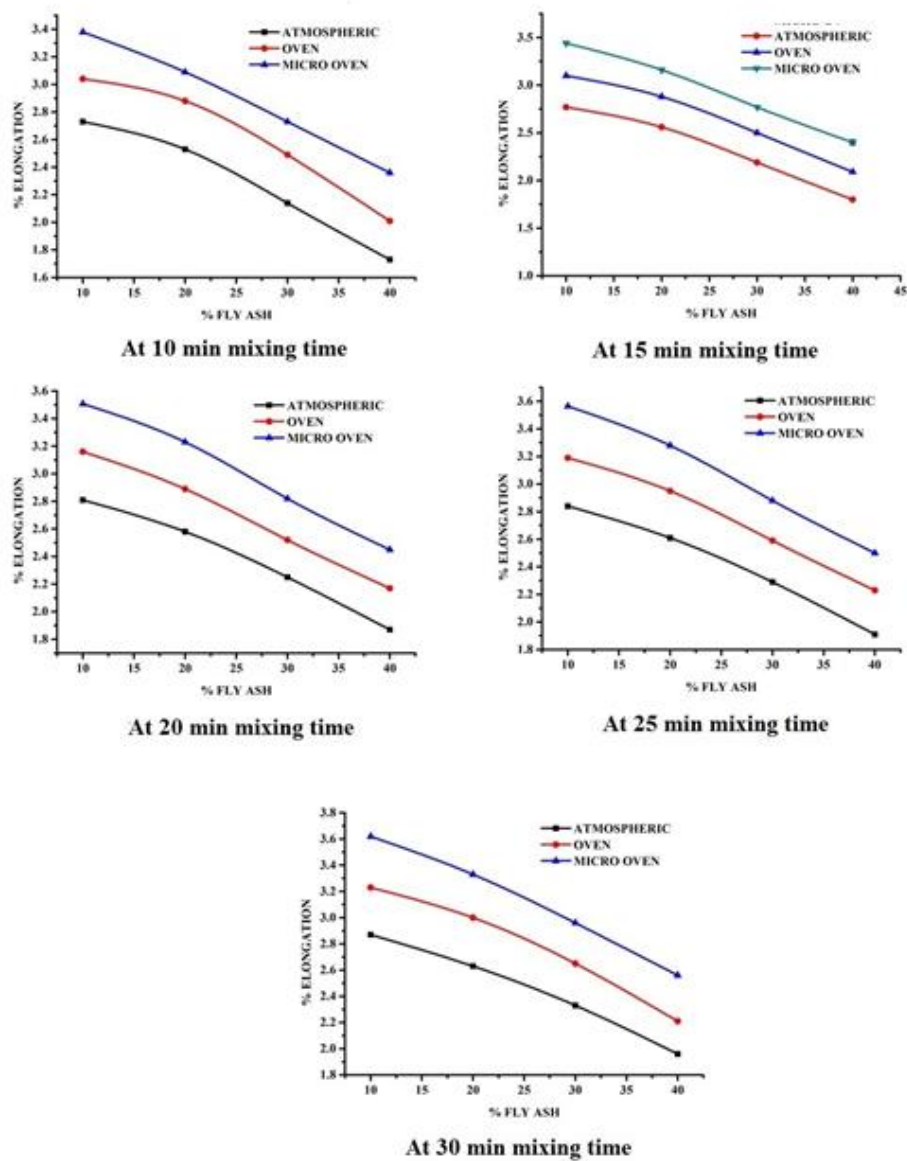


Figure 4.4: Variation of percentage elongation with different fly ash percentage at different mixing times.

It may be due to the reason that, at lower percentage reinforcement of fly ash there is continuous matrix network which carries the load and helps in elongation of the material. As the filler percentage increases, discontinuity in matrix network retards the elongation percentage.

4.1.3 Flexural properties

The flexural strength of the composite for different conditions is plotted in figure 4.5 and figure 4.6. The flexural test was carried out with INSTRON 1195 following ASTM D 790. Figures 4.5 plotted between mixing time and strength show that flexural strength takes an increasing trend with an increase in mixing time. The growing trend in all the graphs is also evident and mixing time of 30 minutes is found as the most suitable duration to get the maximum flexural strength.

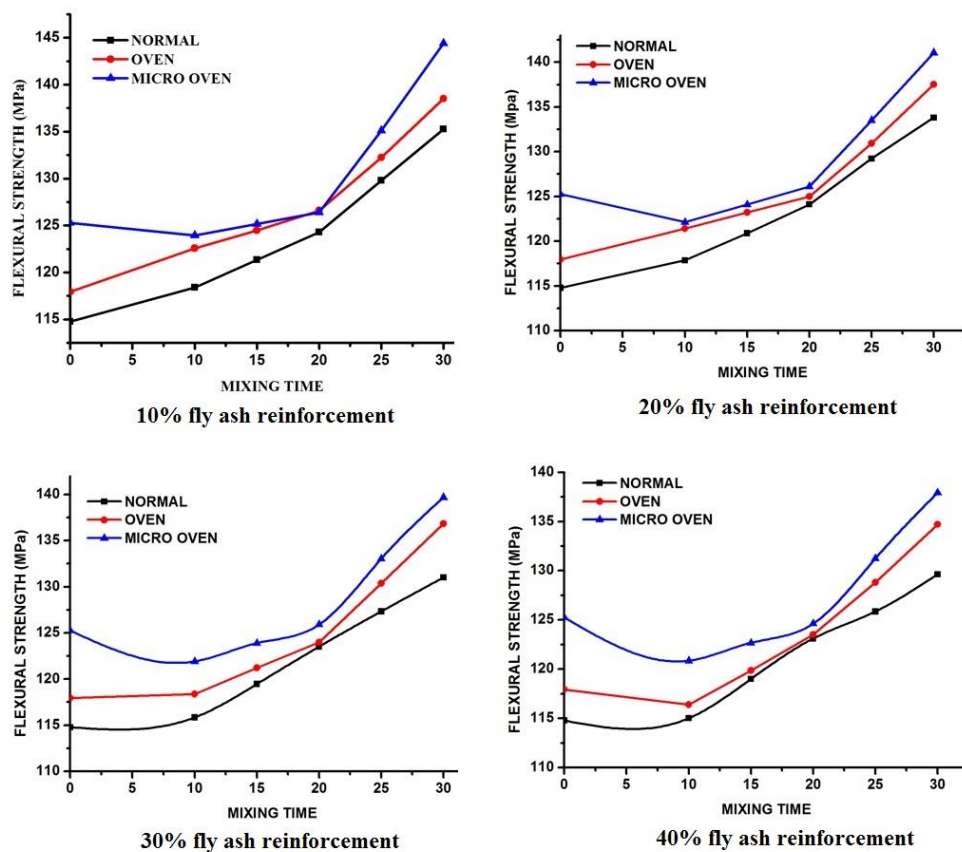


Figure 4.5: Variation of flexural strength with mixing time for different fly ash percentage.

The increase in strength may be due to a decrease in viscosity resulting from coating over the fly ash particles. At higher mixing time, there must be the formation of the amount

of crystallinity in the polymer matrix structure which might be the cause for the increase in strength.

Figure 4.6 shows the variation of flexural strength for different compositions. It is visible that flexural strength increases with curing conditions. But there is not much of change in values as compared to the tensile strength properties. The flexural strength is found to be maximum for microwave curing specimens.

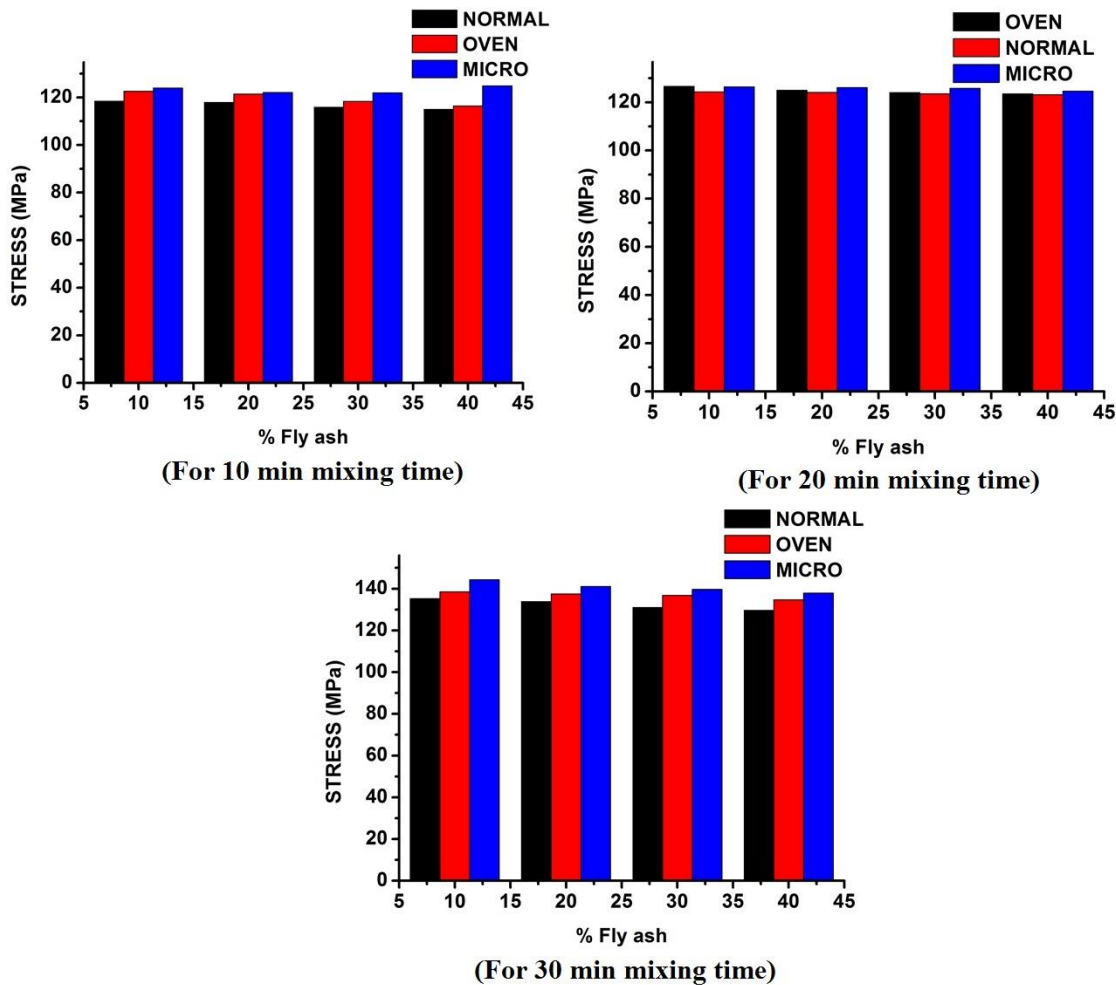


Figure 4.6: Variation of flexural strength with percentage fly ash addition at different curing condition and mixing time.

As curing takes place, there is a change in internal bonding chain structure and favouring the formation of more crystalline regions in the matrix which helps in the inter-particle bonding of fly ash. Modification in the chemical bonding may also be the reason for an increase in flexural strength.

The flexural strength of neat epoxy is found to be 110MPa. Being a ceramic filler fly ash have high hardness and compressive strength. So, from a theoretical point of view, it has a very negligible chance of increasing the flexural strength which is seen from the following

graphs. The flexural strength is found to be maximum 135.26MPa for 30 minutes of mixing (for 10% reinforcement/microwave curing). But after curing, there may be uniformity in its crystallinity which enhances the result and is found to be 144.38MPa.

Figure 4.7 is plotted between percentage reinforcement of fly ash and strain at different mixing times. It is seen from the graphs that strain decreases with increase in the percentage of fly ash irrespective of curing condition.

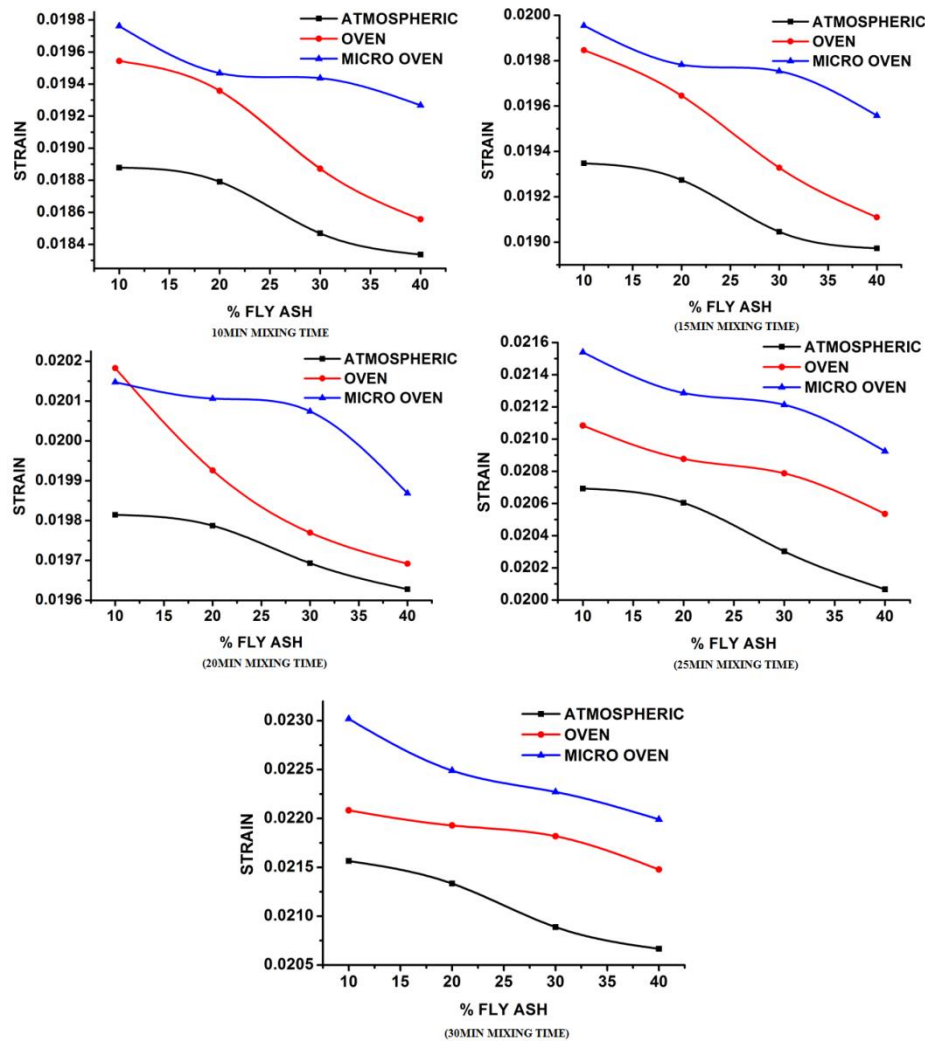


Figure 4.7: Variation of strain with different percentage of fly ash at different curing conditions and mixing time.

The lower value of strain in atmospheric curing conditions is due to its low value of load bearing capacity as compared to oven curing and micro oven curing condition. Strain value is lowered due to high rigidity with higher percentage reinforcement of fly ash.

It is known that deflection of the material can be related to the damping capacity, (of course damping is not under the scope of this piece of research). Figure 4.8 is plotted between the percentage of fly ash reinforcement and maximum deflection at various mixing times.

Maximum deflection (at peak load) follows a decreasing trend with an increase in the percentage of fly ash reinforcement.

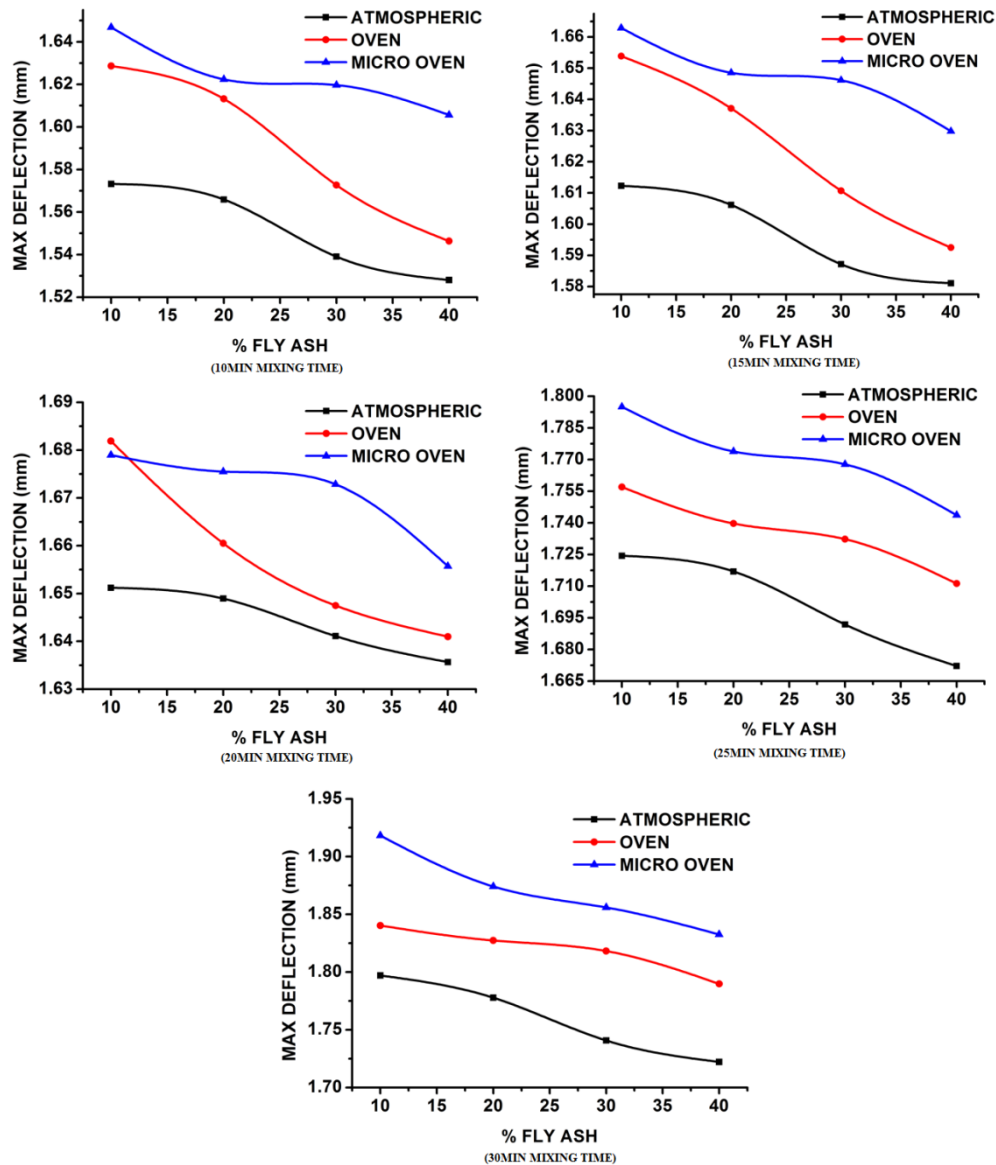


Figure 4.8: Variation of maximum deflection with different fly ash reinforcement for different mixing time and curing conditions.

A maximum deflection of 1.9182mm is obtained for the sample prepared with 10% fly ash and cured in a microwave oven. The decrease in maximum deflection value may be due to increasing the rigidity of the material with percentage reinforcement of fly ash. Deflection for micro oven cured sample found to be higher than that of the oven and atmospheric condition. It may be due to modification and rearrangement of polymer chain structures during post curing operation.

4.1.4 Impact properties

The impact strength of the fly ash reinforced epoxy composite for different curing conditions is plotted in figure 4.9 and figure 4.10. Impact strength was carried out according to ASTM D 256 in VEEKAY TLVS4 impact tester. In figure 4.9, it is observed that the impact strength increased from 1.752J to 1.986J in normal atmospheric treatment, 1.802J to 2.087J in oven curing and 1.821J to 2.124J for microwave curing condition for composite with 10% fly ash reinforcement. Similarly, in 20% fly ash reinforcement composite; the impact strength reaches a maximum value of 1.746J in microwave curing at 30 minutes of mixing time. With 30% addition of fly ash, impact strength varies from 0.761J (atmospheric curing) to 1.425J (microwave curing). For 40% fly ash addition, impact strength increases from 0.619J to 1.042J in atmospheric curing, 0.637J to 1.061J in oven curing and 1.044J to 1.208J in microwave curing condition.

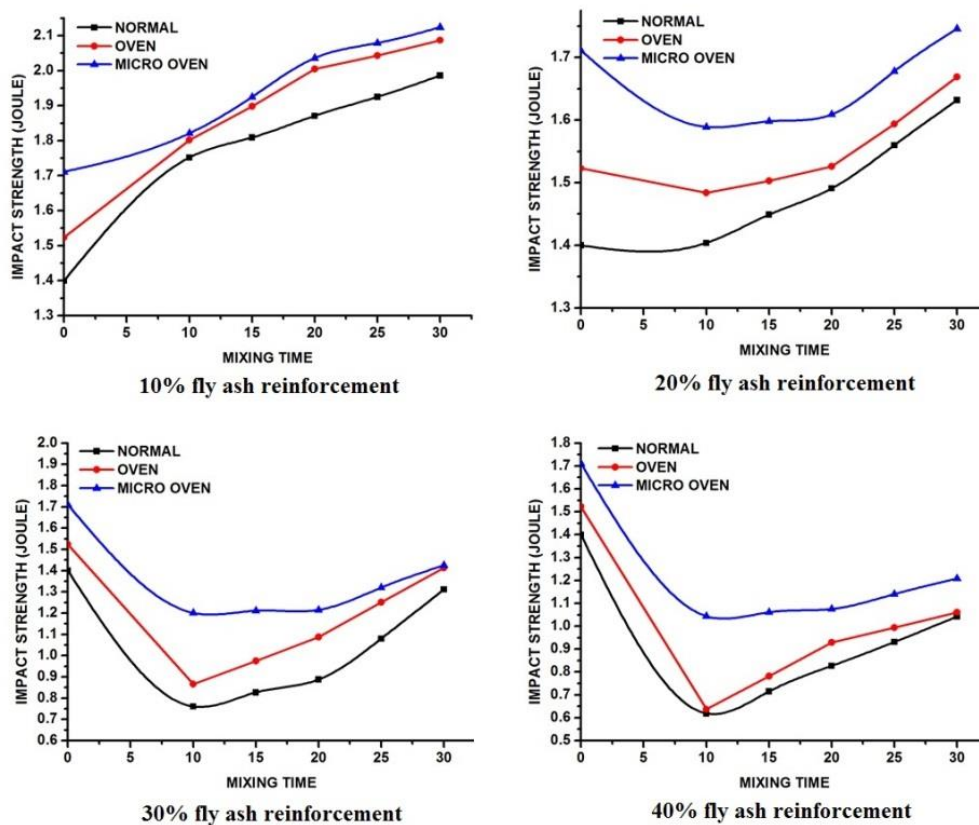


Figure 4.9: Variation of impact strength with mixing time at different curing conditions and percentage reinforcement of fly ash.

The increasing trend of impact strength may be due to uniform grain distribution throughout the epoxy matrix which helps in absorbing the energy. The maximum amount of

energy is absorbed and transferred to the matrix material. So, once there is an increase in percentage reinforcement of fly ash, the continuity of matrix breaks resulting in a decrease in strength which is evident that impact resistance decreases with the percentage of fly ash.

Figure 4.10 shows the effect of curing condition at different mixing times. It is seen that; impact strength varies primarily with the curing condition. It is highest for micro oven curing followed by oven curing and atmospheric curing condition irrespective of time of mixing.

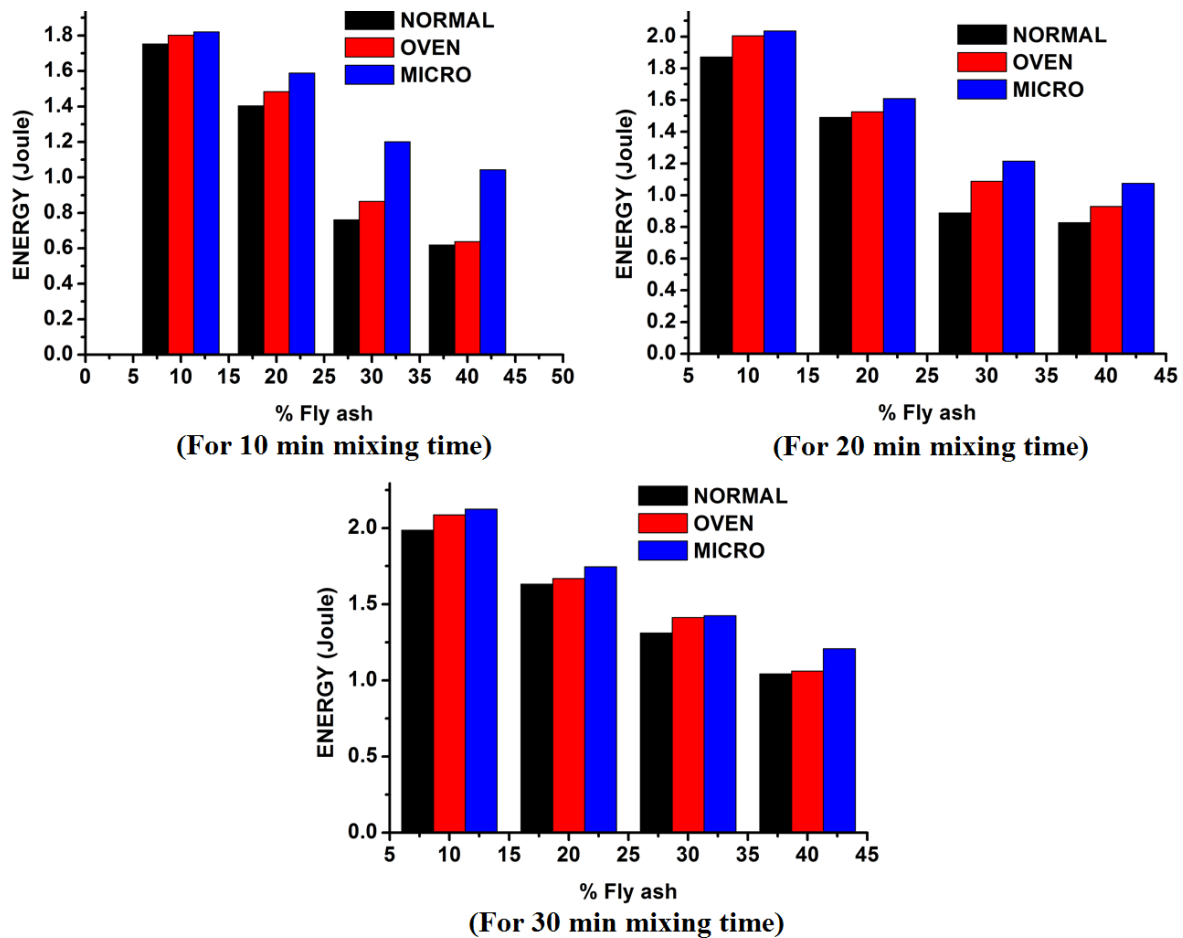


Figure 4.10: Variation of impact energy with percentage of fly ash for different curing conditions and mixing time.

A maximum value of 2.124J of energy is absorbed by the sample prepared with 10% fly ash reinforcement, 30 minutes of mixing time and for microwave curing condition. It may be due to uniform mixing and release of internal stress and/or stretching/bending vibrations occurred during microwave interaction with polymer chains at the above mentioned parametric condition. During microwave oven curing, the energy absorbing capacity increases which are obvious from the figure i.e. figure.4.10.

4.1.5 Microstructural aspect

Fractured samples are observed under a scanning electron microscope for understanding the mechanism of failure.

Surface morphology of the composite

In figure 4.11 (A) the surface morphology of 90%epoxy+10%fly ash composite, some agglomerated zones are seen. That is because of proper interface bonding and uniform distribution of fly ash particles in the matrix material. Figure 4.11 (B) show some fly ash particles which are trapped inside the matrix. These entrapped fly ash particles restrict the flow of stress and act as stress concentration zones and also responsible for void formation/cavitation etc.

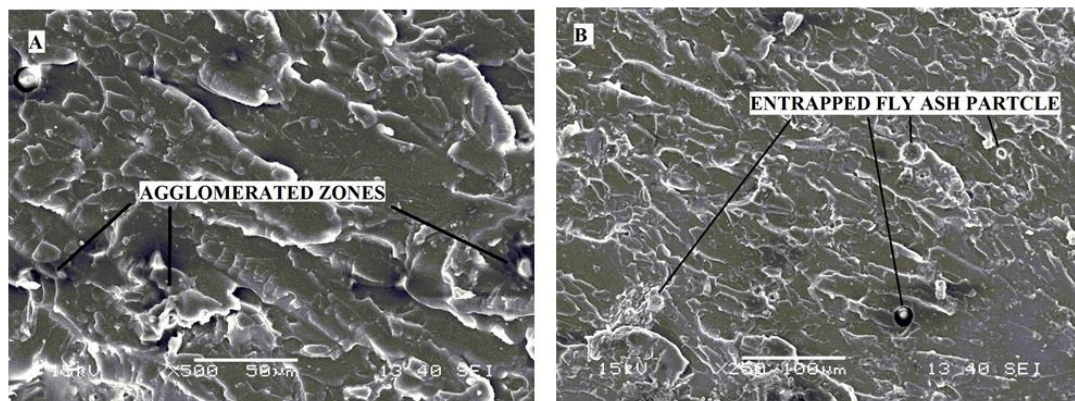


Figure 4.11: Micrographs are showing proper mixing of fly ash and epoxy resin (10%FA+90%EP).

Fracture surface of tensile test specimens

Figure 4.12, fracture surface of the tensile tested specimen, show some crests on the fracture surface. Protruded structures are seen as a result of dislocation of matrix material due to the application of load.

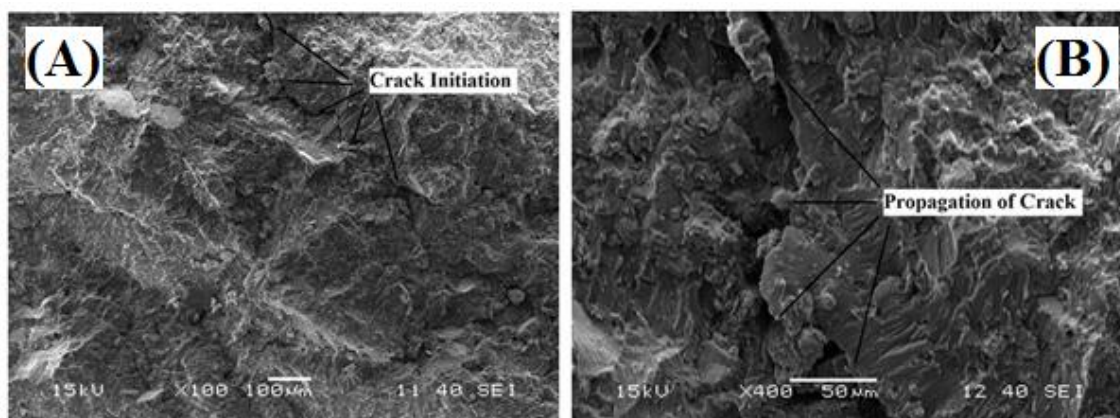


Figure 4.12: SEM micrograph showing initiation and propagation of crack at the breaking point (10%FA+90%EP in microwave curing condition).

When the thermosetting resin is embedded with fibres, there is pull out of fibres from the matrix. But in the case of particle reinforced polymer composite, stress distribution varies from point to point. So the load is mainly taken by the matrix material and then transfers to the reinforced particles. Initially, a small crack is formed/joining of cracks/cavities takes place and propagates along the boundaries of the particles i.e. the stress concentration zones, to the entire area.

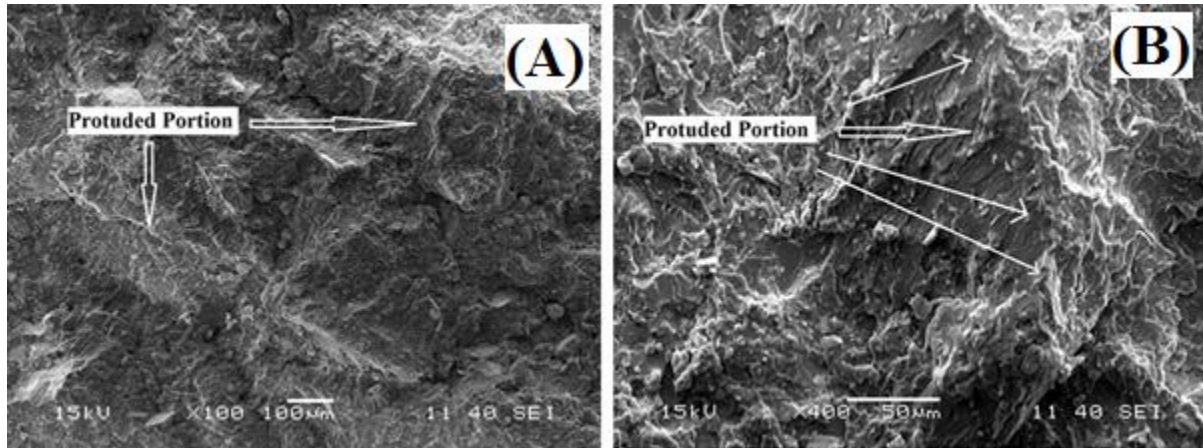


Figure 4.13: SEM micrograph showing protruded a portion of the tensile test specimen (10%FA+90%EP in microwave curing condition).

Fracture surface of flexural test specimens

Figure 4.14 show the fracture surface of the specimen failed with flexural loading. Two different types of morphology are seen which may be due to; in the flexural test, the side of the specimen to which load is applied, faces compressive force and the opposite side face a tensile force i.e. different types of loading conditions occurs on the material. Figure 4.14 (A & B) show the lower portion having protruded regions which face tensile loading and Figure 4.14 (C & D) show the upper part which is under compressive loading. It shows river flow like pattern which is due to matrix flow under loading condition.

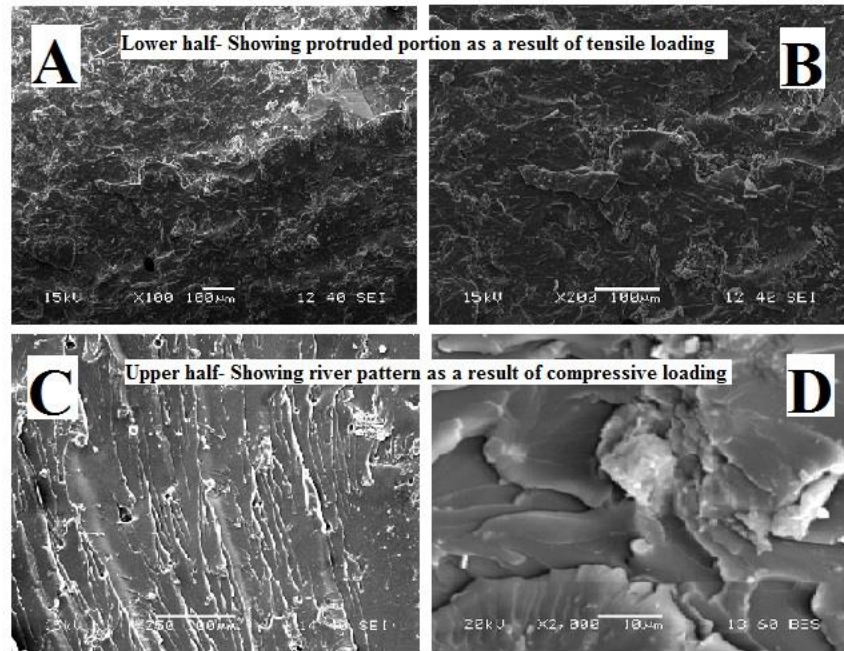


Figure 4.14: SEM micrographs of flexural test samples (10%FA+90%EP in microwave curing condition).

The protruded portion shown is the result of tensile loading while the river pattern in the specimen is the result of compression in the upper half. So, SEM micrograph of flexural testing samples shows both ductile and brittle type of fracture.

Fracture surface of impact tests specimens

Figure 4.15 show the fracture surface of the impact test specimen. It gives the impression of the directional flow of material. The material flows in the direction of applied load. During the impact test, the potential energy stored is converted to kinetic energy and that amount of energy is transferred to the specimen depending on its capacity of energy absorbance, producing a tidal flow/river flow.

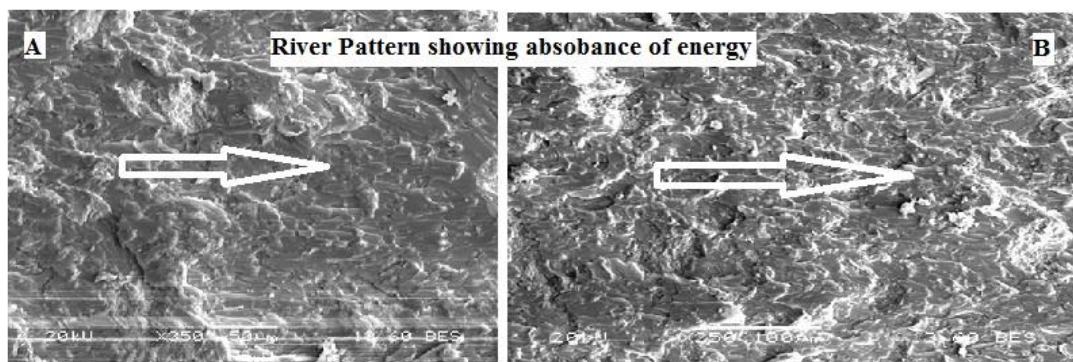


Figure 4.15: SEM micrograph of impact test sample showing the direction of energy flow (20%FA+80%EP in microwave curing condition).

Figure 4.16 (A) show the notch area which is manually made for crack initiation in the impact specimen. The pendulum strikes right at the notch and the crack originates from there. Figure 4.16 (B) show the crater formed at the notch.

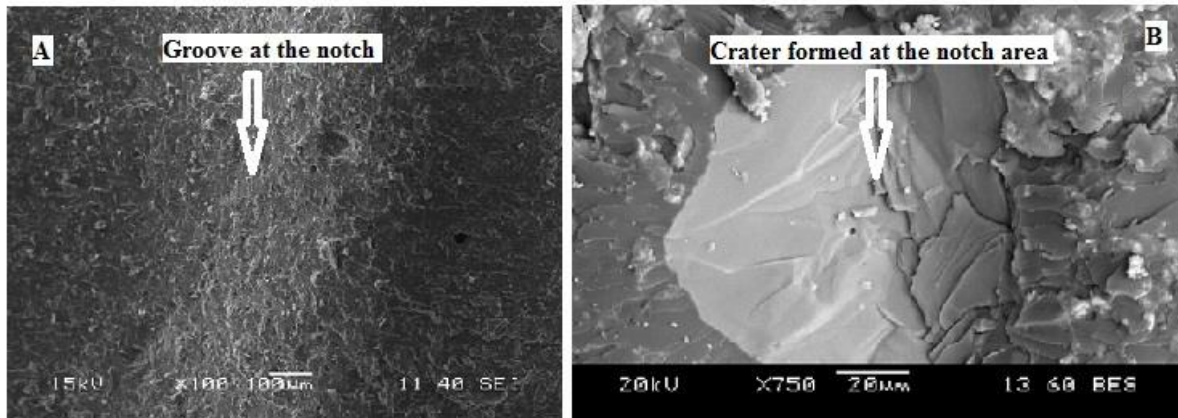


Figure 4.16: SEM micrograph of impact test specimen showing crater (20%FA+80%EP in microwave curing condition).

4.1.6 Differential scanning calorimetry

The glass transition temperatures of various percentages reinforced of fly ash composites made at different curing conditions are determined. DSC analysis of fly ash epoxy composites made at four different weight percentages of reinforcements and three different curing conditions is shown in figure 4.17.

Effect of post curing on T_g

Graphs have been plotted between temperature and amount of heat absorbed. Figure 4.17 (a, b, c) shows the DSC curves for different percentages of fly ash at various curing conditions viz. atmospheric, oven and microwave curing respectively. In all the cases, the T_g is shifted towards lower temperature side with an increase in fly ash content. From the graphs, it is evident that the T_g increases after treatment/curing in the oven and micro oven.

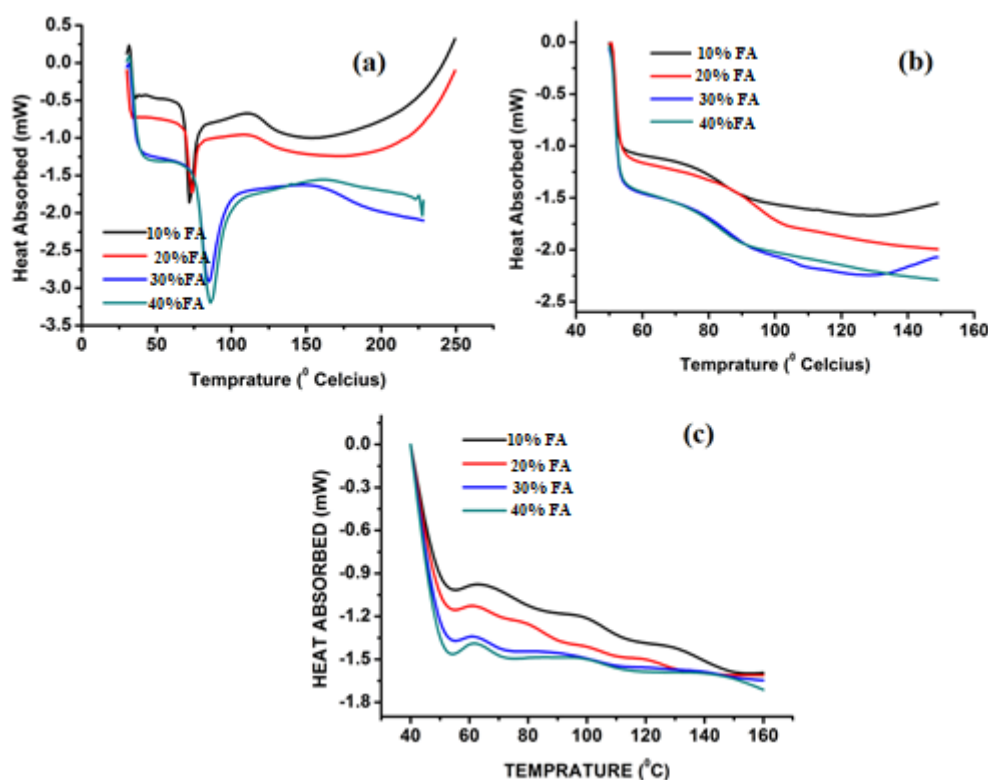


Figure 4.17: Variation of the amount of heat absorbed with temperature for different curing conditions.

The glass transition temperature is the temperature where the material is converted into a glassy state/amorphous material and its properties are changed [142, 143].

Curing of a polymer occurs when individual chains form strong bonds with other neighbouring chains, a process that is sometimes referred to hybridization and/or cross-linking. Like crystallisation, this process of chain ordering and bond formation is exothermic reaction product. The increase in glass transition temperature may be due to main chain rigidity, bulky or rigid side groups, increased cohesive energy density, increased molecular weight and increased polarity and cross-linking. As the T_g increases, the crystallinity increases in the composite; hence microwave cured samples exhibit more strength than others.

4.1.7 Spectroscopic analysis

The effect of curing condition and an increase in reinforcement to the polymer matrix affect the composite properties. Infrared spectroscopy is one of the best tools to analyse the bonding type and mechanism of the polymer composite, which affect the strength properties of the material.

Figure 4.18 shows the IR spectra obtained for atmospheric cured specimens. From the spectra obtained for atmospheric curing condition, shows six numbers of different band patterns and possible chemical bonding and are tabulated in Table 4.1. Similarly, Figure 4.19 (A & B) shows the IR spectra obtained from oven curing and microwave oven curing conditions and possible chemical bonding are tabulated in Table 4.2. In each case, six different chemical bonds with high intensity are indicated which may be the reason of affecting the strength of the material.

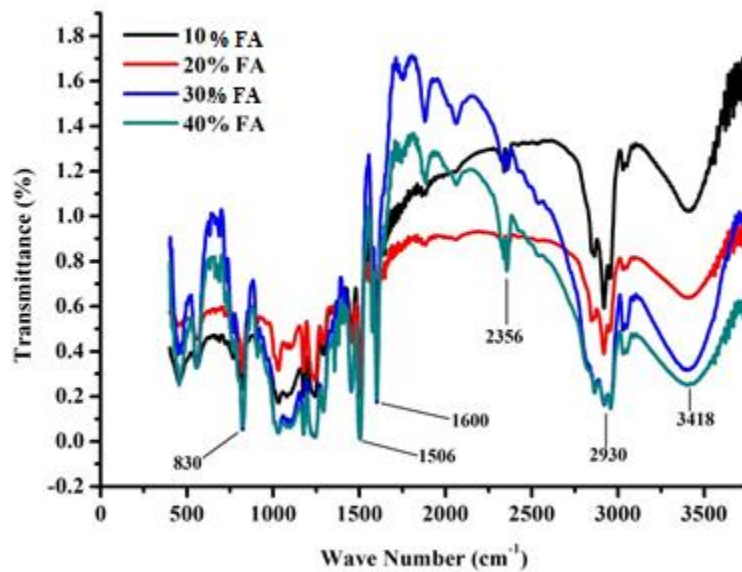


Figure 4.18: FTIR plot between wave number and percentage transmittance for atmospherically cured samples.

Four different lines have been plotted for four different percentage reinforced fly ash composite. Here wave numbers of 830, 1506, 1600, 2356, 2930 and 3418 have been mentioned. The possible chemical bonding in that range is indicated in Table 4.1 below.

Table 4.1: Wave numbers showing possible bonding in atmospheric curing samples.

| Wave Number | Possible Bond |
|-------------|---------------------------------|
| 830 | Aromatic C-H |
| 1506 | C-N=O (Monomer) |
| 1600 | C-N=O (Monomer) |
| 2356 | =NH ₂ ⁺ |
| 2930 | R-C=O |
| 3418 | Crystal water/ -NH ₂ |

Figure 4.19 (A&B) have been plotted for the oven and micro oven cured samples. By comparing the figure 4.18 and 4.19, the wave intensity matches for all the reinforcement percentage of fly ash. Wave numbers match in both the curing conditions but the intensity varies. Out of the four compositions, 40% reinforced composite show some deviations from the other three.

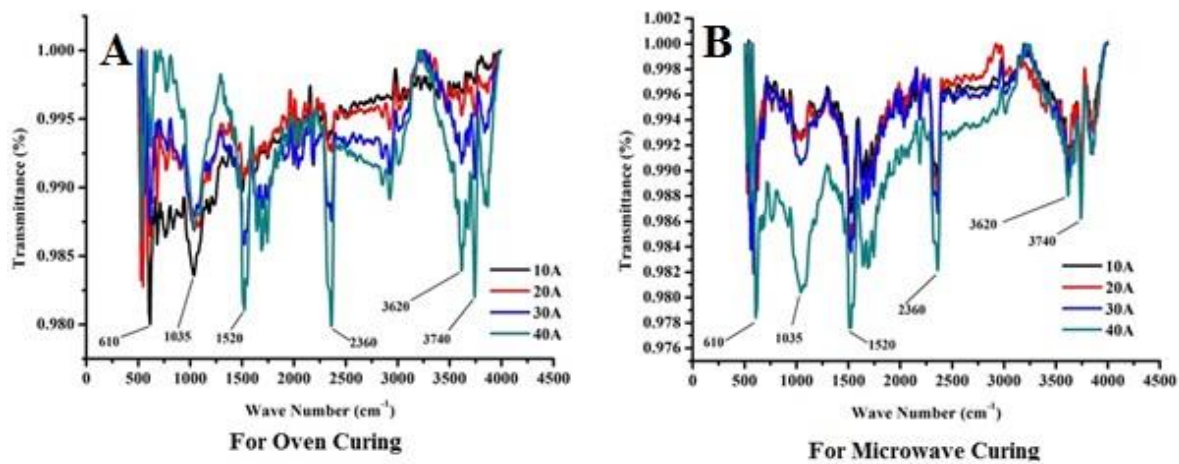


Figure 4.19: FTIR plot between wave number and percentage transmittance for the oven and micro oven cured samples.

Wave number of 610 and 1035 were visible in oven curing for 10% reinforcement of fly ash, but the same wave numbers vanish after micro oven and become visible for 40% of fly ash. Mechanical properties also reveal the change due to curing conditions also. The DSC analysis also indicates that there is a change in glass transition temperature of the material after the material is cured. All the relative properties imply that there must some change in chemical structure of the material. In both the curing condition, there is almost same intensity except the line drawn for 40% of fly ash reinforcement. It may be, as the percentage of fly ash increases, the rate of silicon increases which is tough to cure/not responds to any reaction product/types. Table 4.2 shows the wave numbers and possible bonding in the material. In the case of standard atmospheric curing, the maximum transmittance percentage lies in the range of 0 to 1.8 whereas for other two curing conditions this lies in the range of 0 to 1.0.

Table 4.2: Wave numbers showing possible bonding in oven & micro oven cured samples.

| | Oven Curing | Micro Oven Curing | Possible Bonding |
|------|-------------|-------------------|-------------------------------|
| i. | 610 | 610 | C-Cl/C-Br |
| ii. | 1035 | 1035 | P-O-Alkyl |
| iii. | 1520 | 1520 | C-N=O (monomer) |
| iv. | 2360 | 2360 | =NH ₂ ⁺ |
| v. | 3620 | 3620 | O-H free |

By comparing both tables number 4.1 and 4.2, it is evident that wave number 830 is absent after curing. This implies the stretching of the P-O-Alkyl bond, bending of (=NH₂⁺ and O-H free) bonds and scissoring of C-Cl/C-Br and C-N=O (monomer) bonds. This may be the possible reason of reducing the percentage transmittance.

4.2 Electrical Properties

Epoxy resin is widely used as an insulating material in electrical and other applications. Ceramic fillers are always added to the polymer to enhance its mechanical properties. But at the same time, filler materials decrease the electrical properties. So while making the fly ash epoxy composite, it is obvious to detect the effect of fly ash reinforcement on the dielectric behaviour of the material [144]. The dielectric properties of the composites are measured and described below.

4.2.1 Dielectric constant

Variation of dielectric constant with frequency

Figure 4.20 is plotted between frequency and dielectric constant at various percentage reinforcement of fly ash. It indicates that at lower frequencies dielectric constant decreases at a faster rate may be due to the contribution of the space charge for polarisation, but at higher frequencies, there is decline trend and becomes almost frequency independent may be due to the domination of the ionic and electronic contribution for polarisation.

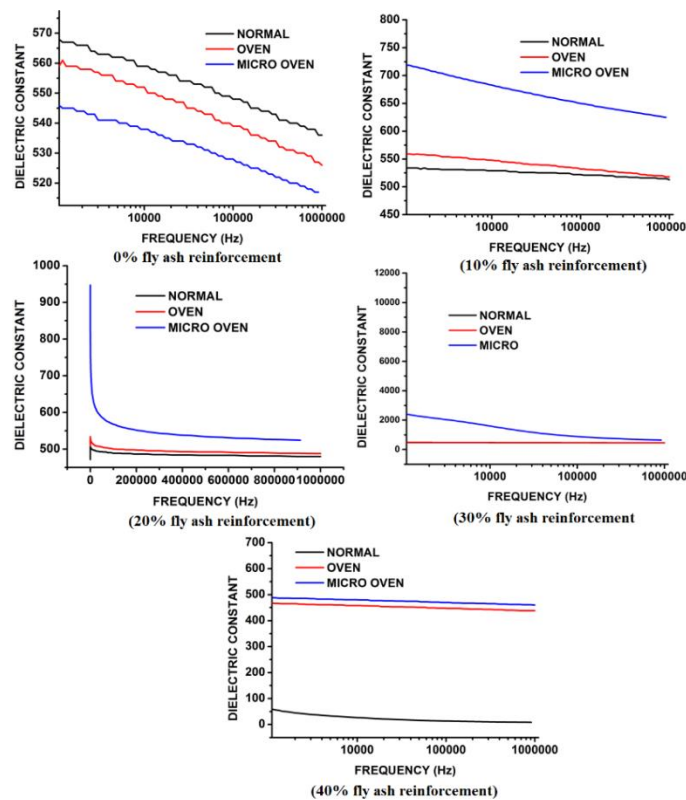


Figure 4.20: Variation of dielectric constant with frequency for different percentage of fly ash reinforcement.

In each figure, three different treatment conditions have been shown. From the figure, it is clear that the dielectric constant decreases with increasing frequency as is the expected behaviour for most of the polymeric materials. As the frequency increases, charges become more random and start to oscillate out of phase with the applied voltage and contribute to the alternating current causing decrease in K value. It is also seen that the dielectric constant is in decreasing order for normal, oven treated and micro oven treated samples only for epoxy resin without fly ash addition, once fly ash added the trend is reversed. It may also be due to the dielectric relaxation which is the cause of anomalous dispersion. At higher frequencies, the orientation of polar molecules along the direction of applied field is disturbed. The charge conveyance controls the dielectric properties of polymers. The polarisation of a dielectric is contributed by ionic, electronic and dipole polarisation. The electric polarisation happens amid a short time of 10-20 sec, however, is more than for electronic polarisation [65].

Free volume is additionally imperative for deciding the dielectric quality of the material. Free volume is resolved as the space that is not possessed by the polymeric material. The free volume connected with one mole of rehashed units of the polymer may be evaluated by subtracting the involved molar volume of rehashed unit [66].

Variation of dielectric constant with curing condition

From the Figure 4.21, it is clear that dielectric constant is decreasing with increase in frequency for a particular percentage of fly ash. A deviation in the trend of the curves is observed at about 100Hz frequency range which is more pronounced for 30% addition of fly ash in the case of atmospheric cured specimens. But in the case of the oven and micro-oven cured samples the deviation is observed at 20% fly ash added specimens.

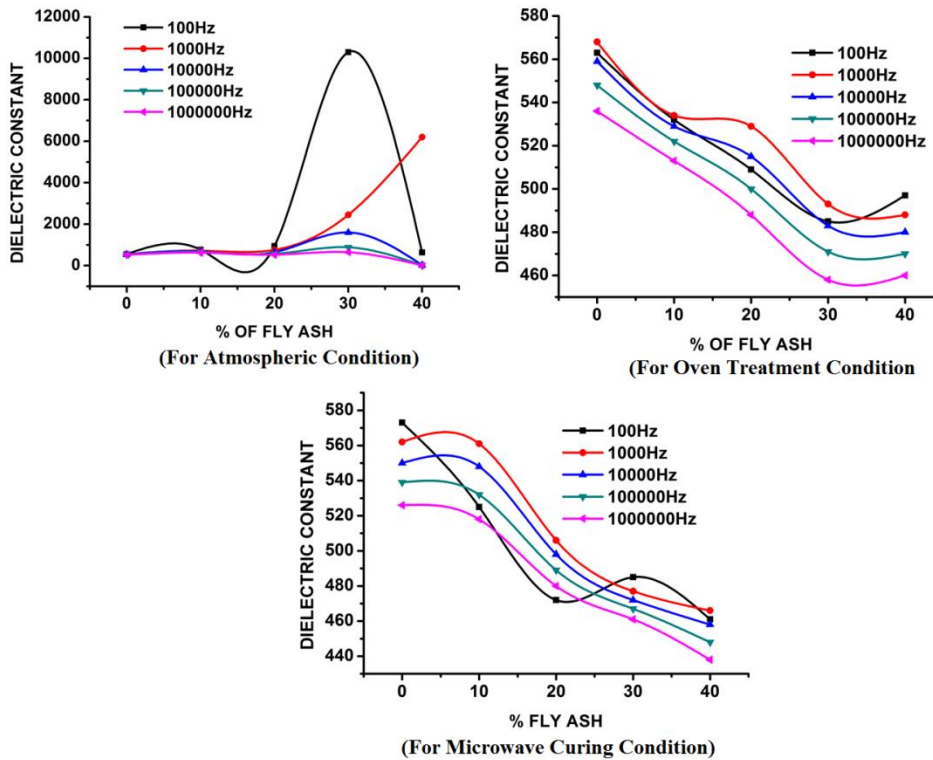


Figure 4.21: Variation of dielectric constant with percentage of fly ash for different curing conditions.

It may be due to the following reasons-

Polymers are known to be a blend of shapeless and sometimes with some crystalline districts. In crystalline regions, the chains are methodical organised. Charge transporters are trapped at the crystalline-formless interfaces make a huge commitment to the dielectric parameters at lower frequencies [67].

The introduction of inorganic fillers having permittivity value higher than the base polymer increases the effective permittivity of the polymer composite due to the influence of filler particles, hence with an increase in filler content, the dielectric constant increases. The dielectric constant of a polymeric material depends on interfacial, dipole, electronic and atomic polarisation. The dielectric behaviour involves different polarisation and the polarisation rate is dependent on temperature and frequency. At low frequencies, the polarisation will have more time to complete compared with that of at high frequencies. Thus, the degree of polarisation of material is high and the dissipation of polarisation is small at low frequencies. The decrease in dielectric constant with an increase in frequency is ascribed to the reason that, the interfacial dipoles have less time to orient themselves in the direction of applied field. It reveals the decrease in dielectric constant with increase in frequency.

The dielectric properties of materials in combination with the applied electromagnetic fields results in the conversion of electromagnetic energy to heat. As polymers and their composites have low thermal conductivity, many of the technical challenges associated with conventional processing also do exist for polymers. As thermosets undergo cross-linking, the dielectric properties change as a result of a change in the network structure. These variations in the dielectric properties correspond directly with resin viscosity also.

4.2.2 Effect of frequency on impedance

Figure 4.22 is plotted between frequency and impedance at various percentage reinforcement of fly ash. There is almost no change in impedance for all types of curing condition irrespective of percentage of fly ash reinforcement.

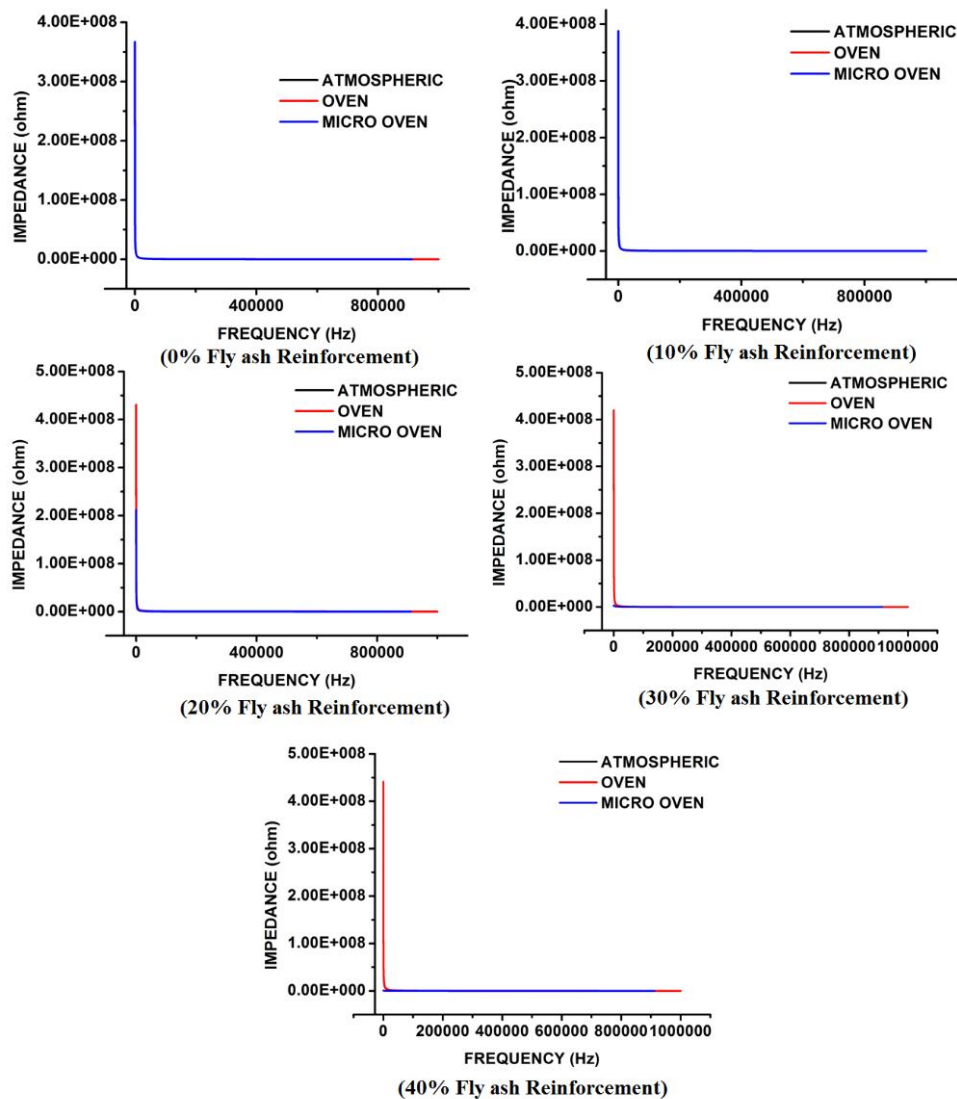


Figure 4.22: Variation of impedance with frequency at different percentage of fly ash reinforcement.

Figure 4.23 plotted between frequency and impedance at various curing conditions viz. on atmospheric, oven and micro oven cured specimens. The graphs show that the impedance remains almost same irrespective of curing conditions.

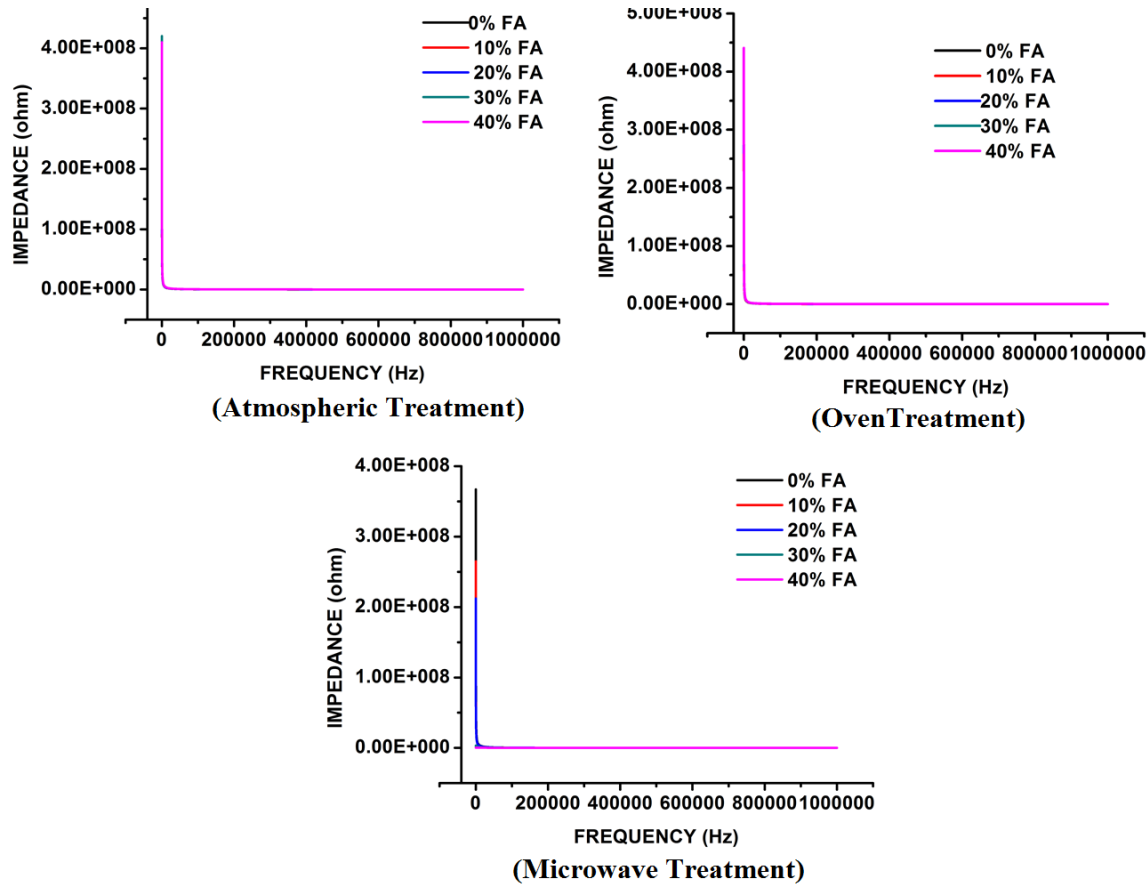


Figure 4.23: Variation of impedance with frequency at different curing conditions.

Impedance is the frequency domain ratio of voltage to current. In other words, it is the measure of opposition that a circuit gives to current when a voltage is applied. So, it is evident from the above graphs that, neither the percentage reinforcement of fly ash nor curing condition alters the resistance to the flow of current.

4.2.3 Effect of frequency on loss factor

Figure 4.24 plotted between frequency and loss factor at different reinforcement percentage of fly ash. It is evident from the figure that, the curing condition has almost no effect on the neat epoxy material but, once the fly ash is added there is an alternation in its loss factor. The loss factor decreases drastically with the addition of fly ash which is evident from the graph. The loss factor is maximum for micro oven cured samples followed by the oven and atmospheric cured samples.

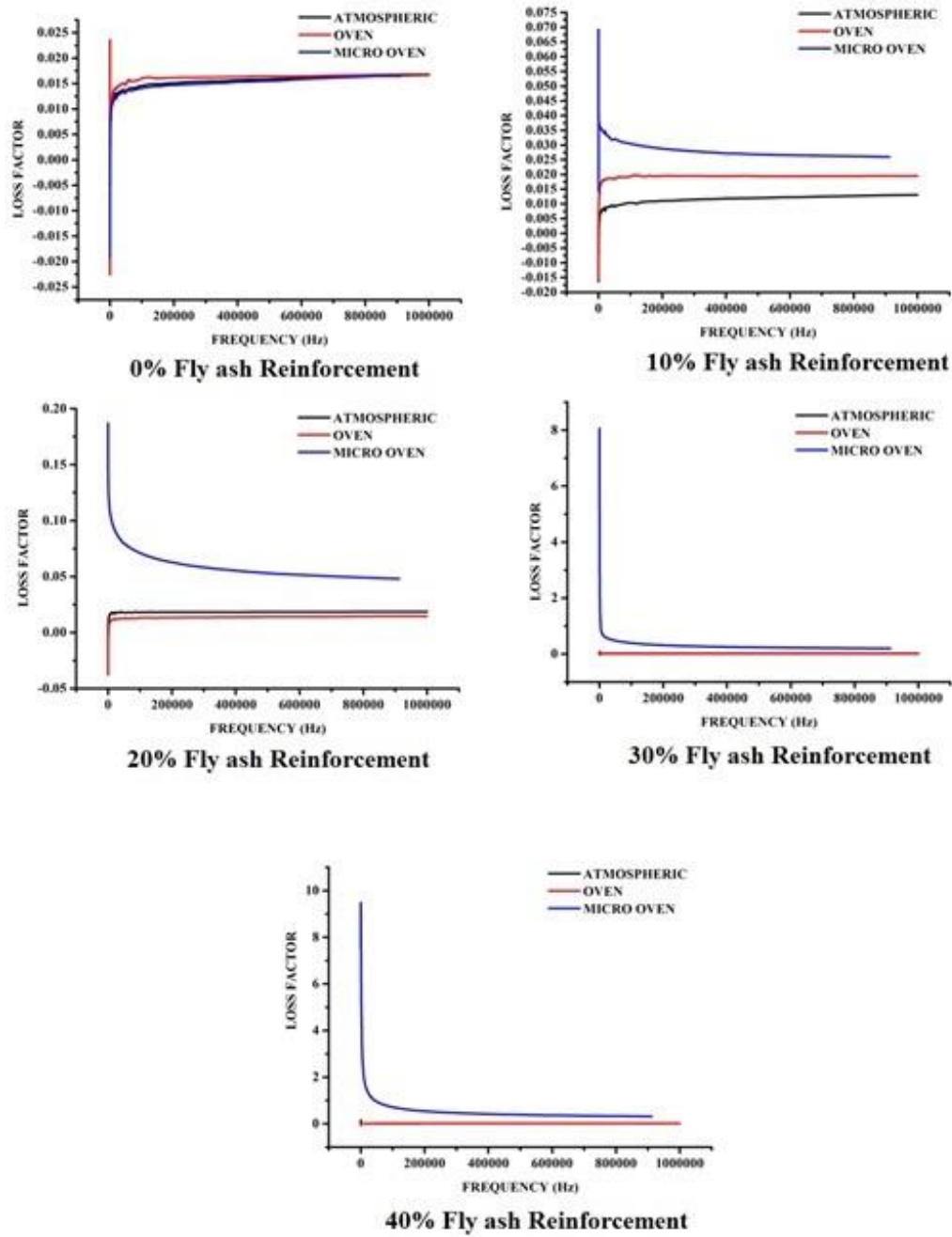


Figure 4.24: Variation of loss factor with frequency for various percentage reinforcement of fly ash.

Figure 4.25 is plotted between frequency and loss factor for samples with different curing conditions. The loss factor trend to increase immediately and remains constant at higher frequencies in case of atmospherically and oven cured specimens. Whereas, a reverse trend is observed in the case of microwave-treated samples. Dielectric loss quantifies a dielectric material's inherent dissipation of electromagnetic energy (and is beyond the scope of this research project to analyse this effect).

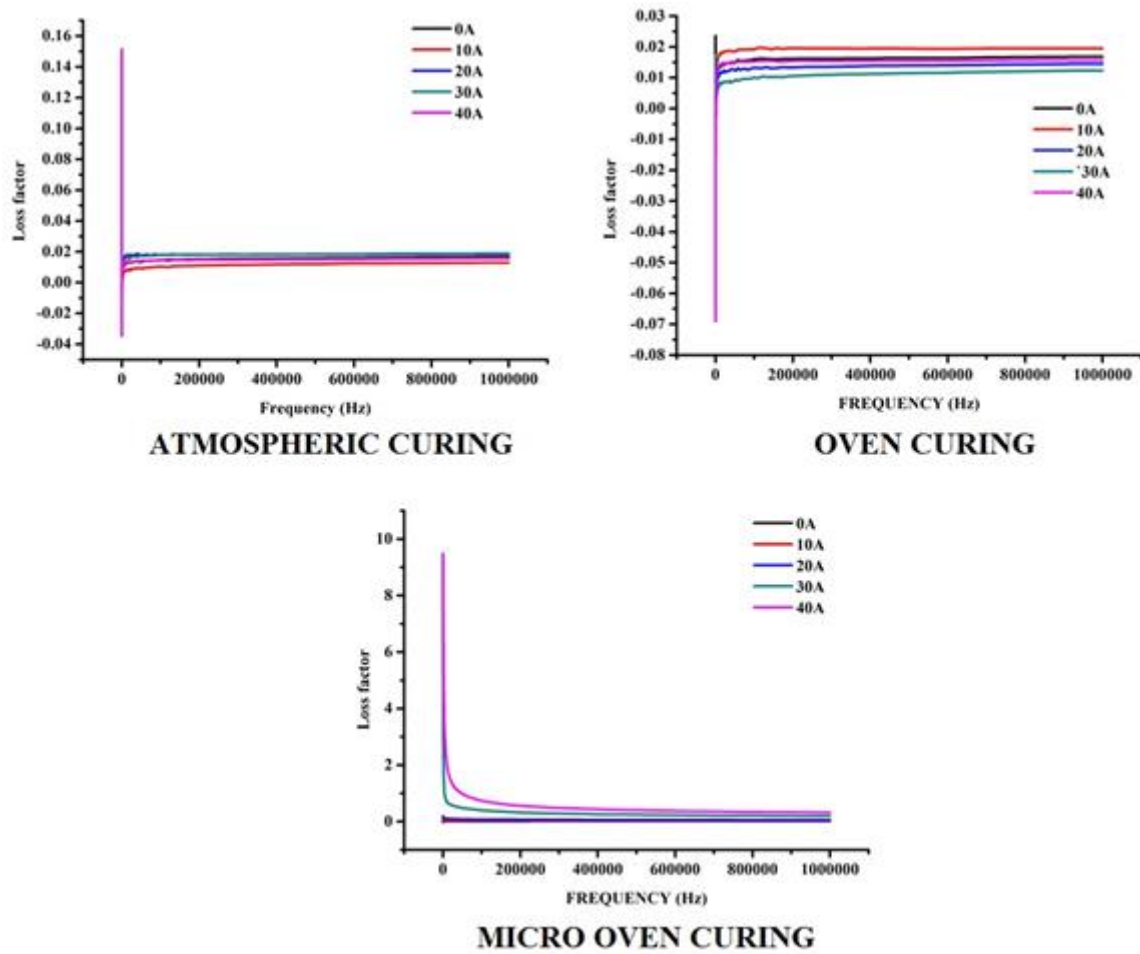


Figure 4.25: Variation of loss factor with frequency at different curing conditions.

4.2.4 Effect of frequency on resistance

Figure 4.26 is plotted between frequency and resistance for different percentage reinforced fly ash epoxy composite. At 0 % fly ash reinforcement i.e. neat epoxy has a very low value of resistance, but once the fly ash is added, resistance is increased. Resistance is found to be increasing with increase in fly ash addition.

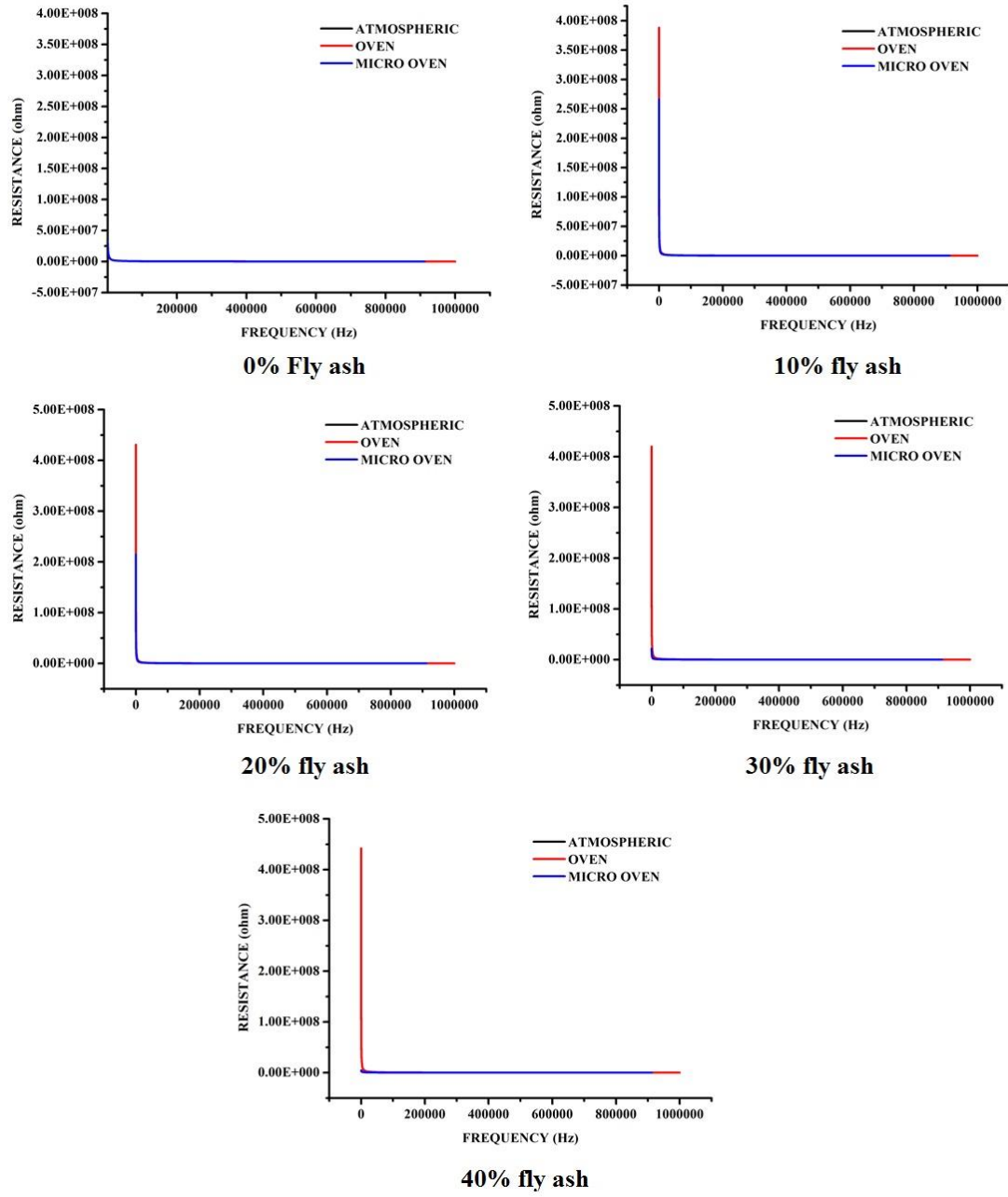


Figure 4.26: Variation of resistance with frequency for different fly ash percentage.

Figure 4.27 is plotted between frequency and resistance of the material at different curing conditions. Results show that curing has no effect on the resistivity of the composite.

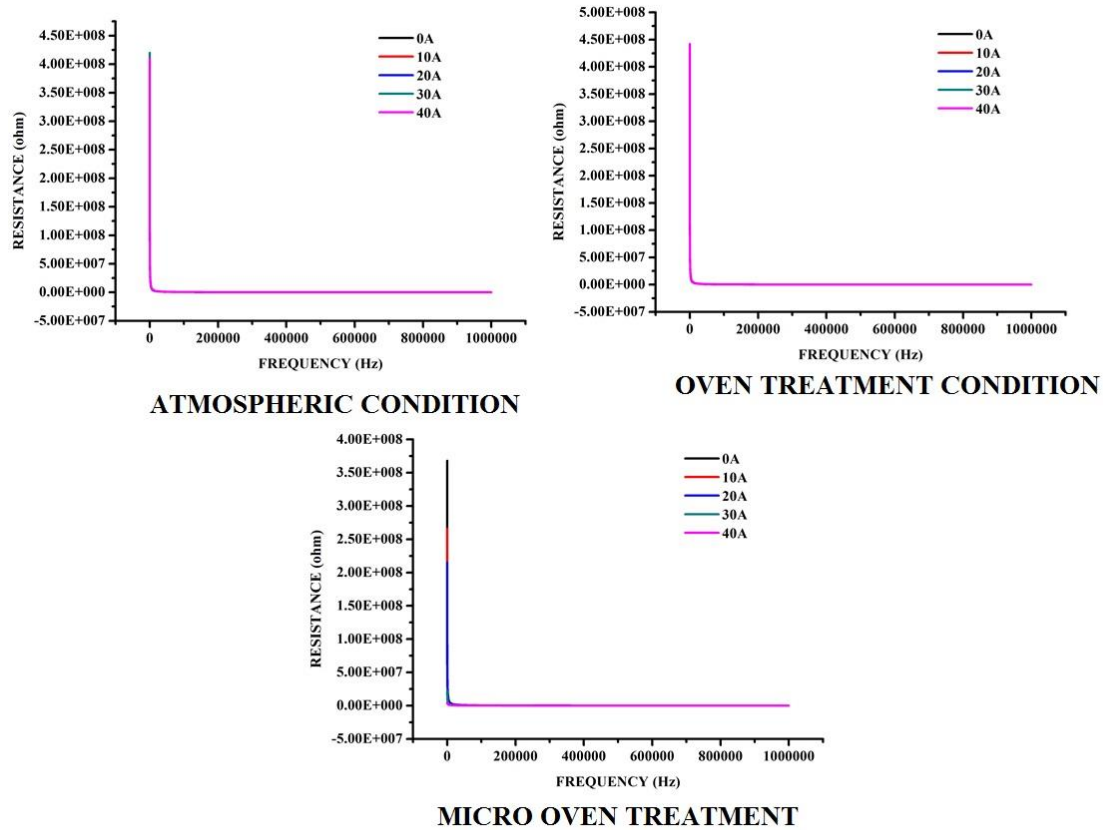


Figure 4.27: Variation of resistance with frequency at different curing conditions.

In simple words, the electrical resistance is the measure of the difficulty/obstruction to pass the electric current. Figure 4.26 clears that, there is no extra resistance force acting with the increase in the percentage of fly ash addition. Curing conditions also have no effect on resistance.

4.2.5 Effect of frequency on capacitance

Figure 4.28 is plotted between frequency and capacitance at various percentage reinforcement of fly ash. In each figure, three different treatment conditions have been mentioned. At 0% fly ash reinforcement, the capacitance of atmospherically cured samples is more than an oven and micro oven cured specimens. But once the reinforcement is added, it reverses its order i.e. capacitance of micro oven cured samples are more than oven cured and atmospherically cured samples.

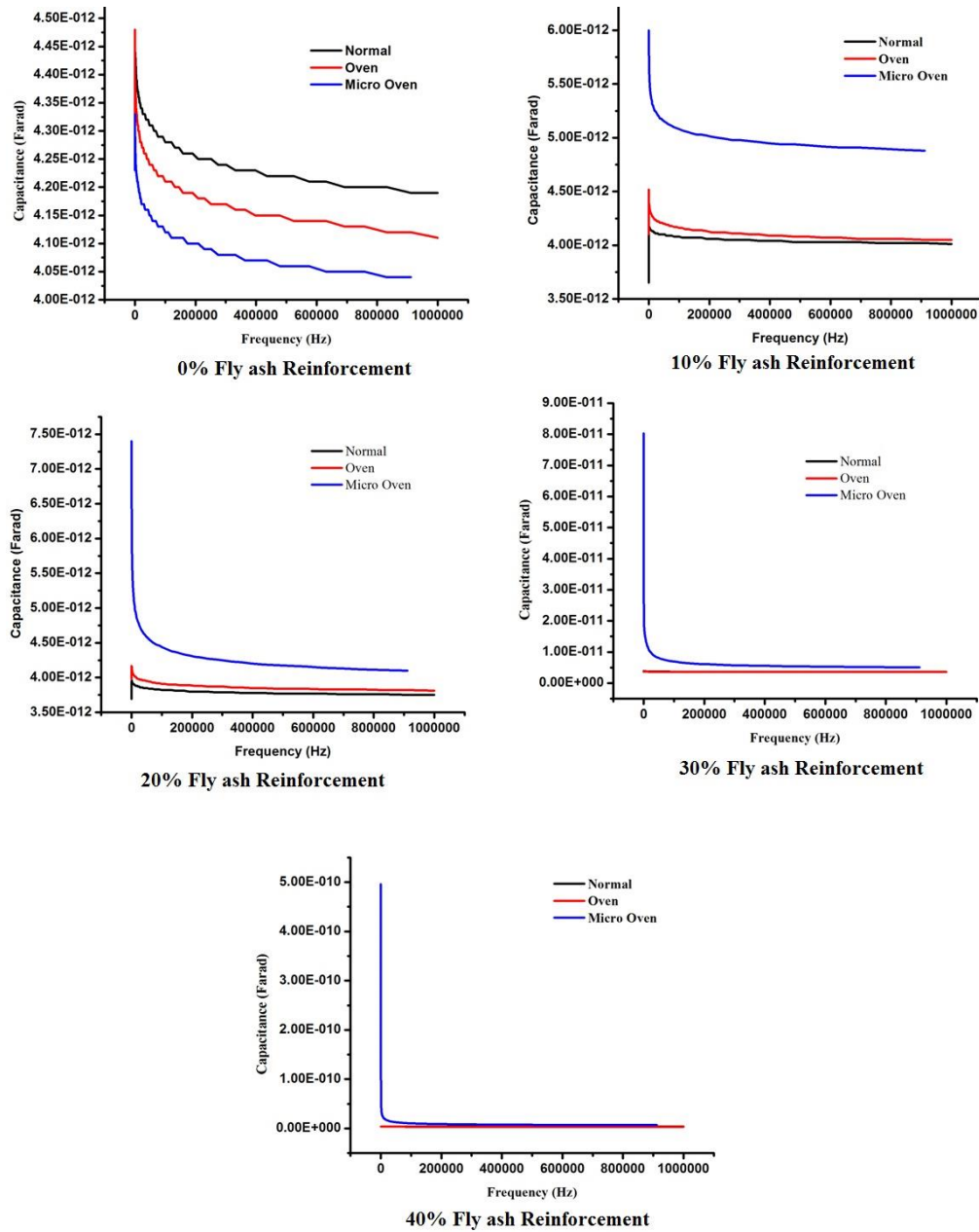


Figure 4.28: Variation of capacitance with frequency for different percentage reinforcement of fly ash.

Figure 4.29 is plotted between frequency and capacitance at various curing conditions. It is clear from the graphs that, capacitance decreases rapidly at lower frequencies than at higher frequencies. It is also evident that, with the addition of fly ash, capacitance decreases. For micro oven curing, capacitance remains unaltered irrespective of percentage fly ash reinforcement.

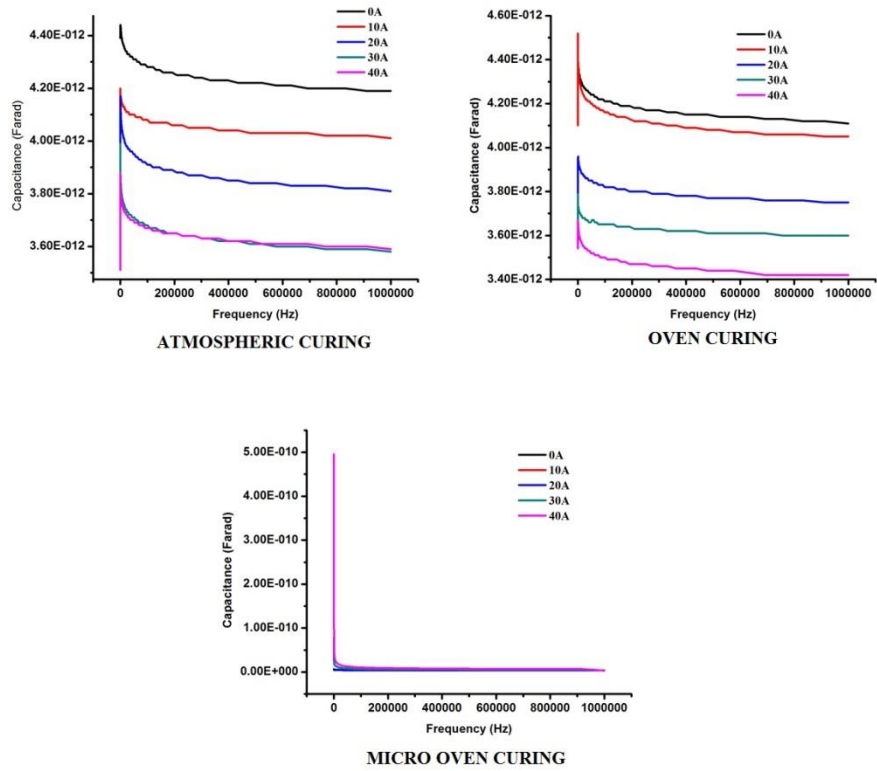


Figure 4.29: Variation of capacitance with frequency at various curing conditions.

4.3 Corrosion Behaviour

In both aerospace and other sectors, which include marine, civil infrastructure and energy, environmental conditioning operating environment is a major concern for durability and efficiency. In such applications, materials are often required to function in service conditions that involve exposure to multiple factors that causes ageing in polymeric composites, including high/low temperatures, environmental conditions, moisture, UV rays and oxidation, etc. In marine applications, ageing mechanisms include differential swelling, residual stress relaxation and hydrolysis [145]. Cracking, creep, leaching, post-crystallization and even biodegradation may occur simultaneously. Vinyl ester reinforced with carbon fibre composite finds its main application in marine industry. The Marine environment consists of simultaneous action of UV rays and moisture. UV rays alter the chemical structure of the polymer and moisture cause deeper damage in polymers by affecting the matrix and the reinforcement simultaneously [146].

Common practice in ageing research is to increase exposure temperature to accelerate moisture ageing because low/room temperature ageing requires long times to cause observable changes in properties. Hydrothermal ageing causes substantial changes to polymer composites often limiting service life and restricting applications. Physical ageing occurs regardless of moisture level [147]. The long-term behaviour of composite materials may be affected by physical (change in T_g) and chemical (change in molecular, oxidation, change in density of reticulation). It is a structural relaxation process and a movement towards equilibrium state in which the free volume shrinks. The capabilities of polymers in combination with other materials to form new, synthetic structures of improved mechanical properties, has led to a real expansion in the employment of composite material. The main disadvantage of these polymeric materials is that these are not cost effective when compared to conventional materials for emerging applications like rehabilitation of civil engineering structures and oil industry.

In actual use of any material, only one side is exposed to the environmental condition. But here the samples are completely dipped inside different mediums and it's tensile, flexural and impact strength has been evaluated on time of treatment. The mechanical property of any composite material is the most relevant property to be evaluated since it determines the utility of the composite as a structural material. Structural materials require strength, stiffness and toughness.

4.3.1 Variation of weight

Figures 4.30 show the change in weight of specimens dipped in different mediums for different time periods. From the figure, it can be concluded that 40% reinforced fly ash composites have the highest weight change and maximum weight gain is observed with basic solution dipped samples followed by an acid solution, sea water and fuel immersed specimens.

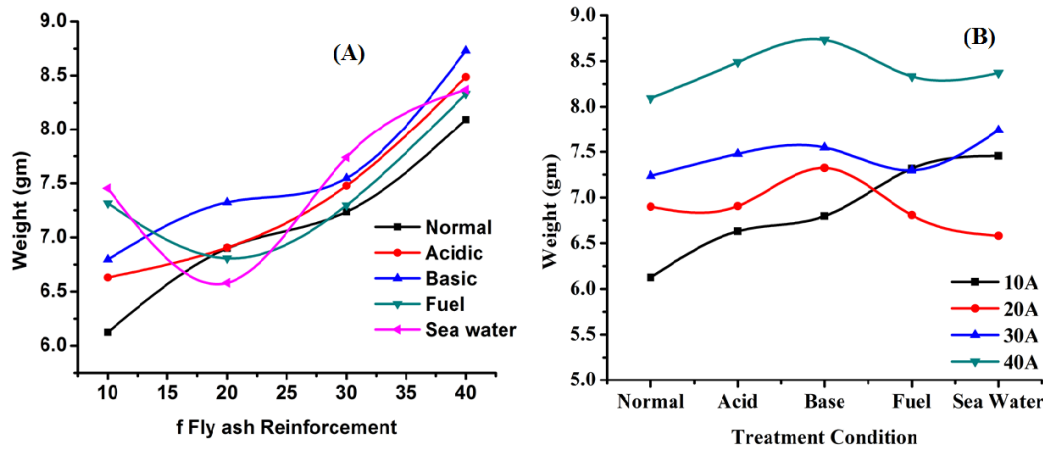


Figure 4.30: Variation of weight with different fly ash percentage, treated in different environmental condition.

When the samples are immersed in the fluids, the fluids enter inside the material through the microcracks and pores. Once they enter inside, there is swelling in the matrix and increasing in weight of the sample. Again, these swelling portions act as stress concentration zones during application of load.

As the samples are immersed in the solution medium, the solution is absorbed into it. The water absorption in weight percentage (Wt. %) can be calculated by using the following equation (4.1).

$$\text{Wt. \%} = \left(\frac{\text{CWW} - \text{DW}}{\text{DW}} \times 100 \right) \quad 4.1$$

Where DW= Dry weight

CWW= Current wet weight

Figure 4.30, indicates that 10% weight samples vary enormously and it is maximum in case of sea water. It may be due to the effect of other ionic minerals present in the sea water. The ionic minerals must have struck over the samples resulting in the increase in sample weight. The reason for an increase in weight may be due to the high percentage of silica, which absorbs water through micro cracks. These micro cracks act as capillary tube helping the solution entering to the core of the specimen [146].

4.3.2 Change in surface morphology

In normal working condition, only one surface of the sample is exposed to the environmental situation. So, degradation takes place only from that side only. But, in this experiment, the total sample is immersed in the solution. So, degradation starts simultaneously from all the sides of the specimen.

It has been observed that basic solution corrodes more than any other solution. So, SEM micrographs have been taken of the basic solution treated samples. In figure 4.31, the degradation is marked, i.e. the sample surface is roughened by the solution attack. Due to high stiffness and high aspect ratio of polymer composites, these are better resistance to electrochemical corrosion as compared to metals.

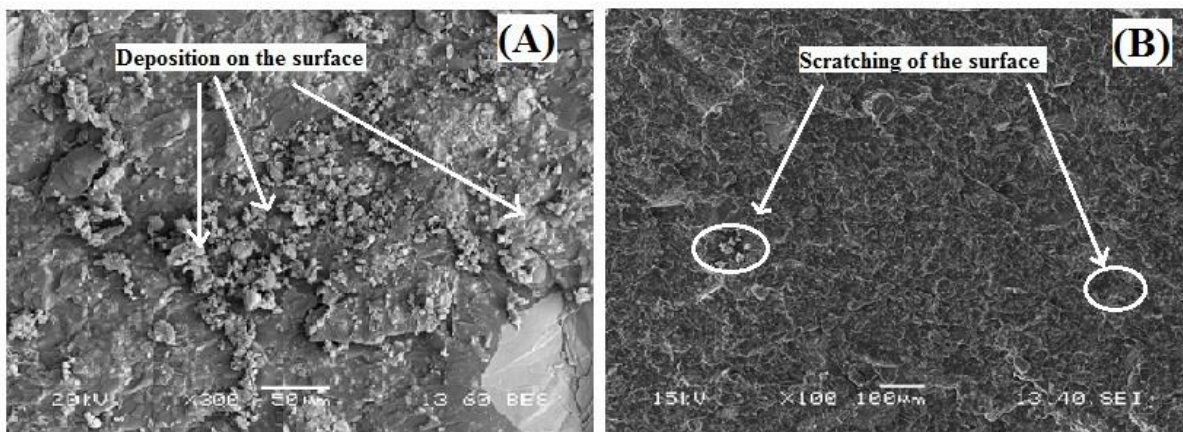


Figure 4.31: SEM micrographs showing deposition of materials in sea water (40%FA+60%EP).

Figure 4.31 show some deposition of salt materials on the sample surface during the exposed time. The amount of deposition on the surface increases the weight of the sample and in the long term, this deposition may help in developing an additional coating on the surface of the sample. Moisture causes deeper damage in polymeric materials. Due to initial scratching on the surface of the sample, moisture diffuses into through plasticization process and hydrolysis takes place, reducing the strength of the composite.

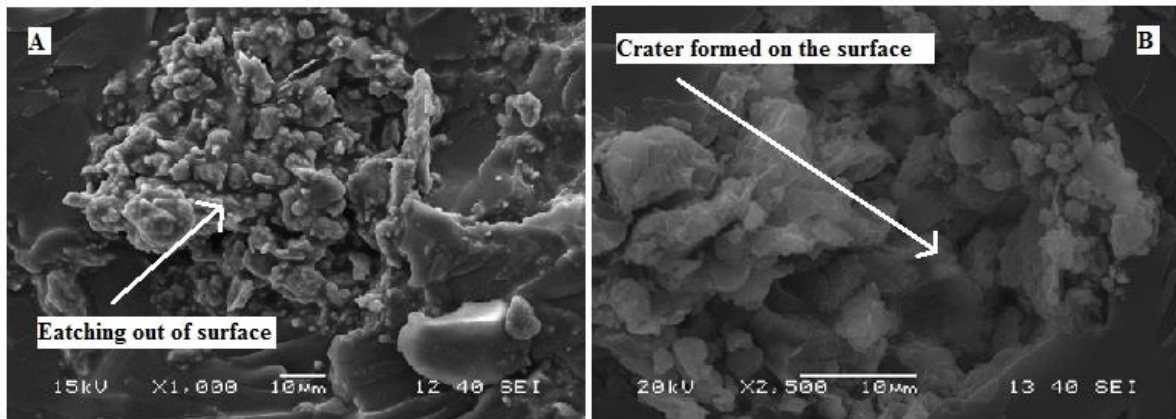


Figure 4.32: SEM micrographs showing crater and etching of surface in the acid solution treated specimen (40%FA+60%EP).

Figure 4.32 show etching and cavity formed at the surface of the sample in acid solution. It may be due to the reason that the acidic environment dissolves the alkali and alkali earth metals (present in traces in fly ash) and at the same time, it extracts aluminium and boron that is present either in the matrix or reinforcement. This extraction leads to the formation of a crater on the surface of the sample.

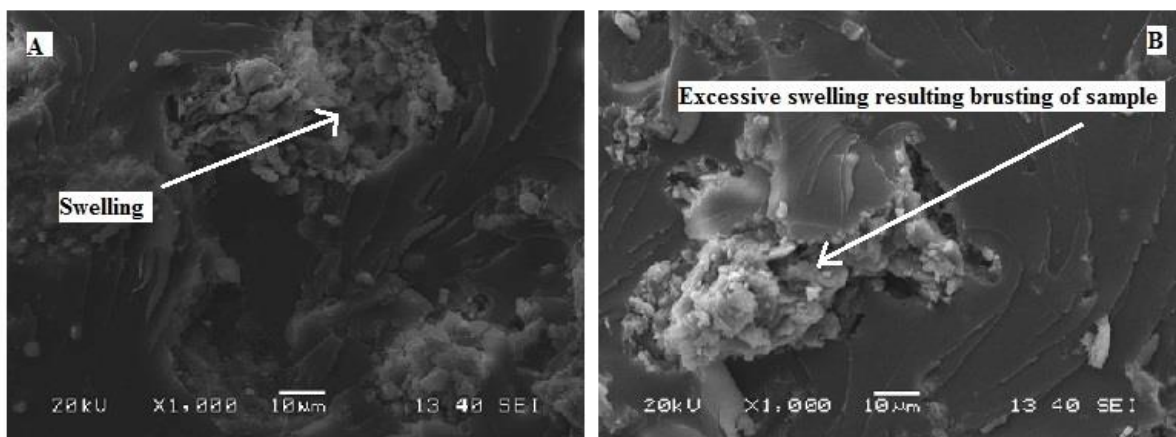


Figure 4.33: SEM micrographs showing swelling of the sample in sea water (40%FA+60%EP).

Figure 4.33 show degradation of the sample surface. Usually, deterioration of the fibre matrix interface is caused by matrix dehydration/swelling, as well as penetration of the solution through micro cracks. Polymers absorb water and the amount of water absorbed depends on their structure, the degree of crystallinity and polarity of molecules.

Once the moisture diffuses into the polymer matrix and gets attached to the fly ash particle, it shows pozzolana effect. So, there is swelling of the sample and ultimately that particular point bursts causing the crack initiation and propagation in the material. The greatest influence of water is the matrix that swells. In this way, the interface between the

matrix and reinforcement is weakened and an inhomogeneous stress originates/results[145, 146].

4.3.3 Tensile properties of different environmentally treated samples

The tensile test is carried out using INSTRON 1195 for the samples prepared according to ASTM D 638 and treated for a maximum period of 28 days in different environmental conditions. Their properties have been evaluated in every seven days interval. Each data point is the mean value of five tests with maximum 5% deviation.

Figure 4.34 (A, B, C & D) have been plotted between time dependence of tensile strength for samples treated with four different types of solutions. Four different graphs have been plotted for four different percentage of reinforcement of fly ash. It is evident from all the figures that the tensile strength decreases with increase in time duration. For 10% fly ash reinforced composite, tensile strength varies from 90MPa to 77.69MPa in acid solution, 89.62MPa to 75.06MPa in basic solution, 90.01MPa to 88.25MPa in fuel and 91.03MPa to 86.22MPa in sea water; for a maximum duration of 28 days. Similarly, for 20% fly ash reinforced composite tensile strength varies from a maximum value of 83.13MPa in fuel to minimum value of 74.59MPa in basic solution. In the case of 30% and 40% fly ash reinforced composite, it follows the same trend of decreasing in its value.

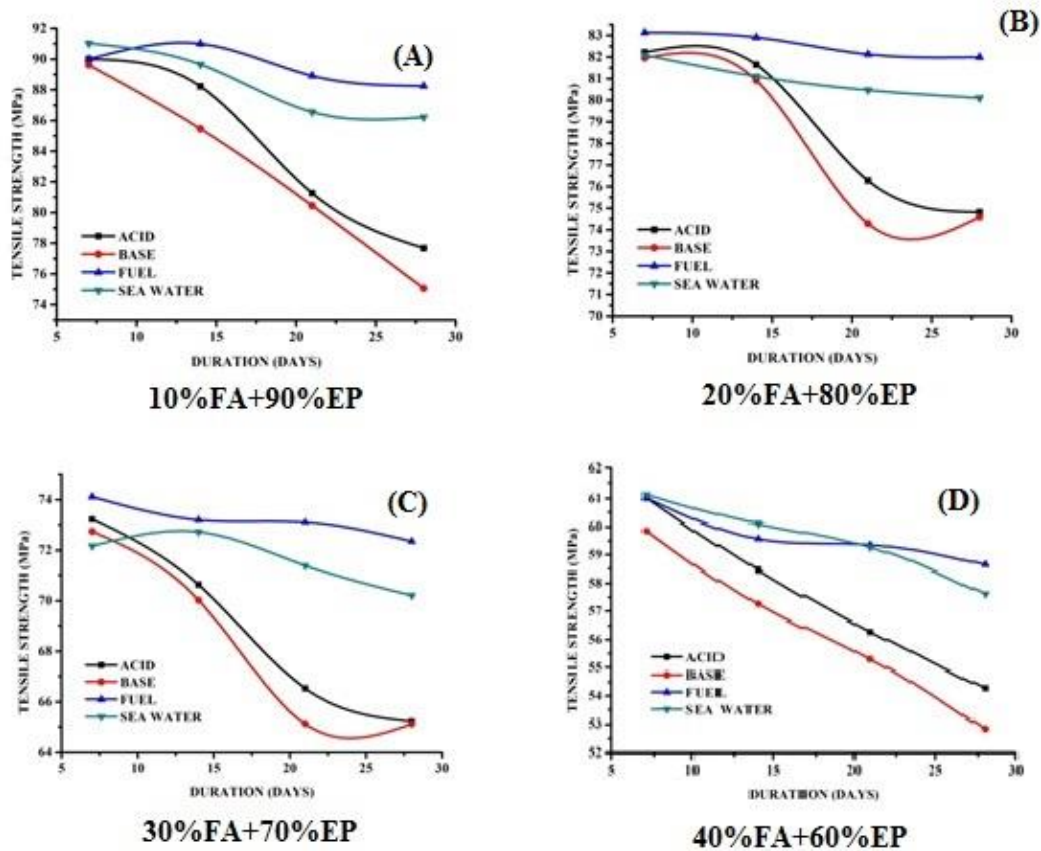


Figure 4.34: Variation of tensile strength with duration time (A) for 10% fly ash (B) for 20% fly ash (C) for 30% fly ash (D) for 40% fly ash reinforcement.

The basic solution is found to be most effective for the degradation of tensile strength followed by an acid solution, sea water and fuel. For 40% reinforced fly ash composite, a minimum value of 52.84MPa is obtained for the sample treated in basic solution for a maximum duration of 28 days. There is some increase in tensile strength of 20% and 30% reinforcement of fly ash after it is treated in basic solution. It may be due to formation/deposition (of some newly formed material) on the surface of the specimens.

The decrease in tensile strength may also be attributable to the presence of voids and microcracks. With the increase in dwelling time in the solution, the solution in which it is immersed enters into the composite by capillary action which leads to matrix expansion and failure of the material. Increasing the volume fraction of filler material in a composite helps in increasing more particle/matrix interfacial area for reaction. Thus, more energy can be dissipated at/by the interface.

Figure 4.35 shows the variation of percentage elongation in tensile tests at various days of treatment. The percentage elongation is found to be decreasing with increase in percentage fly ash reinforcement. During the treatment process, there is a change in its

internal properties so as the modulus of the material that impacts/responsible for the strength and the percentage elongation of the material. Elongation percentage is found to be maximum for the 10% reinforced fly ash composite in sea water immersion for seven days. It reaches a minimum value of 1.68 for the sample treated in basic solution for 28 days. Percentage elongation is the minimum for basic treated samples followed by acid, seawater and fuel treated samples.

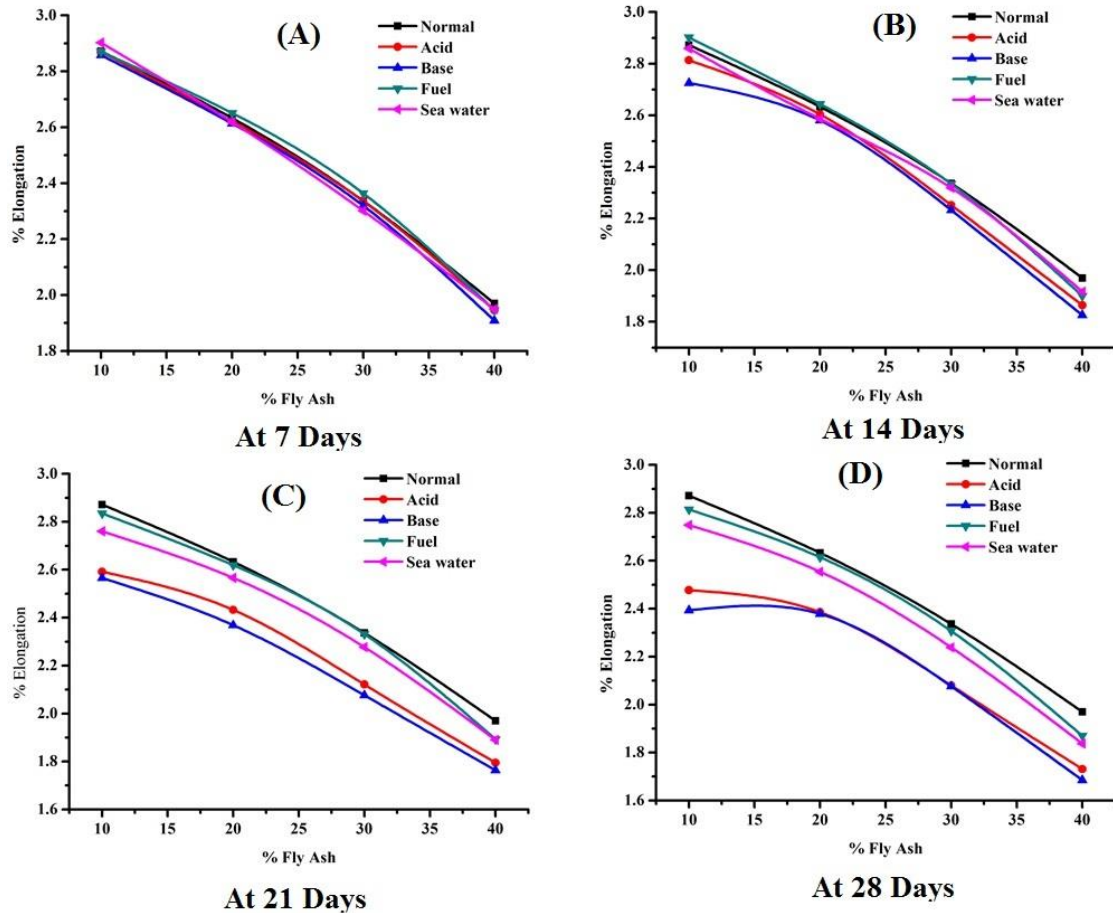


Figure 4.35: Variation of the percentage elongation with different amount of fly ash reinforcement for different durations.

Due to change in modulus of the material, percentage elongation decreases sharply. From the figure 4.35, samples treated in basic solution found to have the least resistance towards the elongation of the material whereas fuel treated samples have maximum elongation towards the application of tensile load. As the immersion time is increased, the interaction between water and epoxy resin became complex. The water existed as a viable resin/fluid binding complex and promoted secondary crosslinking with hydrophilic groups in

epoxy resin (hydroxyls & Amines), or the water stayed in the micropores even causing the micro cracks.

It is known that the mechanical properties of composites are closely related to their structure and the macroscopic failure modes are even more dependent on microscopic damage mechanisms.

4.3.4 Flexural properties of different environmentally treated samples

Figure 4.36 have been plotted between flexural strength and duration of immersion in four different types of liquid solutions. For 10% reinforced fly ash composite, it decreases from 134.96MPa to 120.54MPa in acid solution, 135.11MPa to 120.11MPa in basic solution, 135.98MPa to 131.42MPa in fuel and 137.22MPa to 131.05MPa in sea water for a maximum duration of 28days. Similarly, for 20% reinforced fly ash composite it varies from a maximum of 131.59MPa in sea water to 122.02MPa in basic solution. For other two reinforcement percentage of fly ash, it follows the same trend of decreasing. Here basic and acid solutions have found to have a dominant effect in reducing the flexural strength. Sea water and fuel also show a decreasing trend in flexural strength but at a lower rate. Fuel has the least impact on the flexural strength of the material.

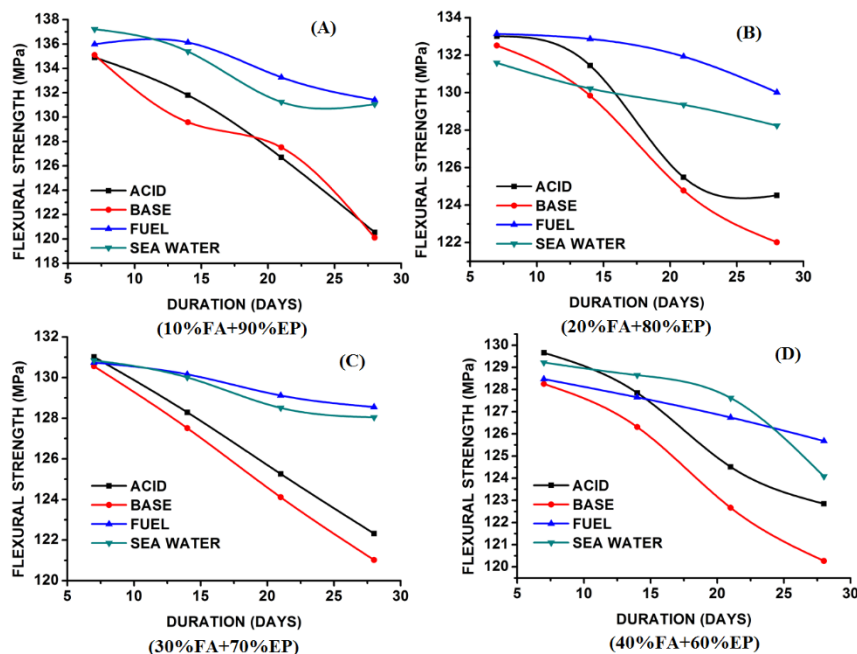


Figure 4.36: Variation of flexural strength with treatment duration periods(A)for 10% fly ash (B) for 20% fly ash (C) for 30% fly ash (D) for 40% fly ash reinforcement.

The decrease in flexural strength may be due to the chemical reactions taking at the surface of the samples and entering of solutions to the core of the composite through microcracks and voids. More surface area and exposure time of exposure impart more changes in the specimens. The mechanism of attack at the interface is decisively governed by the chemistry, structure and morphology, etc. at the interface.

Effect of % fly ash on strain

The variation of strain with curing time for the different amounts of fly ash reinforced composites are shown figure 4.37. Each plot is for the samples treated with four different environmental conditions viz. acid solution, basic solution, sea water and fuel. The strain is found to be decreasing with increase in the percentage of fly ash content. The strain is found to be maximum for 10% fly ash reinforced composite in sea water treatment condition for seven days. The strain is maximum for the fuel treated samples followed by sea water, acid and basic solution treated samples.

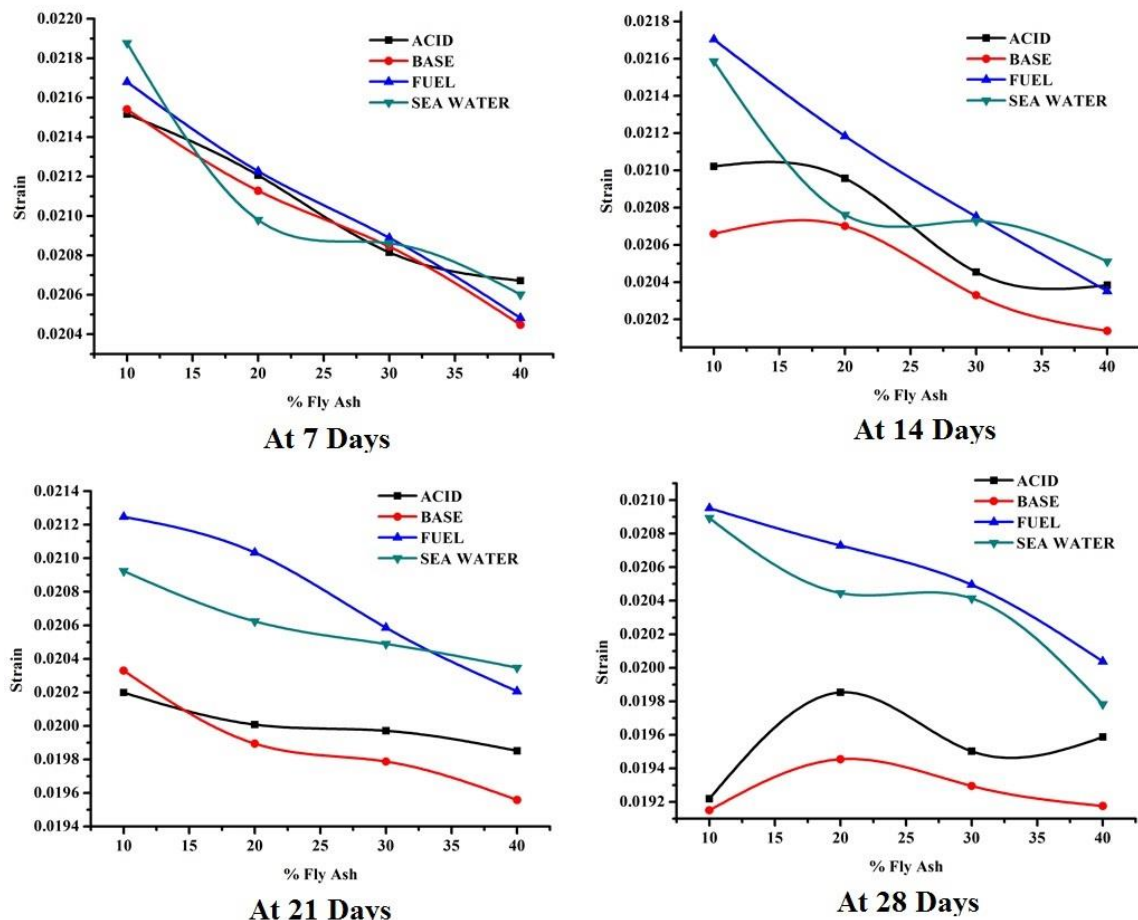


Figure 4.37: Variation of strain with different percentage of fly ash reinforcement for different duration of immersion.

The decrease in strain value is due to decrease in rigidity of the material. From the above graph, it is clear that fuel treated samples are more resistance to applied load having a very negligible change in strain. Water absorption speeds up the damages/crack initiation inside the composites and causes damages. During water or sea water immersion test, many properties of the composites are altered. The effects of water absorption on the mechanical properties of composites are mainly for the matrix plasticization and interface debonding. As the immersion time increases, the interface became weaker and water molecule diffuses into the inner part of the composite through the matrix-particle interface in capillary paths and then stored in the void regions. This is the cause of deterioration and failure of the material.

Effect of percentage fly ash on (maximum) deflection

In the flexural test, maximum elongation/compression depth/height before the fracture is taken/considered as the maximum deflection i.e. the amount of strain (accumulated) on the specimen before starting of plastic deformation (the IIIrd stage of deformation in the polymer) is measured. Figure 4.38 illustrates the variation of maximum deflection of the flexural specimens with different percentage of fly ash reinforcement. There is a maximum deflection of 0.1823mm for 10% reinforced sample treated in sea water for seven days and minimum deflection of 0.1597mm for 40% reinforced sample in basic solution.

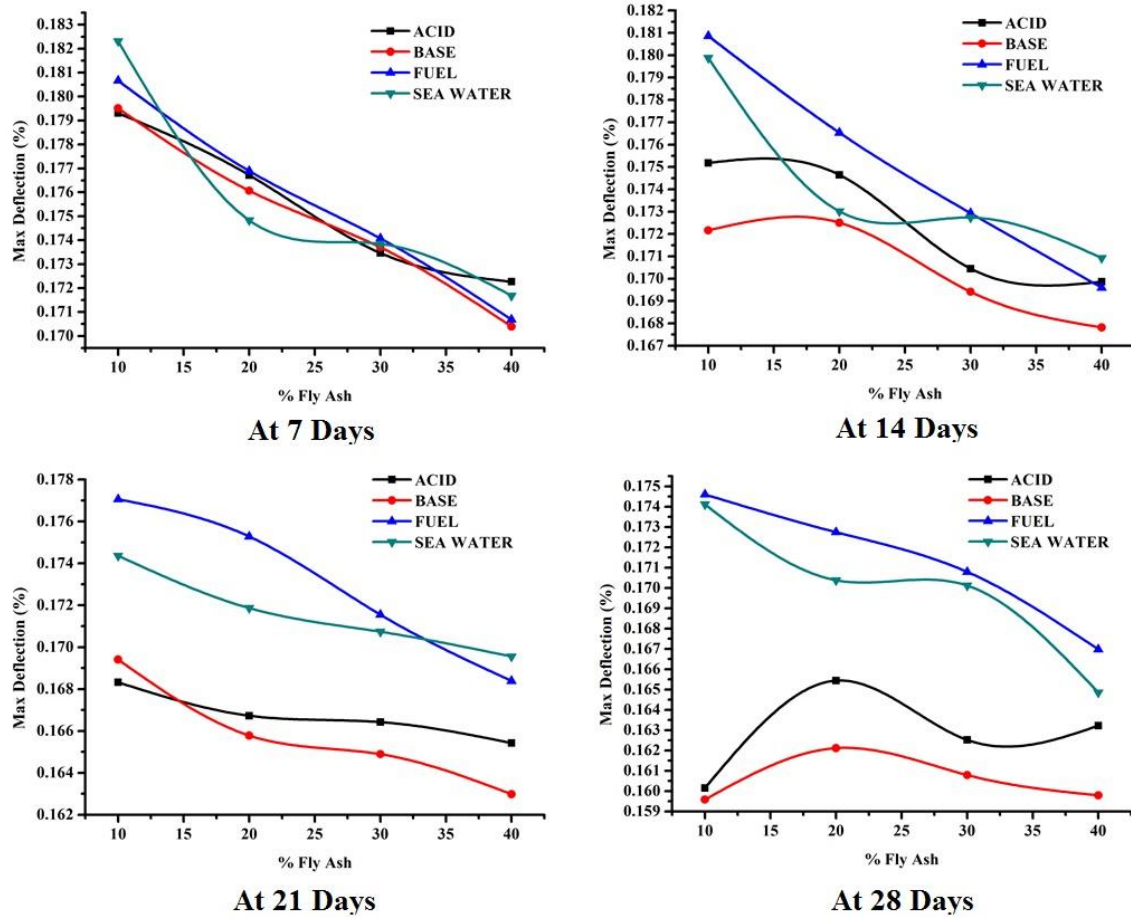


Figure 4.38: Variation of maximum deflection with different percentage of fly ash reinforcement for different duration of immersion.

The decrease in maximum deflection is due to the rigidity of the material. As the samples are treated in various environmental conditions, rigidity varies/affected so as the maximum deflection. The increase in fly ash content also reduce the rigidity of the material and making it more brittle and lowering the maximum deflection.

4.3.5 Impact properties of different environmentally treated samples

Figure 4.39 is plotted between impact strength and duration of treatment for a different amount of fly ash reinforcement. The impact strength decreases with duration of immersion as revealed in the figure. For 10% fly ash composite, impact strength varies from 2.001J to 1.318J in acid solution, 1.941J to 1.003J in basic solution, 1.965J to 1.644J in fuel and 1.973J to 1.649J in sea water, for a maximum duration of 28 days. Similarly, for 20% fly ash composite, it ranges from 1.64J in acid (7days) solution to 1.21J in basic solution (28days). For 30% and 40% fly ash composites, it follows the same trend and reaches a minimum value

of 0.98J and 0.518J respectively. Like earlier, the basic solution has the highest impact on decreasing the impact strength followed by an acid solution, sea water and fuel. The decline in impact energy may be due to the following reason.

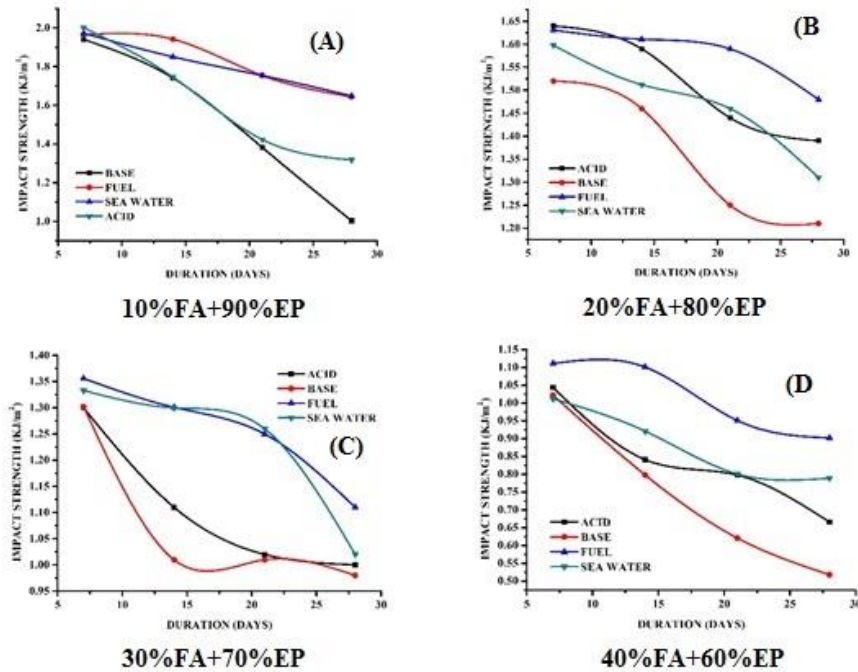


Figure 4.39: Variation of impact strength with duration time (A) for 10% fly ash (B) for 20% fly ash (C) for 30% fly ash (D) for 40% fly ash reinforcement.

As the material corrodes with time in different environments, the internal bonding is also affected. As the internal structure changes, there is the development of initial/residual strain. This residual strain helps in initiation and propagation of crack and decreases the capability of storing energy. Larger swellings are also evident with the composites those are saturated with water. This promotes larger dimensional change that can affect the performance of the composite and even led to failure by mechanical constraints at stress concentration zones. The decrease in rigidity may also be the reason of reduction in impact strength of the material.

4.3.6 Microstructural analysis

For tensile test specimens

Figure 4.40 have been taken on the fracture surface after the sample failed during tensile testing. The dog bone shaped samples are stretched and breaks at the midpoint due initiation

of crack at the fly ash embedded site. The morphologies of the fracture surfaces show that the failure occurred catastrophically.

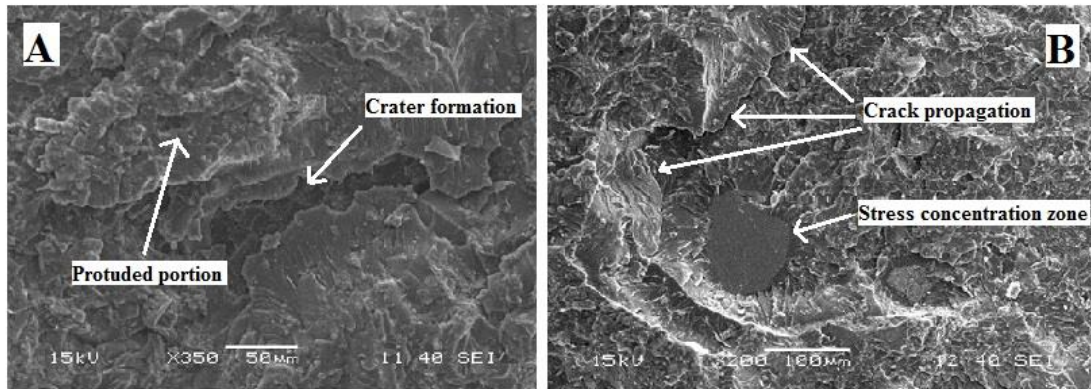


Figure 4.40: SEM micrograph of the fractured surface of tensile test specimen (for 10% fly ash treated in basic solution after 28 days).

In the figure, propagation of crack is visible and stress concentration zone is also seen. Protruded structures are the result of stretching of material at amorphous regions of the composite.

For flexural test specimens

In three point bend test, a normal load is applied within a fixed span. As the load increases, the upper part is imparted by a compressive force and the lower part of a tensile force. Figure 4.41 (A), shows fracture surface, indicating the path formation as a result of compression loading. Figure 4.41 (B), shows the lower part/side (tensile loaded zone) which exhibits river like flow pattern. At the site of embedded fly ash particle, stress concentration increases which initiate the crack inside the specimen.

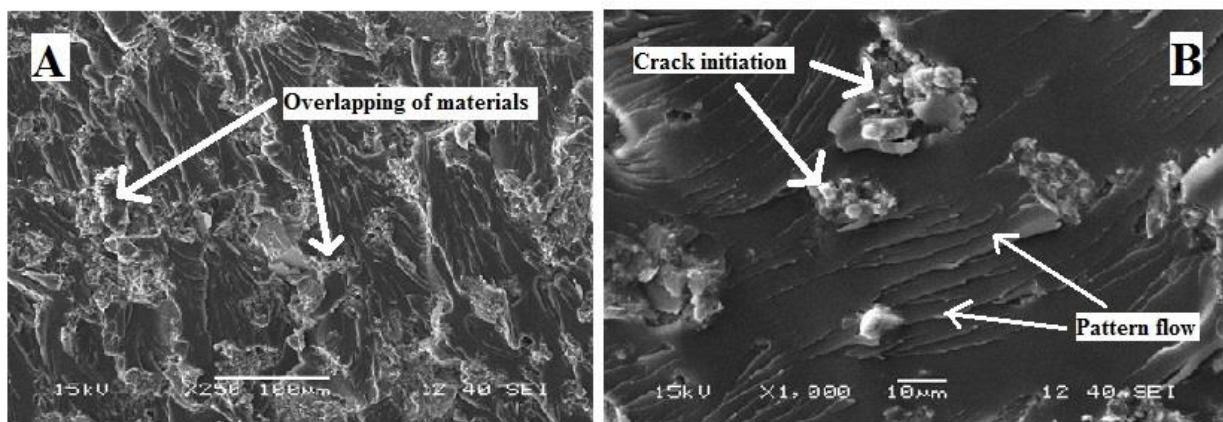


Figure 4.41: SEM micrograph of the fractured surface in flexural test specimen (for 10% fly ash treated in basic solution after 28 days).

For impact test specimens

In figures 4.42, there is a flow of material from right to left and river-like patterns are visible. The river like pattern in the fracture surface is due to energy transfer and the plastic flow occurs in the material.

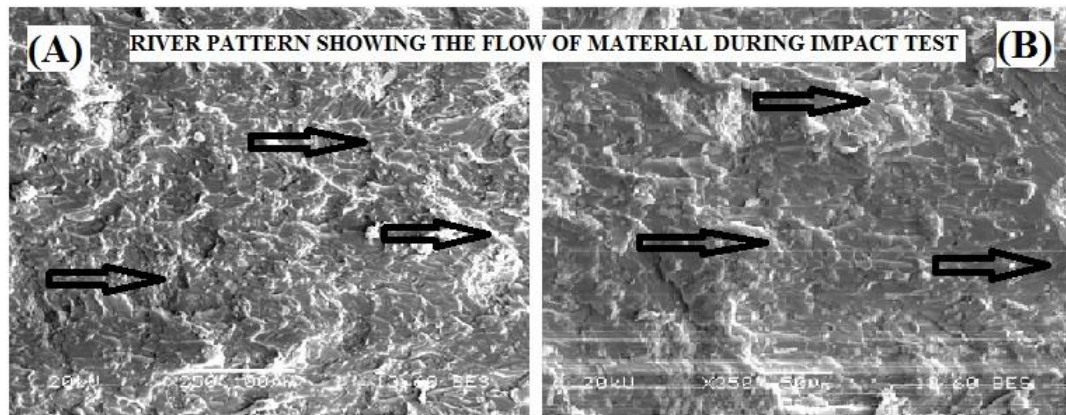


Figure 4.42: SEM micrograph of the fractured surface in impact test specimen (for 10% fly ash treated in basic solution after 28 days).

The amount of energy absorbed is directly proportional to the strength and modulus of the material. Impact specimens are subjected to absorb energy. The fracture is due to the suddenly applied load, but the fracture is initiated by the maximum amount of energy stored per unit area. As the energy flow takes place in a direction, so as the movement of material. Hence, there is always some flow pattern observed on the surfaces of impact test specimens.

4.3.7 Thermal analysis

Glass transition temperature

Figure 4.43 shows the plot between heat and temperature which is a measure of enthalpy. The area under the curve illustrates the amount of heat energy required/used for completion of reaction during the curing operation. The fuel treated sample has the minimum area of groove that implies least energy consumption/amount of energy spent/absorbed during the reaction. The area of the groove for a basic solution has the highest value which indicates; there may be a decrease in crystalline regions with this treatment. The same trend is followed by all (reinforce percentage of fly ash i.e. 20, 30, 40) composites.

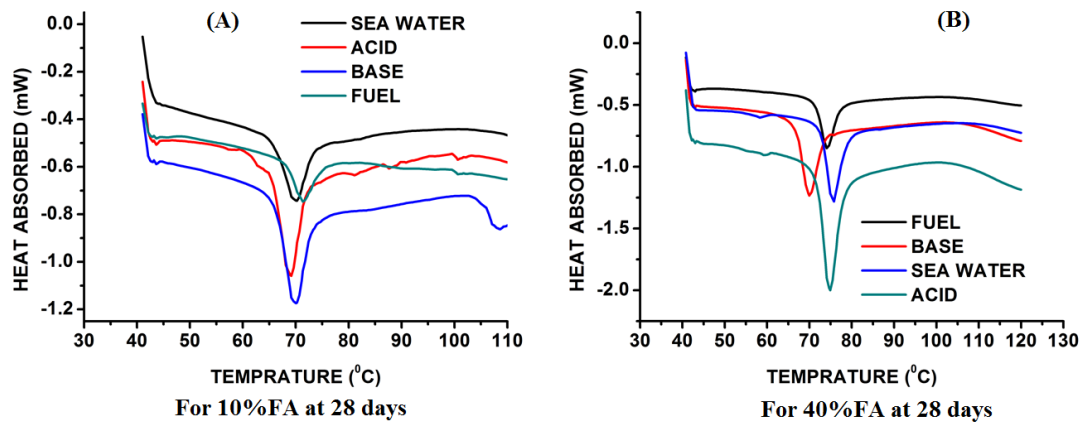


Figure 4.43: Variation of the amount of heat absorbed with temperature treated in different ways (10%FA after 28 days & 40%FA after 28 days).

The glass transition temperature of 10, 20, 30 & 40 % fly ash reinforced sample treated with different mediums for 28 days is evaluated and shown in figure 4.44 below.

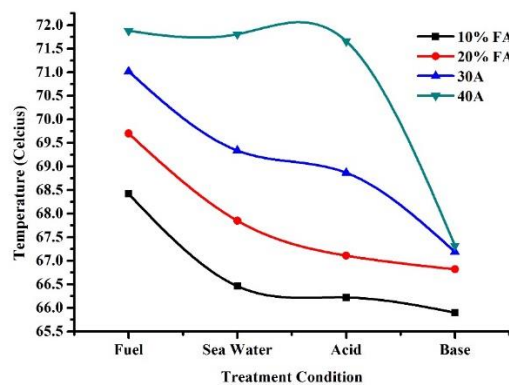


Figure 4.44: Variation of glass transition temperature with different treatment conditions (10% fly ash after 28days).

From the figure, it is evident that the glass transition temperature decreases from the normal value with increase in the time duration of the treatments. It also indicates that fuel has the least impact on T_g whereas basic solution exhibits the highest impact. Water can cause plasticization of the polymeric matrix composite reducing its glass transition temperature and affecting the particle-matrix interface strength. For any material, T_g is directly proportional to the crystallinity and the crystallinity is commensurate with the strength of the material. So, these T_g temperatures show that fuel has the least impact on decreasing the strength of these composite material.

4.3.8 Spectroscopic analysis

IR spectra of 10% fly ash reinforced specimens after 28 days treatment is shown in figure 4.45. Here the percentage transmittance does not vary so much. Wave numbers like 610, 1035, 1520, 2360 and 3620 are also present (as was in previously discussed cases) in the normal sample. The fingerprint of the samples in the form of wave number indicates the structural change in the specimens.

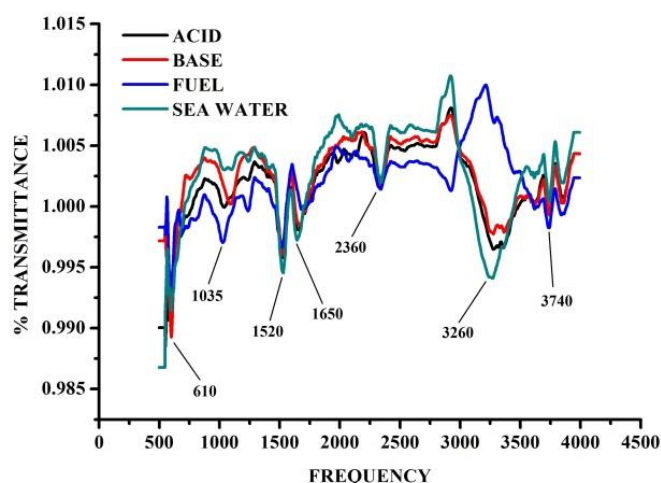


Figure 4.45: IR spectra of 10% fly ash reinforced specimens after 28 days of treatment.

One addition wave number of 1650 is observed which is a (-NH_2) bond. The addition of (-NH_2) might be helping in altering the strength properties of the sample. These structural changes ultimately result in the decrease in strength of the composite.

Figure 4.46 represent the IR spectra of 40% fly ash reinforced specimens at 28 days treatment. There is a lot of change between 10% and 40% fly ash reinforced composites. Here the wave numbers like 610, 1035, 1520 and 2360 are absent.

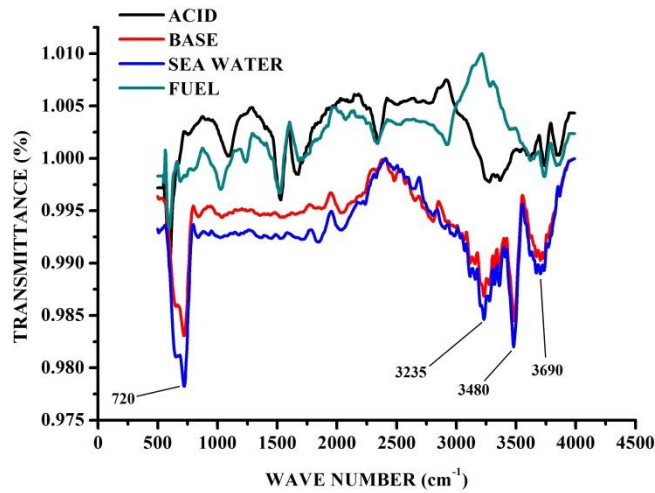


Figure 4.46: IR spectra of 40% fly ash reinforced specimens after 28 days immersion.

One new wave number of 720 is found which also represents the same bond of C-Cl. The percentage transmittance does not change much in both the cases. But there is a deviation in both the cases. The spectral line obtained for fuel immersed sample deviates, a pattern opposite to samples with other treatment conditions.

Table 4.3: Wavenumbers are showing possible bonding in oven & microwave curing samples.

| Sl No | Wave number | Probable chemical bonding | Existence in 10%reinforced FA composite | Existence in 40% reinforced FA composite |
|-------|-------------|-------------------------------|---|--|
| i. | 610 | C-Cl / C-Br | Present | Present |
| ii. | 720 | C-Cl / C-Br | Absent | Present |
| iii. | 1035 | =C-O-C= | Present | Absent |
| iv. | 1520 | C-N=O | Present | Absent |
| v. | 1650 | -NH ₂ | Present | Absent |
| vi. | 2360 | =NH ₂ ⁺ | Present | Absent |
| vii. | 3260 | =CONH ₂ | Present | Present |

Table 4.3 represent the possibility of bonding and corresponding wavenumbers. It is evident from the above table that most of the bonds vanish in 40% fly ash reinforced composite after immersion duration of 28 days. It may be the possible reason of losing strength in a higher percentage of fly ash reinforced epoxy composite.

4.3.9 XRD analysis

Figure 4.47 shows the X-ray diffractograms of 10% and 40% fly ash reinforced samples treated in different environmental conditions. It illustrates the compounds formed and the amount of crystallinity in the specimens. In X-ray analysis, large broader peaks show the amorphous regions while the stiff peaks show the crystalline regions

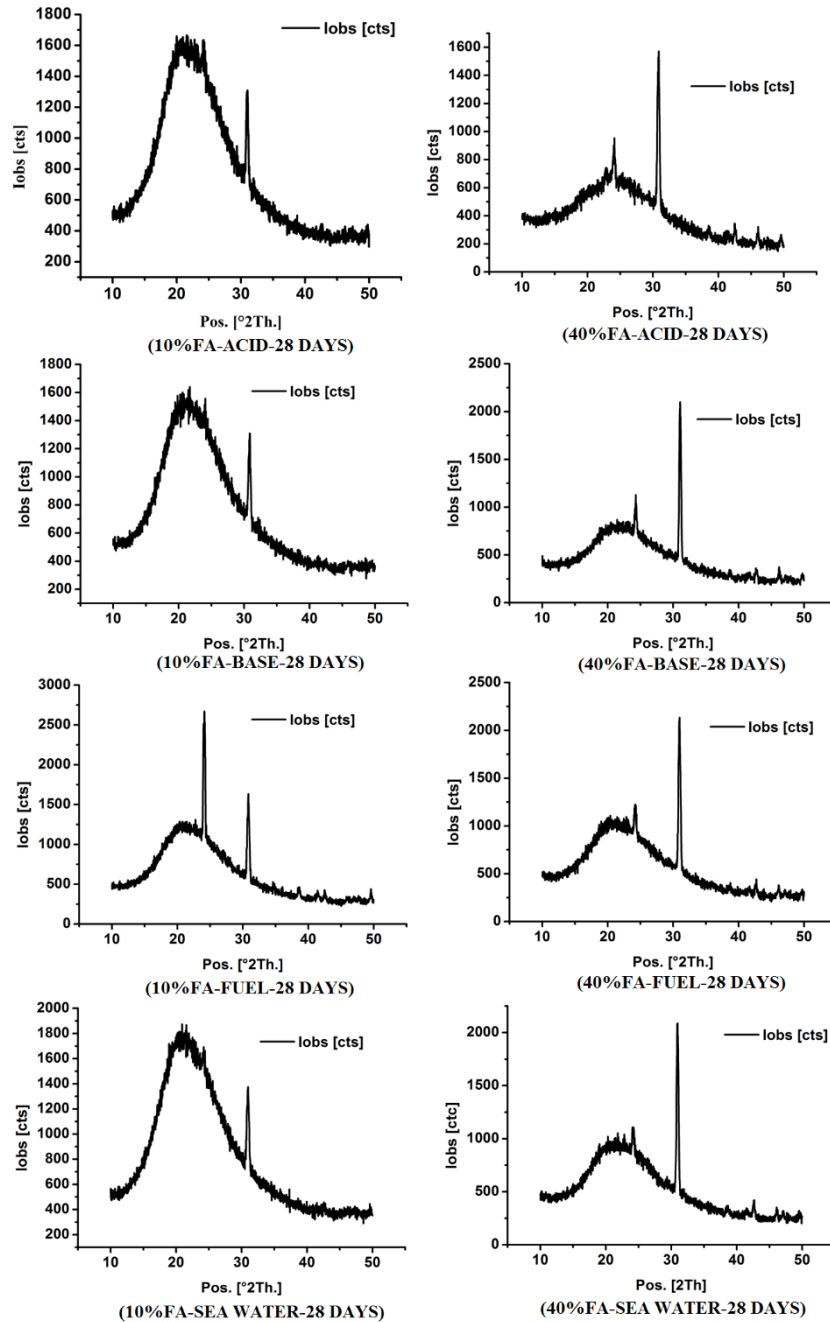


Figure 4.47: XRD analysis of various samples treated in different environmental conditions (after 28 days).

The crystallinity of the polymeric samples is measured by-

$$X_c = \frac{I_c}{I_c + I_a}$$

Where, X_c = % crystallinity

I_c = Intensity of crystalline region

I_a = Intensity of amorphous region

Table 4.4: % Crystallinity of fly ash reinforced composites.

| Sl No | Treatment Condition | Crystallinity of 10% FA Resin | Crystallinity of 40% FA Resin | % change in crystallinity |
|-------|---------------------|-------------------------------|-------------------------------|---------------------------|
| 1 | Acid Solution | 44.56 | 69.23 | 24.67 |
| 2 | Basic Solution | 45.80 | 72.06 | 26.26 |
| 3 | Fuel | 68.30 | 67.19 | 1.11 |
| 4 | Sea Water | 43.68 | 68.49 | 24.81 |

Table 4.4 indicate that change in percentage crystallinity is minimum for fuel treated and maximum for basic solution treated samples. It indicates that samples treated in fuel undergo a very minimal change in its properties and samples treated in basic solution have the highest change in its mechanical properties. It is evident from the figure that, with the addition of fly ash, crystallinity increases. By analysing the diffractograms, it is clear that presence of silica in fly ash might be influencing the crystallinity and amorphous regions and transformations in their amount during curing and chemical treatments.

4.4 Wear Behaviour

4.4.1 Statistical Analysis

The statistical analysis method is used for considering the experimental variables responsible for wear. Experiments have been carried out for 32 numbers of samples for each treatment condition and result in the form of wear, frictional force and coefficient of friction are obtained by the change in parameters as demonstrated in Table 4.5, Table 4.6 and 4.7. In all the three cases, these are multi-objective parametric conditions are converted to the single objective state by applying TOPSIS. A relative closeness value is obtained for each condition which is the combined output of all the software estimated outputs. The optimal parametric combination is then assessed which come about most noteworthy relative closeness value.

Table 4.5: L32 Orthogonal array with results for atmospheric curing condition.

| Sl no | % FA | Time (Min) | Speed (RPM) | Load (N) | Track diameter (cm) | Wear (μm) | Frictional force (N) | COF (μ) | Relative closeness coefficient (P) |
|-------|------|------------|-------------|----------|---------------------|------------------------|----------------------|---------------|------------------------------------|
| 1 | 10 | 5 | 200 | 10 | 40 | 140 | 2.77 | 0.04 | 0.82856 |
| 2 | 10 | 5 | 400 | 20 | 50 | 250.78 | 10.17 | 0.04 | 0.615883 |
| 3 | 10 | 5 | 600 | 30 | 60 | 147.09 | 14.79 | 0.05 | 0.643091 |
| 4 | 10 | 5 | 800 | 40 | 70 | 371.35 | 22.18 | 0.05 | 0.260846 |
| 5 | 10 | 10 | 200 | 40 | 40 | 136.15 | 20.17 | 0.04 | 0.562478 |
| 6 | 10 | 10 | 400 | 30 | 50 | 171.58 | 11.2 | 0.05 | 0.684963 |
| 7 | 10 | 10 | 600 | 20 | 60 | 333.52 | 6.34 | 0.05 | 0.566212 |
| 8 | 10 | 10 | 800 | 10 | 70 | 60.08 | 9.98 | 0.04 | 0.826147 |
| 9 | 20 | 5 | 200 | 10 | 50 | 134.27 | 3.83 | 0.05 | 0.822666 |
| 10 | 20 | 5 | 400 | 20 | 40 | 47.91 | 11.43 | 0.05 | 0.788616 |
| 11 | 20 | 5 | 600 | 30 | 70 | 297.03 | 17.13 | 0.05 | 0.434593 |
| 12 | 20 | 5 | 800 | 40 | 60 | 272.15 | 23.03 | 0.06 | 0.362369 |
| 13 | 20 | 10 | 200 | 40 | 50 | 505.83 | 27.39 | 0.06 | 3.80E-06 |
| 14 | 20 | 10 | 400 | 30 | 40 | 145.41 | 14.01 | 0.05 | 0.65989 |
| 15 | 20 | 10 | 600 | 20 | 70 | 395.76 | 9.98 | 0.05 | 0.458599 |
| 16 | 20 | 10 | 800 | 10 | 60 | 108.99 | 2.05 | 0.05 | 0.853708 |
| 17 | 30 | 5 | 200 | 20 | 60 | 60.98 | 7.93 | 0.04 | 0.873544 |
| 18 | 30 | 5 | 400 | 10 | 70 | 21.87 | 3.84 | 0.04 | 0.999999 |
| 19 | 30 | 5 | 600 | 40 | 40 | 197 | 16.92 | 0.05 | 0.552097 |
| 20 | 30 | 5 | 800 | 30 | 50 | 91.48 | 13.36 | 0.05 | 0.720155 |
| 21 | 30 | 10 | 200 | 30 | 60 | 222.23 | 12.77 | 0.04 | 0.607281 |
| 22 | 30 | 10 | 400 | 40 | 70 | 248.9 | 19.45 | 0.05 | 0.450608 |
| 23 | 30 | 10 | 600 | 10 | 40 | 281.17 | 3.31 | 0.05 | 0.648674 |
| 24 | 30 | 10 | 800 | 20 | 50 | 408.76 | 7.48 | 0.05 | 0.484069 |

| | | | | | | | | | |
|----|----|----|-----|----|----|--------|-------|------|----------|
| 25 | 40 | 5 | 200 | 20 | 70 | 110.65 | 5.13 | 0.05 | 0.845886 |
| 26 | 40 | 5 | 400 | 10 | 60 | 54.78 | 2.21 | 0.05 | 0.909899 |
| 27 | 40 | 5 | 600 | 40 | 50 | 297.21 | 13.22 | 0.05 | 0.504077 |
| 28 | 40 | 5 | 800 | 30 | 40 | 46.83 | 9.71 | 0.05 | 0.827162 |
| 29 | 40 | 10 | 200 | 30 | 70 | 144.34 | 8.81 | 0.05 | 0.757246 |
| 30 | 40 | 10 | 400 | 40 | 60 | 120.27 | 11.85 | 0.05 | 0.726858 |
| 31 | 40 | 10 | 600 | 10 | 50 | 31.02 | 3.31 | 0.05 | 0.931367 |
| 32 | 40 | 10 | 800 | 20 | 40 | 43.88 | 9.85 | 0.05 | 0.825404 |

Table 4.6: L32 Orthogonal array with results for oven curing condition.

| Sl no | % FA | Time (Min) | Speed (RPM) | Load (N) | Track diameter (cm) | Wear (μm) | Frictional force (N) | COF (μ) | Relative closeness coefficient (P) |
|----------|---------|---------------|----------------|-------------|---------------------------|---------------------------|----------------------------|------------------|---|
| 1 | 10 | 5 | 200 | 10 | 40 | 59.84 | 5.59 | 0.2 | 0.914565 |
| 2 | 10 | 5 | 400 | 20 | 50 | 32.25 | 9.61 | 0.2 | 0.770425 |
| 3 | 10 | 5 | 600 | 30 | 60 | 92.07 | 11.67 | 0.2 | 0.887507 |
| 4 | 10 | 5 | 800 | 40 | 70 | 79.24 | 12.13 | 0.2 | 0.867243 |
| 5 | 10 | 10 | 200 | 40 | 40 | 60.78 | 15 | 0.2 | 0.802059 |
| 6 | 10 | 10 | 400 | 30 | 50 | 41.44 | 11.53 | 0.2 | 0.78233 |
| 7 | 10 | 10 | 600 | 20 | 60 | 223.31 | 5.69 | 0.2 | 0.975153 |
| 8 | 10 | 10 | 800 | 10 | 70 | 14.58 | 3.52 | 0.3 | 0.805525 |
| 9 | 20 | 5 | 200 | 10 | 50 | 45.64 | 1.56 | 0.2 | 0.966949 |
| 10 | 20 | 5 | 400 | 20 | 40 | 22.7 | 0.05 | 0.2 | 0.997802 |
| 11 | 20 | 5 | 600 | 30 | 70 | 112.76 | 9.09 | 0.3 | 0.9254 |
| 12 | 20 | 5 | 800 | 40 | 60 | 85.1 | 9.61 | 0.3 | 0.898532 |
| 13 | 20 | 10 | 200 | 40 | 50 | 98.06 | 13.9 | 0.3 | 0.875849 |
| 14 | 20 | 10 | 400 | 30 | 40 | 30.44 | 12.94 | 0.2 | 0.701706 |
| 15 | 20 | 10 | 600 | 20 | 70 | 31.41 | 6.31 | 0.3 | 0.832715 |
| 16 | 20 | 10 | 800 | 10 | 60 | 48.23 | 4.43 | 0.3 | 0.915875 |
| 17 | 30 | 5 | 200 | 20 | 60 | 102.96 | 14.26 | 0.1 | 0.878348 |
| 18 | 30 | 5 | 400 | 10 | 70 | 19.27 | 20.38 | 0.1 | 0.486003 |
| 19 | 30 | 5 | 600 | 40 | 40 | 96.72 | 15.59 | 0.1 | 0.861188 |
| 20 | 30 | 5 | 800 | 30 | 50 | 35.03 | 11.76 | 0.1 | 0.748664 |
| 21 | 30 | 10 | 200 | 30 | 60 | 162.92 | 14.77 | 0.1 | 0.916878 |
| 22 | 30 | 10 | 400 | 40 | 70 | 259.91 | 14.21 | 0.1 | 0.948161 |
| 23 | 30 | 10 | 600 | 10 | 40 | 26.77 | 40.15 | 0.1 | 0.40003 |

| | | | | | | | | | |
|----|----|----|-----|----|----|-------|-------|-----|----------|
| 24 | 30 | 10 | 800 | 20 | 50 | 46.17 | 1.64 | 0.2 | 0.965698 |
| 25 | 40 | 5 | 200 | 20 | 70 | 62.75 | 1.64 | 0.2 | 0.97453 |
| 26 | 40 | 5 | 400 | 10 | 60 | 36.25 | 3.89 | 0.2 | 0.903089 |
| 27 | 40 | 5 | 600 | 40 | 50 | 25.77 | 15.56 | 0.1 | 0.623518 |
| 28 | 40 | 5 | 800 | 30 | 40 | 10.42 | 10.3 | 0.1 | 0.502896 |
| 29 | 40 | 10 | 200 | 30 | 70 | 26.61 | 11.51 | 0.2 | 0.698059 |
| 30 | 40 | 10 | 400 | 40 | 60 | 15.7 | 13.8 | 0.2 | 0.532203 |
| 31 | 40 | 10 | 600 | 10 | 50 | 26.38 | 4.99 | 0.2 | 0.840931 |
| 32 | 40 | 10 | 800 | 20 | 40 | 29.37 | 11.44 | 0.2 | 0.719677 |

Table 4.7: L32 Orthogonal array with results for micro oven curing condition.

| Sl no | % Fa | Time (min) | Speed (rpm) | Load (N) | Track diameter (cm) | Wear (μm) | Frictional force | COF (μ) | Relative closeness COF (P) |
|-------|---------|---------------|----------------|-------------|---------------------------|---------------------------|---------------------|------------------|----------------------------------|
| 1 | 10 | 5 | 200 | 10 | 40 | 80.32 | 4.41 | 0.2 | 0.052048 |
| 2 | 10 | 5 | 400 | 20 | 50 | 126.66 | 11.16 | 0.3 | 0.080975 |
| 3 | 10 | 5 | 600 | 30 | 60 | 103.55 | 13.47 | 0.2 | 0.115109 |
| 4 | 10 | 5 | 800 | 40 | 70 | 110.72 | 20.83 | 0.4 | 0.158343 |
| 5 | 10 | 10 | 200 | 40 | 40 | 98.13 | 17.01 | 0.3 | 0.147733 |
| 6 | 10 | 10 | 400 | 30 | 50 | 70.91 | 12.32 | 0.3 | 0.148024 |
| 7 | 10 | 10 | 600 | 20 | 60 | 280.53 | 7.07 | 0.3 | 0.024583 |
| 8 | 10 | 10 | 800 | 10 | 70 | 41.8 | 6.82 | 0.6 | 0.140271 |
| 9 | 20 | 5 | 200 | 10 | 50 | 102.74 | 1.98 | 0.17 | 0.018908 |
| 10 | 20 | 5 | 400 | 20 | 40 | 39.79 | 3.99 | 0.23 | 0.091138 |
| 11 | 20 | 5 | 600 | 30 | 70 | 198.63 | 13.93 | 0.5 | 0.065534 |
| 12 | 20 | 5 | 800 | 40 | 60 | 143.25 | 18.63 | 0.72 | 0.115085 |
| 13 | 20 | 10 | 200 | 40 | 50 | 147.05 | 21.27 | 0.3 | 0.126366 |
| 14 | 20 | 10 | 400 | 30 | 40 | 82.43 | 16.91 | 0.22 | 0.170223 |
| 15 | 20 | 10 | 600 | 20 | 70 | 67.92 | 9.03 | 0.24 | 0.117349 |
| 16 | 20 | 10 | 800 | 10 | 60 | 58.89 | 5.02 | 0.39 | 0.078548 |
| 17 | 30 | 5 | 200 | 20 | 60 | 50.68 | 11.92 | 0.35 | 0.190415 |
| 18 | 30 | 5 | 400 | 10 | 70 | 23.77 | 5.88 | 0.38 | 0.198314 |
| 19 | 30 | 5 | 600 | 40 | 40 | 54.41 | 17.73 | 0.21 | 0.245772 |
| 20 | 30 | 5 | 800 | 30 | 50 | 72.43 | 12.37 | 0.18 | 0.145873 |
| 21 | 30 | 10 | 200 | 30 | 60 | 181.22 | 15.06 | 0.17 | 0.076727 |

| | | | | | | | | | |
|----|----|----|-----|----|----|--------|-------|------|----------|
| 22 | 30 | 10 | 400 | 40 | 70 | 221.49 | 17.92 | 0.11 | 0.074851 |
| 23 | 30 | 10 | 600 | 10 | 40 | 183.17 | 5053 | 0.8 | 0.965018 |
| 24 | 30 | 10 | 800 | 20 | 50 | 163.77 | 3.46 | 0.6 | 0.02069 |
| 25 | 40 | 5 | 200 | 20 | 70 | 84.55 | 5.22 | 0.2 | 0.058149 |
| 26 | 40 | 5 | 400 | 10 | 60 | 41.57 | 4.04 | 0.32 | 0.088577 |
| 27 | 40 | 5 | 600 | 40 | 50 | 138.49 | 11.36 | 0.4 | 0.075809 |
| 28 | 40 | 5 | 800 | 30 | 40 | 23.98 | 10.11 | 0.1 | 0.296568 |
| 29 | 40 | 10 | 200 | 30 | 70 | 58.63 | 10.85 | 0.23 | 0.15616 |
| 30 | 40 | 10 | 400 | 40 | 60 | 84.72 | 14.1 | 0.28 | 0.142684 |
| 31 | 40 | 10 | 600 | 10 | 50 | 35.8 | 4.46 | 0.34 | 0.11078 |
| 32 | 40 | 10 | 800 | 20 | 40 | 36.87 | 10.15 | 0.41 | 0.215866 |

The average wear values for diverse levels of selected parameters are indicated in Tables 4.8, 4.9 and 4.10. From the table 4.8 below, the mean value of time at level 1 is higher than the average value of time at level 2 which indicates that level 1 is better than level 2. Similarly, better choices have been found out in other parameters. The same comparison has been carried out and given in table 4.9 and table 4.10.

Table 4.8: Mean response table for relative closeness coefficient for atmospheric curing condition.

| Level | Time | % FA | Speed | Load | Track diameter |
|-------|---------|---------|---------|---------|----------------|
| 1 | -3.764 | -4.529 | -15.742 | -1.445 | -3.067 |
| 2 | -10.229 | -17.476 | -2.961 | -3.573 | -16.644 |
| 3 | | -3.813 | -4.784 | -3.652 | -3.508 |
| 4 | | -2.168 | -4.499 | -19.316 | -4.767 |
| Delta | 6.465 | 15.308 | 12.782 | 17.871 | 13.576 |
| Rank | 5 | 2 | 4 | 1 | 3 |

Table 4.9: Mean response table for relative closeness coefficient for oven curing condition.

| Level | Time | % FA | Speed | Load | Track diameter |
|-------|---------|---------|---------|---------|----------------|
| 1 | -12.717 | -11.364 | -11.684 | -13.341 | -12.299 |
| 2 | -11.050 | -12.521 | -12.600 | -13.269 | -13.757 |
| 3 | | -9.444 | -10.119 | -11.442 | -10.427 |

| | | | | | |
|-------|-------|---------|---------|--------|---------|
| 4 | | -14.207 | -13.133 | -9.483 | -11.053 |
| Delta | 1.667 | 4.763 | 3.014 | 3.859 | 3.330 |
| Rank | 5 | 1 | 4 | 2 | 3 |

Table 4.10: Mean response table for relative closeness coefficient for micro oven curing condition.

| Level | Time | % FA | Speed | Load | Track diameter |
|-------|--------|--------|--------|--------|----------------|
| 1 | -1.770 | -2.058 | -1.562 | -3.967 | -3.485 |
| 2 | -3.088 | -2.052 | -1.693 | -2.039 | -1.965 |
| 3 | | -4.020 | -4.127 | -1.526 | -2.189 |
| 4 | | -1.586 | -2.334 | -2.184 | -2.078 |
| Delta | 1.317 | 2.434 | 2.565 | 2.441 | 1.520 |
| Rank | 5 | 3 | 1 | 2 | 4 |

Figure 4.48, 4.49 and 4.50 show the S/N ratio plots for mean values which are the output result of Table 4.8, 4.9 and 4.10 respectively. Taguchi suggested a robust method having a minimum sensitive to all noise factors. In this, the loss function is used to find out the deviation between the experimental value and calculated/desired value. Moreover, this loss function can be converted from signal to noise ratio. The loss functions are categorised into lower-the-better, higher-the-better and nominal-the-better.

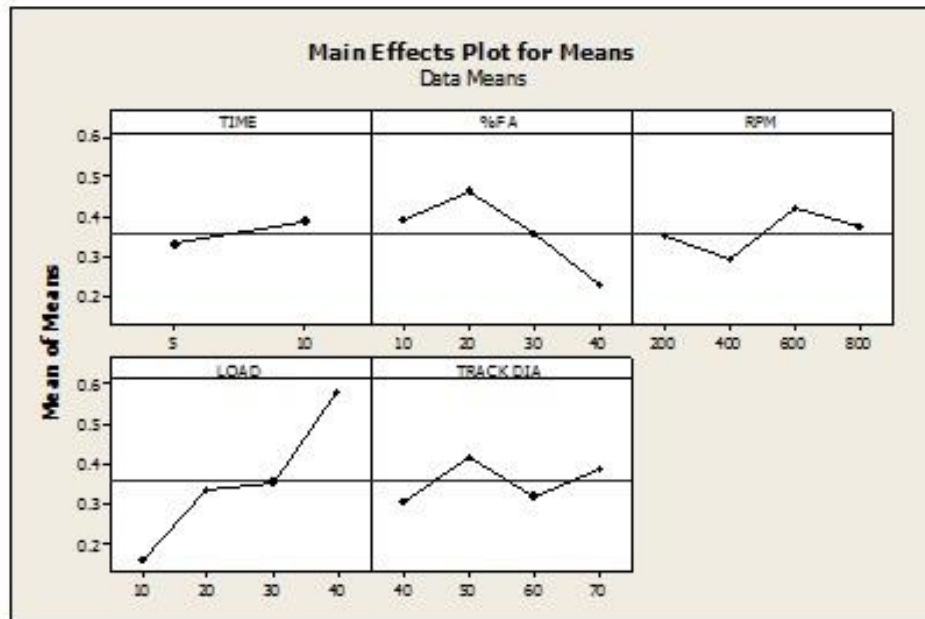


Figure 4.48: S/N ratio plot (atmospheric condition).

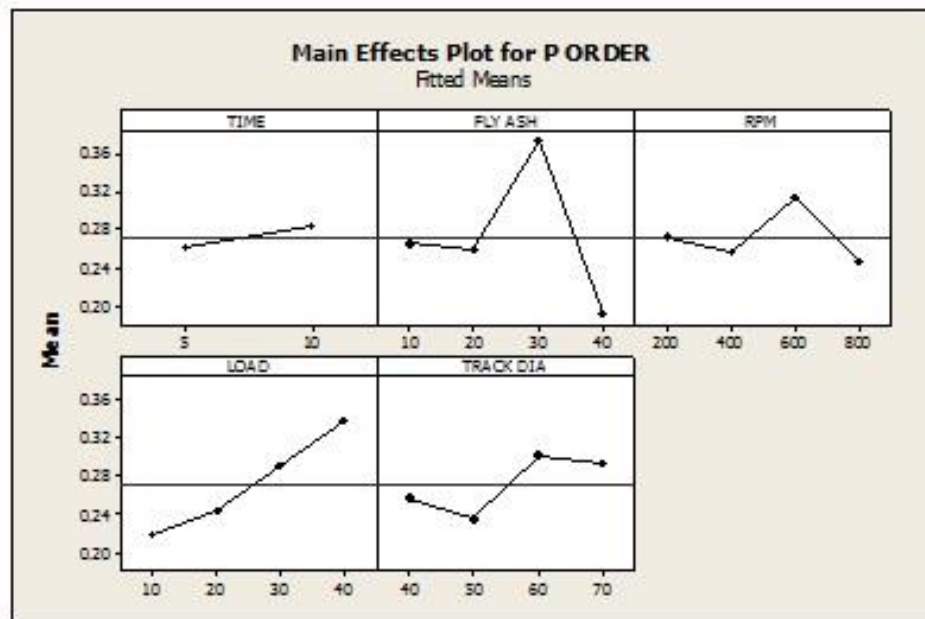


Figure 4.49: S/N ratio plot (oven treated the condition).

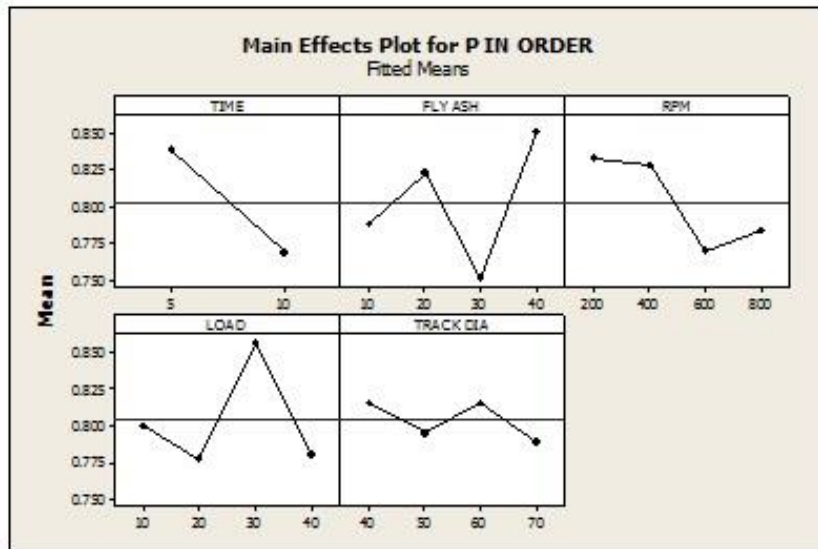


Figure 4.50: S/N ratio plot (micro oven treated the condition).

The above three main effect plots ultimately show the optimum parametric condition to get minimum wear, frictional force and coefficient of friction.

The contribution of each parameter viz. time, the percentage of reinforcement, speed, load and track diameter on wear rates found out using ANOVA and results have been shown in Table 4.11- 4.13. The procedure is to a high degree accommodation to reveal the level of essentialness of effect of factor(s) on a particular reaction. It secludes the total variability of the response (total of squared deviations about the terrific mean) into commitments rendered by each of the parameter and the blunder [148-150]. The analysis has been carried out with at 95% level of confidence. The last column in each table below shows the significance of each parameter having very lower value. At the same time, it also shows which parameter has no direct impact on the outputs. From Table 4.11, the percentage of fly ash reinforcement and load has the highest significance and time has the least significance.

Table 4.11: ANOVA table with adjusted sum of square for tests (atmospheric treatment)

| Source | DF | Seq SS | Adj SS | Adj MS | F | P |
|----------------|----|----------|----------|----------|-------|-------|
| Time | 1 | 0.018507 | 0.018507 | 0.018507 | 2.65 | 0.121 |
| % FA | 3 | 0.262953 | 0.262953 | 0.087651 | 12.57 | 0 |
| Speed | 3 | 0.093677 | 0.093677 | 0.031226 | 4.48 | 0.016 |
| Load | 3 | 0.785823 | 0.785823 | 0.261941 | 37.56 | 0 |
| Track diameter | 3 | 0.078732 | 0.078732 | 0.026244 | 3.76 | 0.029 |
| Error | 18 | 0.125542 | 0.125542 | 0.006975 | | |
| Total | 31 | 1.365234 | | | | |

Table 4.12: ANOVA table with adjusted sum of square for tests (oven treatment).

| Source | DF | Seq SS | Adj SS | Adj MS | F | P |
|----------------|----|----------|----------|----------|-------|-------|
| Time | 1 | 0.003924 | 0.003924 | 0.003924 | 5.79 | 0.027 |
| %FA | 3 | 0.134776 | 0.134776 | 0.044925 | 66.29 | 0.000 |
| Speed | 3 | 0.020945 | 0.020945 | 0.006982 | 10.30 | 0.000 |
| Load | 3 | 0.068034 | 0.068034 | 0.022678 | 33.46 | 0.000 |
| Track diameter | 3 | 0.023958 | 0.023958 | 0.007986 | 11.78 | 0.000 |
| Error | 18 | 0.012198 | 0.012198 | 0.000678 | | |
| Total | 31 | 0.263834 | | | | |

From Table 4.12, only time has the least significance while other parameters have an influence on the output.

Table 4.13: ANOVA table with adjusted sum of square for tests (micro oven treatment).

| Source | DF | Seq SS | Adj SS | Adj MS | F | P |
|----------------|----|----------|----------|----------|--------|-------|
| Time | 1 | 0.039258 | 0.039258 | 0.039258 | 214.81 | 0.000 |
| %FA | 3 | 0.044797 | 0.044797 | 0.014932 | 81.71 | 0.000 |
| Speed | 3 | 0.023814 | 0.023814 | 0.007938 | 43.44 | 0.000 |
| Load | 3 | 0.031945 | 0.031945 | 0.010648 | 58.27 | 0.000 |
| Track diameter | 3 | 0.004484 | 0.004484 | 0.001495 | 8.18 | 0.001 |
| Error | 18 | 0.003290 | 0.003290 | 0.000183 | | |
| Total | 31 | 0.147587 | | | | |

From Table 4.13, only track diameter has no impact on the output while others have some influence on the output.

Confirmatory experiment for minimum wear rate: The confirmatory test helps in determining and analysing the actual experimental value with the predicted value. In the wake of assessing the optimal parameter settings, the following step is to be anticipated and check the enhancement of quality characteristics utilising the optimal parametric

combination. The estimated relative closeness coefficient $\hat{\gamma}$ using the optimal level of the design parameters can be calculated as:

$$\hat{\gamma} = \gamma_m + \sum_{i=1}^n (\bar{\gamma} - \gamma_m)$$

Where γ_m = total is mean Grey relational grade

$\bar{\gamma}$ = mean Grey relational grade at the optimal level

n = number of the main design parameters

Table 4.14, 4.15 and 4.16 compares the value between predicted value of input parameters and actual value using optimal parametric condition. The error is calculated by the difference in actual value and the predicted value. In all the three conditions, a minimum percentage of error is obtained which confirms that the results are least varied.

Table 4.14: Confirmatory test results (atmospheric condition).

| | Initial parameter setting | Optimal parameter condition | |
|---|------------------------------|-----------------------------|--------------------|
| | | Predicted value | Experimented value |
| Level of factors | A2B3C1E3D2 | A1B4C2D1E1 | A1B4C2D1E1 |
| Time | 10 | | 5 |
| % FA | 30 | | 40 |
| Speed | 200 | | 400 |
| Load | 30 | | 10 |
| Track diameter | 50 | | 40 |
| Relative coefficient value | 0.9999 | | |
| S/N ratio of relative coefficient value | | 14.5811 | 14.4461 |
| Improvement in relative coefficient value = 0.93% | | | |

Table 4.15: Confirmatory test results (oven treatment condition).

| | Initial parameter setting | Optimal parameter condition | |
|------------------|------------------------------|-----------------------------|--------------------|
| | | Predicted value | Experimented value |
| Level of factors | A1B2C1D1E2 | A2B3C3D4E3 | A2B3C3D4E3 |

| | | |
|---|----------|---------|
| Time | 5 | 10 |
| % FA | 20 | 30 |
| Speed | 200 | 600 |
| Load | 10 | 40 |
| Track diameter | 50 | 60 |
| Relative coefficient value | 0.142315 | |
| S/N ratio of relative coefficient value | -3.84420 | -3.6830 |

Improvement in relative coefficient value = 0.97%

Table 4.16: Confirmatory test results (micro oven condition).

| | Initial parameter setting | Optimal parameter condition | |
|---|---------------------------|-----------------------------|--------------------|
| | | Predicted value | Experimented value |
| Level of factors | A2B3C1E3D2 | A1B4C1D3E2 | A1B4C1D3E2 |
| Time | 5 | | 5 |
| % FA | 20 | | 40 |
| Speed | 200 | | 200 |
| Load | 10 | | 30 |
| Track diameter | 50 | | 50 |
| Relative coefficient value | 0.870022 | | |
| S/N ratio of relative coefficient value | | 1.30663 | 1.24129 |

Improvement in relative coefficient value = 0.95%

4.4.2 Morphology of worn surfaces:

Morphology of worn out surfaces reveals the actual cause of wear during the process of sliding. Two figures of each type of treatment condition are shown in figure 4.51. It is very difficult to differentiate between normal; oven treated and micro oven treated sample surfaces. White marks in the figure indicate the plastic flow region of the material. The plastic movement of material is due to the unidirectional rotation of the sample and also may

be due to heat generated at the sliding surface. Although there is no micro-crack seen around the void, the smoothness of the specimen surface was deteriorated so as to affect the wear resistance.

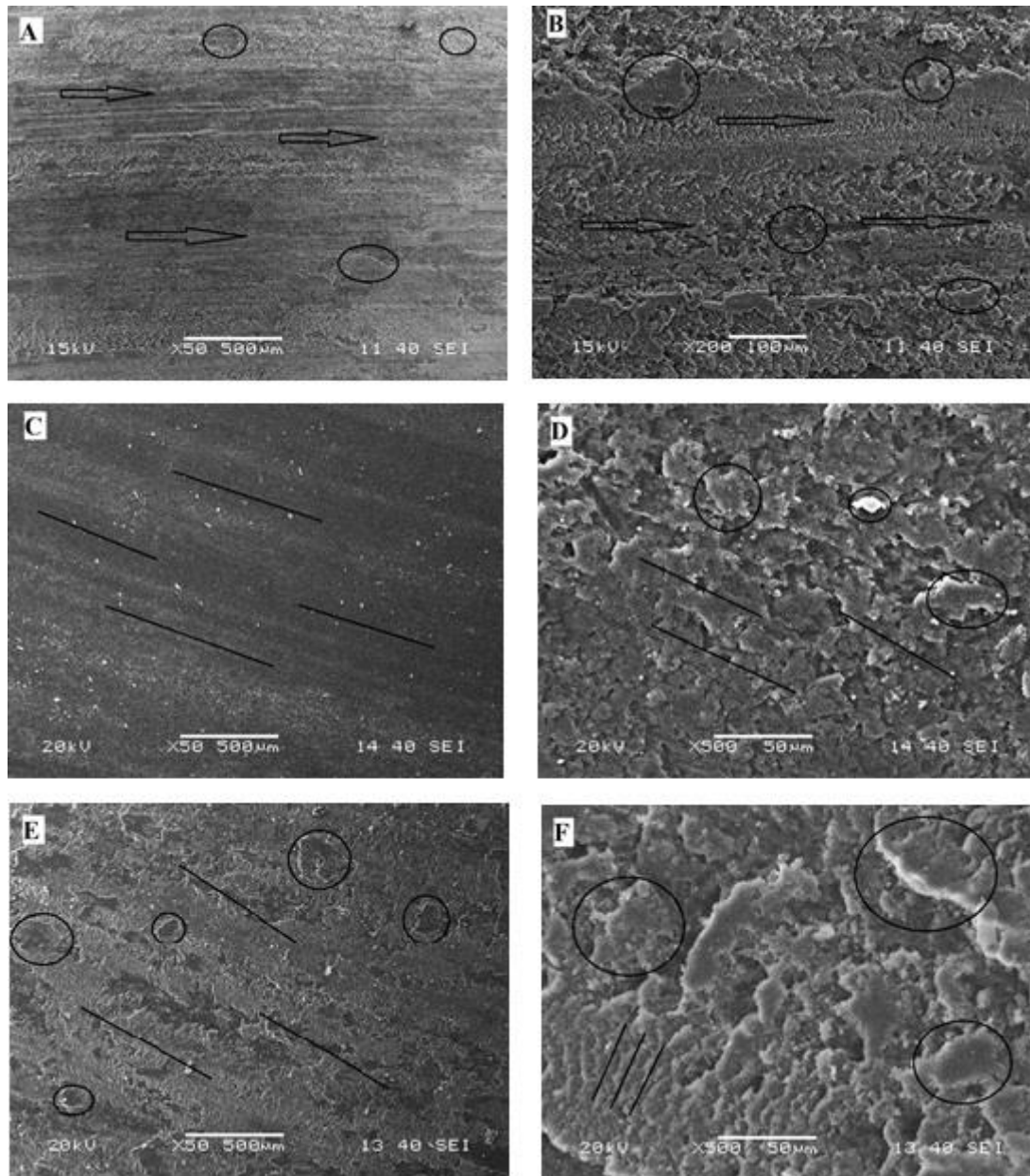


Figure 4.51: SEM micrographs of worn surfaces (for 10% fly ash reinforced, microwave cured specimen).

Figure 4.51 (A & B) are the surface morphology of the samples for the normal atmospheric treatment condition, (C & D) for the oven treated the condition and (E & F) for the micro oven treatment condition. The straight lines in the above figures show the direction of sliding. The circular marks indicated the protruded surfaces where only matrix epoxy material is accumulated due to overheating. Figure 4.51(C) seems to be smoothest of all as it is oven treated. In figure (B and D) crack propagation and erosion of reinforcement material

are visible. Track broadening has taken place due to the secondary erosion which is due to the entrapment of eroded fly ash particle at the initial stages of wear. Figure 4.51(F) which is at 500X magnification shows that matrix material is highly responsible for the erosion of the material. River pattern which is visible in the figure is due to the overheating and overlapping of material.

Chapter 5

Discussion

5.1 Effect of ultrasonic mixing

Ultrasonic vibration/sonication acts as a special initiator for chemical bonds to break and reformation etc., thus enhance polymerization. It has been found that under same conditions, the molecular weight of composites prepared by ultrasonication is higher than that fabricated by conventional method [151]. It has also been observed that ultrasonic stirring/mixing has given improved mechanical properties of fly ash reinforced composites than that of the same composite made with magnetic stirring even [152]. So we have chosen this technique to process our composite to have better interfacial bonding of polymer chains on the surface of the fly ash (ceramic) particles.

Ultra-sonication around monomer droplets provides sufficient radicals for polymerization. Therefore, compared with conventional polymerization it can be regarded that sonication offers some attractive features such as low reaction temperature, faster polymerization rates and higher molecular weight of polymers. Overlapping of different segments of polymer chain during polymerization reaction process increases with the increase of molecular weight. So under ultrasonication, the increment of polymer-polymer interaction in composites affect the viscosity with more distinct shear thinning behaviour, this might also be a cause factor for better interfacial bonding of polymer chains on the surface of (fly ash) ceramic particles.

Meanwhile, a continuing ultrasound leads to the degradation of polymer chains, resulting in a low molecular weight [151]. So, in our work, a pulse time of 5 sec is used during the time of sonication and the process is restricted to 30 minutes only to prevent degradation of the composite. Increasing the mixing time causes air entrapment and void formation in the composite, for which we have restricted the mixing time to 30 minutes for fabrication of the composite (to minimise void formation) and to retain homogeneous distribution of fly ash particles in the composite.

5.2 Effect of post curing treatment

The response of interface within the composite plays an important role in determining the gross mechanical performance because it is transmitting the load from the matrix to the

reinforcement, which contributes the greater portion of the composite strength [153]. Adhesion chemistry at the interface influenced by post curing phenomenon and this effect is supposed to increase with conditioning time [154]. Thermal conditioning also causes matrix shrinkage due to volatile loss and additional cure of matrix, but above the glass transition temperature, polymer composites are susceptible to thermo-oxidative degradation [155]. Thermal conditioning is to induce further polymerization process with the development of penetrating and/or semi-penetrating network at the interface. Thermal conditioning (i.e. microwave curing) at/above ambient temperature might improve adhesion at the interface. It is also found that, during microwave curing, the material will not only absorb heat but also dissipate heat to the cold surrounding. In the prophase, the material absorbs more heat energy than it dissipates, so the temperature increases with increase in time. When heat absorption equals to heat dissipation a thermal equilibrium will be created in the material, so the temperature gradually tends to stabilise and levels off to a constant value [155]. So, these mechanisms in microwave curing (of our specimens) help in improving/increasing the mechanical properties.

It has also been observed that the FTIR peak at 830cm^{-1} , which corresponds to the vibration of an epoxy ring, is known to be the characteristics after microwave curing the intensity of that peak becomes very weak and hardly distinguishable [155]. This suggests that an epoxy group reforms/disintegrate etc. during microwave curing. In our case, similar observation is also noticed (Figure 4.19), for both oven and microwave cured specimens. From the IR spectra (Page 52-54) it reveals that the peaks at 1365cm^{-1} (Bis-methyl symmetric deformation vibration of Bisphenol-A) and development of new fingerprint at 610cm^{-1} , envisage that, microwave curing has caused a modest change in the cross-linking path and the network structures obtained in oven and microwave curing. Hence microwave cured samples have superior/better mechanical properties than that of the samples cured in an oven or atmospheric condition.

5.3 Effect of viscosity on composite fabrication

Several factors are responsible for the viscosity of polymeric melts. The most significant factors influencing the melt viscosity are temperature, pressure, molecular characteristics, the volume of added filler and structure of the polymeric string and addition of auxiliary processing additives. At high viscosity, the chain termination reaction and eventually the chain propagation reaction becomes diffusion controlled. But as the temperature increases,

the viscosity decreases. At higher temperature, the molecular movement of the polymer is easier due to a decrease of the solvent viscosity, decrease of the inter-chain liaisons but helps in polymer solubility [156]. Hence, the mixing time is found to be an important factor/condition to prepare the composite before casting into desire shaped moulds.

As the polymerization reaction starts, the rate of translational diffusion of the large polymer molecules is reduced by the polymer-polymer interactions. This helps in the formation of a uniform coating of polymer on reinforced particles which helps in increasing mechanical strength; due to the presence of a continuous matrix network and helps in increasing interface bond strength; also helps in making a composite material with a homogenous distribution of reinforced particles. But with an increase in the amount of reinforcement, such effect does not become feasible on each particle surfaces; resulting in a decrease in mechanical properties [157]. A similar trend is also observed in our studies (revealed from Figure 4.2 and Figure 4.3) that, with an increase in the amount of fly ash reinforcement the mechanical property of the composite deteriorate.

5.4 Effect of Tg on mechanical properties

Tg is a parameter considered for evaluating the flexibility of a polymer molecule and the type of response the polymeric material would exhibit to mechanical stress. Polymers above their Tg exhibit a delayed elastic response (viscoelasticity), while those below Tg will exhibit dimensional stability. General common sense prevails that higher the Tg better the mechanical properties [158]. Organic matrix resins such as epoxies soften as the temperature is increased. Above Tg, the resin exhibit a significant decrease in strength and stiffness due to increased chain mobility. There are several factors which influence the magnitude of the temperature region where Tg occurs, i.e. composition of the resin molecule, cross-linking density, the polar nature of the resin molecules, functional group, curing agent/catalyst, curing time and temperature/conditions etc. [37]. In our study, the improvement/variation of mechanical properties are affected due to variation of Tg in case of samples processed at different curing conditions (Figure 4.17 and Figure 4.44) and microwave cured samples offer better mechanical properties than that of the samples cured in oven and atmosphere condition.

It has been suggested by various researchers [145, 146] that, free segmental motion is restricted in chemically cross-linked polymers; because it is cured and cooled through its glass transition temperature. Both capillary effect through the matrix and wicking along the

interface consequently facilitate penetration of the solution through the polymer. Specimens are immersed in different chemicals viz. acid, base, fuel and sea water under the laboratory conditions to determine the sustainability of the composite for various applications. The basic solution found to have maximum impact on the strength of the material while fuel has a negligible impact on the strength. The mechanical and thermal properties deteriorate with increase in duration of treatment. The decrease in strength may be due to the penetration of liquid/solutions into the core of the material through micro cracks resulting swelling, pitting and surface degradation etc.

From the SEM observations, it is found that particle agglomeration takes place with increasing fly ash amount in the composite and shows a mixed mode of fracture; as crack initiations that take place at the agglomerated particles boundary (Figure 4.11) and at inter particle space/voids (Figure 4.12). The polymer composite is a combination of amorphous and crystalline structures. This amorphous portion also helps for the formation of dislocation and initiating a fracture in the material.

From the corrosion tests it is observed that there is weight gain of the samples, which is increasing with increase in fly ash content. This effect is more pronounced for the sample treated with NaOH solution. This is due to high silica content (in fly ash) which might be responsible for formation of different compounds on the sample surface (as revealed from Figure 4.31) and also hydrolysis reaction might be taking place; which is responsible for decrease in strength of the composite. In case of microwave cured specimens these reactions find obstruction due to improved interfacial bonding of polymer chain on particle surface.

5.5 Overview

By incorporating the ceramic particle/particulate filler (i.e. fly ash) into epoxy resin, better mechanical properties have been obtained. The change in chemical bonding structure leads to increase the glass transition temperature which is a good sign for industrial application than normal epoxy resin (for composite casting and forming operations). The increased value of dielectric constant show some hope of using this developed composite replacing the traditional material in electronics applications.

The developed particulate filled composite can also be suitable for use as flooring tiles etc. As the floor is subjected to sliding wear, this developed polymer composite has better sliding wear properties, i.e. with low rate of wear, low coefficient of friction. The influence of various parameters viz. load, percentage of fly ash reinforcement and sliding

distance has been studied. The influence of load is found to be detrimental for wear. Time of operation has the least impact on the wear rate.

By increasing the mixing time and changing the post curing processes, the mechanical properties are affected. The mechanical property increases with the mixing time and found to be maximum for the specimens prepared at 30minutes of mixing. It may be due to low viscosity of epoxy resin mix which helps in good incorporation of filler material. Curing in the oven and micro oven also increase the properties to a larger extent. It may be due to the change in internal structure and chemical bonding during the curing process. The change in bonding and chain structure is confirmed from differential scanning calorimetry and fourier transformation infrared spectroscopic analysis. Curing also helps in increasing the dielectric strength which opens a new path for the composite material to be utilised in electronics devices.

Summary and Conclusions

6.1 Summary

The evaluation of mechanical, thermal and electrical characterization of any newly developed composite material is highly essential to find out its suitable and productive application. In the current research, a set of original research data have been provided for the newly developed fly ash reinforced epoxy composite which can be used in future.

The findings of the current research are broadly classified into three main parts.

- i. The first part consists of the effect of varying parameters on the various properties of fly ash reinforced polymer composite. A novel idea and procedure for making a low-cost polymer composite are described. Mechanical characterization of the polymer composite i.e. tensile strength, flexural strength and impact strength are measured. Its glass transition temperature and its possible chemical bonding have been determined to know the phase transition and structural fingerprint of the composite. The electrical resistivity, dielectric constant and dielectric loss are measured to have an idea of electrical property.
- ii. The second part discussed the environmental conditioning of the polymer composite in different solution/ mediums viz. an acid solution, basic solution, sea water and fuel. The variation in weight, change in surface morphological structure and effect on mechanical properties for the duration of immersion in different mediums have been discussed. DSC and FTIR analysis have also made to find out the change in glass transition temperature due to immersion in different mediums and the possible changes in bond structure.
- iii. The third part discussed for the wear behaviour of the developed polymer composite. Wear parameters were varied and some experiments are restricted with the help of design of the experiment using statistical analysis methods. The wear characteristic, the impact of each parameter on wear is discussed elaborately. So, this chapter gives an idea of using the developed fly ash reinforced polymer composite for various applications.

6.2 Conclusions

The analytical and experimental investigation of the current research work led to the following conclusions.

- i. Successful fabrication of particulate filled epoxy composite is possible by normal casting method without the application of external pressure.
- ii. Mechanical properties are greatly influenced by mixing time of fly ash and epoxy resin.
- iii. Due to the process of post curing, there is an internal modification (structural/bonding) which leads to increase in mechanical strength and change in glass transition temperature.
- iv. Fly ash reinforced epoxy composite show good wear resistance capability as compared to virgin epoxy. Wear resistance decreases with increase in amount fly ash reinforcement.
- v. Out of three differently cured samples, oven treated samples show better sign of wear resistance.
- vi. Various parameters like load, percentage reinforcement of fly ash, duration of operation, speed and track diameter influence the amount of wear of the material. Out of these, the load is the most influencing parameter for an increase in wear rate.
- vii. Mechanical and thermal properties are highly influenced by environmental treatment/conditioning. These properties decrease with increase in durability time of exposure in the solution/medium.
- viii. Out of four mentioned conditions, basic solution affects the most and fuel affects the least to the properties of the material.
- ix. Fly ash reinforced epoxy composite can be commercially used as flooring tiles, especially in fuel industries even for fuel carrying containers.

6.3 Scope of future work

- i. Other wastes, fillers and catalysts can be used for improving the mechanical, electrical and wear properties.
- ii. Surface treatment of fly ash before reinforcement can be made to affect the interface bonding of polymer and ceramic.
- iii. Other post curing/treatment methods viz. γ - ray radiation etc. may be studied.

- iv. Other polymers can be used as matrix material for the making of fly ash reinforced composites.
- v. Fatigue behaviour of the composites needs to be evaluated.
- vi. Damping behaviour is to be studied.

References

1. Agarwal B. D and Broutman L. J, (1990). Analysis and performance of fibre composites, Second Edition, John Wiley & Sons, Inc, pp.2-16.
2. Jang B. Z, (1994). Advanced Polymer Composites: Principles and Applications, ASM International.
3. Kuljanin J, Vuckovic M, Comor M. I, Bibic N, Djokovic V and Nedeljkovic J. M, (2002). Influence of CdS-filler on the thermal properties of polystyrene, European Polymer Journal, 38(8), PP. 1659-1662.
4. Weidenfeller B, Höfer M and Schilling F, (2004). Thermal conductivity, thermal diffusivity and specific heat capacity of particle filled polypropylene, Composites Part A: Applied Science and Manufacturing, 35 (4), pp. 423-429
5. Stolarski T. A, (1990). Tribology in Machine Design, Heiman Newnes, UK.
6. Päivi Kivikytö-Reponen, (2006). Correlation of Material Characteristics and Wear of Powder Metallurgical Metal Matrix Composites, Doctoral Theses in Materials and Earth Sciences, Helsinki University of Technology, Laboratory of Materials Science, Espoo.
7. Budinski K. G, (1998). Surface Engineering for Wear Resistance, Prentice Hall, New Jersey.
8. Robinowicz E, (1965). Friction and wear of materials, John Willey, New York, USA.
9. Thomas H. Kosel, (1992). Solid Particle Erosion, ASM Handbook, ASM International, 18, 199-213.
10. T.H. Kosel. & P.J. Blau, Editor, Friction, Lubrication and Wear Technology, ASM Handbook, 18, pp. 207).
11. Takei T, Hatta H and Taya M (1991) Thermal expansion behavior of particulate-filled Composites II: Multi-reinforcing phases (hybrid composites). Materials Science and Engineering-A 131(1): 145–152.
12. Attar S, Nagaral M, Reddappa HN, et al. (2015) A Review on Particulate Reinforced Aluminum Metal Matrix Composites. 2(2): 225–229.
13. Sawyer WG, Freudenberg KD, Bhimaraj P, et al. (2003) A study on the friction and wear behaviour of PTFE filled with alumina nanoparticles. 254: 573–580.
14. Kim J, Kang PH and Nho YC (2004) Positive temperature coefficient behaviour of polymer composites having a high melting temperature. Journal of Applied Polymer Science 92(1): 394–401.

15. Njoku RE, Okon AE and Ikpaki TC (2011) Effects of Variation of Particle Size and Weight Fraction on the Tensile Strength and Modulus of Periwinkle Shell Reinforced Polyester Composite. *Nigerian Journal of Technology* 30(2).
16. Bartczak Z, Argon AS, Cohen RE, et al. (1999) Toughness mechanism in semi-crystalline polymer blends: II. High- density polyethylene toughened with calcium carbonate filler particles. *Polymer* 40(9): 2347–2365.
17. Singla M and Chawla V (2010) Mechanical Properties of Epoxy Resin – Fly Ash Composite. 9(3): 199–210.
18. Jin H, Miller GM, Pety SJ, et al. (2013) Fracture behaviour of a self-healing, toughened epoxy adhesive. *International Journal of Adhesion and Adhesives* 44: 157–165.
19. Fu SY, Feng XQ, Lauke B, et al. (2008) Effects of particle size, particle/matrix interface adhesion and particle loading on mechanical properties of particulate-polymer composites. *Composites Part B: Engineering* 39(6): 933–961.
20. Lee J and Yee AF (2000) Micro-mechanical deformation mechanisms in the fracture of hybrid-particulate composites based on glass beads, rubber and epoxies. *Polymer Engineering and Science* 40(12): 2457–2470.
21. Koh S, Kim J and Mai Y (2006) in *Silica-Filled Epoxy Resin Composites : Effects of Temperature and Loading Rate*. 34(16).
22. Imanaka M, Takeuchi Y, Nakamura Y, et al. (2001) Fracture toughness of spherical silica-filled epoxy adhesives. *International Journal of Adhesion and Adhesives* 21(5): 389–396.
23. Wang H, Bai Y, Liu S, et al. (2002) Combined effects of silica filler and its interface in epoxy resin. *Acta Materialia* 50(17): 4369–4377.
24. Alya A (2012) Friction and Wear of Polymer Composites Filled by Nano-Particles: A Review. *World Journal of Nano Science and Engineering* 02(01): 32–39.
25. Nakamura Y, Yamaguchi M, Kitayama A, et al. (1991) Effect of particle size on impact properties of epoxy resin filled with angular shaped silica particles. *Polymer* 32 (12): 2221–2229.
26. Wetzel B, Hauptert F, Friedrich K, et al. (2013) Mechanical and Tribological Properties of Micro particulate and Nano particulate Reinforced Polymer Composites. *Iccm*: 1–10.
27. Sudár A, Móczó J, Vörös G, et al. (2007) The mechanism and kinetics of void formation and growth in particulate filled PE composites. *Express Polymer Letters* 1(11): 763–772.

28. Patnaik A., Satapathy A., Mahapatra SS, et al. (2008) A Comparative Study on Different Ceramic Fillers Affecting Mechanical Properties of Glass--Polyester Composites. *Journal of Reinforced Plastics and Composites* 28(11): 1305–1318.
29. Nikkeshi S, Kudo M and Masuko T (1998) Dynamic viscoelastic properties and thermal properties of Ni powder-epoxy resin composites. *Journal of Applied Polymer Science* 69(13): 2593–2598.
30. Nielsen L E and Landel R F, (1994) *Mechanical properties of polymers and composites*, 2nd Edition, New York: Marcel Dekker, pp 557
31. Rihan Y and Bary B, (2012) Wear Resistance and Electrical Properties of Functionally Graded Epoxy-Resin / Silica Composites. 23–27.
32. Zhu K and Schmauder S (2003) Prediction of the failure properties of short fibre reinforced composites with metal and polymer matrix. 28: 743–748.
33. Rusu M, Sofian N and Rusu D (2001) Mechanical and thermal properties of zinc powder filled high density polyethylene composites. 20: 409–417.
34. Zhu K and Schmauder S (2003) Prediction of the failure properties of short fibre reinforced composites with metal and polymer matrix. 28: 743–748.
35. Kim J, Kang PH and Nho YC (2004) Positive temperature coefficient behaviour of polymer composites having a high melting temperature. *Journal of Applied Polymer Science* 92(1): 394–401.
36. Zhanwei Y, Fuguo L, Peng Z, et al. (2014) Mechanical properties study of particles reinforced aluminium matrix composites by micro-indentation experiments. *Chinese Journal of Aeronautics, Chinese Society of Aeronautics and Astronautics* 27(2): 397–406.
37. Mehan ML and Schadler LS (2000) Micromechanical behaviour of short- fibre polymer composites. 60(June 1999): 1013–1026.
38. Gungor A (2007) *Materials & Design* Mechanical properties of iron powder filled high density polyethylene composites. 28: 1027–1030.
39. Nikkeshi S, Kudo M and Masuko T (1998) Dynamic viscoelastic properties and thermal properties of Ni powder-epoxy resin composites. *Journal of Applied Polymer Science* 69(13): 2593–2598.
40. Amer MS and Schadler LS (1997) Stress Concentration Phenomenon in Graphite / Epoxy Composites : Tension / Compression Effects. 57: 1129–1137.
41. Mohammadi M, Dryden JR and Jiang L (2011) *International Journal of Solids and Structures* Stress concentration around a hole in a radially inhomogeneous plate. *International Journal of Solids and Structures*, Elsevier Ltd 48(3-4): 483–491.

42. Li M, Gu Y, Liu H, et al. (2013) Investigation the interphase formation process of carbon fibre / epoxy composites using a multi scale simulation method. *Composites Science and Technology*, Elsevier Ltd 86: 117–121.
43. Yang S, Yu S and Cho M (2012) Influence of Thrower – Stone – Wales defects on the interfacial properties of carbon nanotube / polypropylene composites by a molecular dynamics approach. *Carbon* 55: 133–143.
44. Olsson R (2011) A survey of test methods for multi-axial and out-of-plane strength of composite laminates. *Composites Science and Technology*, Elsevier Ltd 71(6): 773–783.
45. Mishra G, Mohapatra SR, Behera PR, et al. (2010) Environmental stability of GFRP laminated composites: an emphasis on mechanical behaviour. *Aircraft Engineering and Aerospace Technology* 82(4): 258–266.
46. Hinton MJ, Kaddour AS (2016) The background to the Second World-Wide Failure Exercise.
47. Zhou G and Silberschmidt V V (2016) Effect of through-thickness compression on in-plane tensile strength of glass / epoxy composites : Experimental study. *Polymer Testing*, Elsevier Ltd 49: 1–7.
48. Arash B, Park HS and Rabczuk T (2015) Tensile fracture behaviour of short carbon nanotube-reinforced polymer composites : A coarse-grained model. *COMPOSITE STRUCTURE*, Elsevier Ltd 134: 981–988.
49. Kaddour AS, Hinton MJ, Smith PA, et al. (2016) The background to the third worldwide failure exercise.
50. Dong C and Davies IJ (2014) Flexural and tensile strengths of unidirectional hybrid epoxy composites reinforced by S-2 glass and T700S carbon fibres. *Materials and Design*, Elsevier Ltd 54: 955–966.
51. Fu S and Lauke B (1996) effects of fibre length and fibre orientation. 56(2): 1179–1190.
52. Yue C and Hu X (2000) Tensile properties of short-glass-fibre- and short-carbon-fibre-reinforced polypropylene composites. 31: 1117–1125.
53. Koh S, Kim J and Mai Y (2006) in *Silica-Filled Epoxy Resin Composites : Effects of Temperature and Loading Rate*. 34(16).
54. Garcia-gonzalez D, Rodriguez-millan M, Rusinek A, et al. (2015) Investigation of mechanical impact behavior of short carbon-fibre-reinforced PEEK composites. *Composite structure*, Elsevier Ltd 133: 1116–1126.

55. Yu B, Geng C, Zhou M, et al. (2016) Impact toughness of polypropylene / glass fibre composites : Interplay between intrinsic toughening and extrinsic toughening. *Composites Part B, Elsevier Ltd* 92: 413–419.
56. Kotoul M and Vrbka J (2003) Crack bridging and trapping mechanisms used to toughen brittle matrix composite. 40: 23–44.
57. Ma H, Jia Z, Lau K, et al. (2016) Impact properties of glass fibre / epoxy composites at cryogenic environment. *Composites Part B, Elsevier Ltd* 92: 210–217.
58. Fan Y, Huang X, Wang G, et al. (2015) Core-Shell Structured Biopolymer@BaTiO₃ Nanoparticles for Biopolymer Nano composites with Significantly Enhanced Dielectric Properties and Energy Storage Capability. *Journal of Physical Chemistry C* 119(49): 27330–27339.
59. Liu S, Xiao S, Xiu S, et al. (2015) Poly(vinylidene fluoride) Nano composite capacitors with a significantly enhanced dielectric constant and energy density by filling with surface-fluorinated Ba_{0.6} Sr_{0.4} TiO₃ Nanofibers. *RSC Adv.* 5(51): 40692–40699.
60. Song Y, Shen Y, Liu H, et al. (2012) Improving the dielectric constants and breakdown strength of polymer composites: effects of the shape of the BaTiO₃ Nano inclusions, surface modification and polymer matrix. *Journal of Materials Chemistry* 22(32): 16491.
61. Stoyanov H, Brochu P, Niu X, et al. (2013) carbon nanotube compliant electrodes.: 2272–2278.
62. Zhang SL and Ito K (2015) Showcasing the study of dielectric elastomer actuator based as featured in: electromechanical performance using slide-ring. *Journal of Materials Chemistry A: Materials for energy and sustainability, Royal Society of Chemistry* 3: 9468–9479.
63. Chem JM, Romasanta LJ, Leret P, et al. (2012) Towards materials with enhanced electro-mechanical response: 24705–24712.
64. Betts T, Kennedy D and Jerrams S (2015) Improving the Electromechanical Performance of Dielectric Elastomers using Silicone Rubber and Dopamine Coated Barium Titanate .: 0–18.
65. Feng Y, Li WL Hou F et al. (2015) Enhanced dielectric properties of PVDF-HFP/BaTiO₃-nanowire composites induced by interfacial polarization and wire-shape BaTiO₃ -nanowire composites induced by.: 1250–1260.
66. Chang J, Shen Y and Chu X et al. (2015) Large d₃₃ and enhanced ferroelectric/dielectric properties of poly (vinylidene fluoride)-based composites filled with Pb(Zr_{0.52}Ti_{0.48})O₃ Nanofibers. *RSC Advances*: 51302–51307.

67. Dang Z, Yuan J, Zha J, et al. (2012) Progress in Materials Science Fundamentals , processes and applications of high-permittivity polymer – matrix composites. Progress in Materials Science, Elsevier Ltd 57(4): 660–723.
68. Zhang L, Yuan S, Chen S, et al. (2015) Preparation and dielectric properties of core – shell structured Ag @ poly dopamine / poly (vinylidene fluoride) composites. Composites science and technology, Elsevier Ltd 110: 126–131.
69. Zhang Zhenchong, Gu Y, Bi J, et al. (2015) SiC and SiO₂ core shell filler reinforced polymer composites with high dielectric permittivity and low loss. Materials Letters, Elsevier 160: 16–19.
70. Bi J, Gu Y, Zhang Zhenchong, et al. (2016) Core shell SiC / SiO₂ whisker reinforced polymer composite with high dielectric permittivity and low dielectric loss. JMADE, Elsevier Ltd 89: 933–940.
71. Zhou W, Zuo J and Ren W (2012) Composites : Part-A Thermal conductivity and dielectric properties of Al / PVDF composites. Composites Part-A, Elsevier Ltd 43(4): 658–664.
72. Yuan J, Yao S, Dang Z, et al. (2011) Giant Dielectric Permittivity Nano composites : Realizing True Potential of Pristine Carbon Nanotubes in Poly vinylidene Fluoride Matrix through an Enhanced Interfacial Interaction.: 5515–5521.
73. Shoude W, Lingchao L and Xin C (2011) Effect of ultra-fine fly ash on the dielectric behaviour of CFSC under stress. 2(1): 12–16.
74. Hanjitsuwan S, Chindaprasirt P and Pimraksa K (2011) Electrical conductivity and dielectric property of fly ash geo polymer pastes. 18(1): 94–99.
75. Jumrat S, Chatveera B and Rattanadecho P (2011) Dielectric properties and temperature profile of fly ash-based geo polymer mortar. International Communications in Heat and Mass Transfer, Elsevier Ltd 38(2): 242–248.
76. Lebedev SM and Ge OS (2015) Evaluation of electric, morphological and thermal properties of thermally conductive polymer composites. 91: 875–882.
77. Chand N and Khare N (1999) Effect of fly ash addition on dielectric properties of polypropylene. 6(December): 342–345.
78. Jin X, Xu X, Zhang X, et al. (2014) Determination of the PCM melting temperature range using DSC. Thermochimica Acta, Elsevier B.V. 595: 17–21.
79. Zvetkov VL and Djoumaliisky S (2014) Microwave curing of initially compatible epoxy – poly (ethylene terephthalate) blends : DSC kinetic study and Nanostructure analysis. Thermochimica Acta, Elsevier B.V. 595: 43–50.

80. Rathgeber C, Miró L, Cabeza LF, et al. (2014) Measurement of enthalpy curves of phase change materials via DSC and T-History : When are both methods needed to estimate the behaviour of the bulk material in applications Sensors & Actuators: B. Chemical, Elsevier B.V. 596: 79–88.
81. Toda A and Konishi M (2014) An evaluation of thermal lags of fast-scan microchip DSC with polymer film samples. *Thermochimica Acta*, Elsevier B.V. 589: 262–269.
82. De JL, Ruiz-bermejo M, Menor-salván C, et al. (2011) Thermal characterization of HCN polymers by TG e-MS, TG, DTA and DSC methods. *Polymer Degradation and Stability*, Elsevier Ltd 96(5): 943–948.
83. Rusu M, Sofian N and Rusu D (2001) Mechanical and thermal properties of zinc powder filled high density polyethylene composites. 20: 409–417.
84. Tavman IH (1996) POWDER Thermal and mechanical properties of copper powder filled poly (ethylene) composites. 91: 63–67.
85. Luyt AS, Molefi JA and Krump H (2006) Thermal, mechanical and electrical properties of copper powder filled low-density and linear low-density polyethylene composites. 91.
86. Toda A, Taguchi K, Nozaki K, et al. (2014) Melting behaviours of polyethylene crystals : An application of fast-scan DSC. *Polymer*, Elsevier Ltd 55(14): 3186–3194.
87. *Enthalpy* (2001): 17–31.
88. Nearingburg B and Elias AL (2011) Characterization of surface plasma energy transduction in gold nanoparticle / polymer composites by photo-DSC. *Thermochimica Acta*, Elsevier B.V. 512(1-2): 247–253.
89. Blaine RL, Determination of Polymer Crystallinity by DSC: 1–3.
90. Malhotra VM, Valimbe PS and Wright MA (2002) Effects of fly ash and bottom ash on the frictional behaviour of composites. 81: 235–244.
91. Chauhan SR and Thakur S (2013) Effects of particle size, particle loading and sliding distance on the friction and wear properties of cenospheres particulate filled vinyl ester composites. *Materials and Design*, Elsevier Ltd 51: 398–408.
92. Srivastava VK and Pawar AG (2006) SCIENCE AND Solid particle erosion of glass fibre reinforced fly ash filled epoxy resin composites. 66: 3021–3028.
93. Jinfeng L, Shoufu T and Guoqin C (2009) Effect of Graphite Particle Reinforcement on Dry Sliding Wear of SiC / Gr / Al Composites. *Rare Metal Materials and Engineering*, Northwest Institute for Nonferrous Metal Research (China) 38(11): 1894–1898.
94. Srinivas K and Bhagyashekar MS (2014) Wear Behaviour of Epoxy Hybrid Particulate Composites. *Procedia Engineering*, Elsevier B.V. 97: 488–494.

95. Chandra CR, Ravikumar TR, Mohan N, et al. Mechanical and Three-body abrasive wear behaviour of Nano-Fly ash / ZrO₂ filled Polyimide Composites. 01(04): 196–202.
96. Esteves M, Ramalho A, Ferreira JAM, et al. (2013) Tribological and Mechanical Behaviour of Epoxy / Nano Clay Composites. 1–10.
97. Mohanty and Chugh YP (2007) Development of fly ash-based automotive brake lining. 40: 1217–1224.
98. Kurahatti R V, Surendranathan AO, Kumar AVR, et al. (2014) Dry Sliding Wear behaviour of Epoxy reinforced with Nano ZrO₂ Particles. Procedia Materials Science, Elsevier B.V. 5: 274–280.
99. Yilmaz MG, Unal H and Mimaroglu A (2008) Study of the strength and erosive behaviour of CaCO₃ / glass fibre reinforced polyester composite. 2(12): 890–895.
100. Supreeth S, Vinod B and Sudev LJ (2014) Influence of Fibre Length on the Tribological Behaviour of Short PALF Reinforced Bisphenol-A Composite. 2(4): 825–830.
101. Raju BR, Suresha B and Swamy RP (2013) Investigations on Mechanical and Tribological Behaviour of Particulate Filled Glass Fabric Reinforced Epoxy Composites. 2013(July): 160–167.
102. Chauhan SR, Kumar A, Singh I, et al. (2010) Effect of Fly Ash Content on Friction and Dry Sliding Wear Behaviour of Glass Fibre Reinforced Polymer Composites - A Taguchi Approach. 9(4): 365–387.
103. P HKTRSR and Chandrashekar TK (2011) Taguchi Technique for the Simultaneous Optimization of Tribological Parameters in Metal Matrix Composite. 10(12): 1179–1188.
104. Kumar GBV, Rao CSP and Selvaraj N (2011) Mechanical and Tribological Behaviour of Particulate Reinforced Aluminium Metal Matrix Composites – a review. 10(1): 59–91.
105. Majhi S, Samantarai SP, Acharya SK, et al. (2012) Tribological Behaviour of Modified Rice Husk Filled Epoxy Composite. 3(6): 1–5.
106. Berhanu T, Kumar P and Singh I (2014) Sliding Wear Properties of Jute Fabric Reinforced Polypropylene Composites. Procedia Engineering, Elsevier B.V. 97: 402–411.
107. Vasconcelos P V, Lino FJ, Baptista M, et al. (2005) Tribological behaviour of epoxy based composites for rapid tooling.
108. Hanumantharaya R, M AKK, G PKB, et al. (2014) Friction and Dry Sliding Wear Behaviour of Granite - Fly Ash Filled Glass Epoxy Composites. 3(7): 14331–14338.
109. Mohan N, Mahesha CR and Rajaprakash BM (2013) Erosive wear behaviour of WC filled glass epoxy composites. Procedia Engineering, Elsevier B.V. 68: 694–702.

110. Fujun Z, Hengjing BA and Xiaojian GAO The Durability of Epoxy Resin Coating. *Journal of Wuhan University of Technology-Mater.* 23(2): 242–244.
111. Hammami A (2004) Durability and Environmental Degradation of Glass-Vinyl Ester Composites. *Polymer composites.* 25(6): 609–616.
112. Kishore, Barpanda P and Kulkarni SM (2005) Compression Strength of Saline Water-exposed Epoxy System Containing Fly Ash Particles. *Journal of Reinforced Plastic & Composites.* 24(15): 1567–1576.
113. Ribeiro MCS, Tavares CML and Ferreira, Chemical resistance of epoxy and polyester polymer concrete to acids and salts.
114. Bledzki A, Spaude R and Ehrenstein GW (1985) Corrosion Phenomena in Glass Fibres and Glass Fibre Reinforced Thermosetting Resins. *Composite Science and Technology.* 23: 263–285.
115. Rakin M, Medjo B and Stamenovic M (2011) Effect of alkaline and acidic solutions on the tensile properties of glass – polyester pipes. *Materials and Design.* 32: 2456–2461.
116. Amaro AM, Reis PNB, Neto MA, et al. (2013) Effects of Alkaline and Acid Solutions on Glass/Epoxy Composites. *Polymer Degradation and Stability, Elsevier Ltd.*
117. Banna MH, Shirokoff J and Molgaard J (2011) Effects of two aqueous acidic solutions on polyester and Bisphenol-A epoxy vinyl ester resins. *Materials Science & Engineering A, Elsevier B.V.* 528(4-5): 2137–2142.
118. Norwood LS and Hogg PJ (1984) G R P in Contact with Acidic Environment a Case Study. *Composite Structure.* 2: 1–22.
119. Pai R, Kamath MS and Rao R (1997) Acid resistance of glass fibre composites with different layup sequencing: Part I-Diffusion studies. *Journal of Reinforced Plastic and Composites.* 16: 1002-11.
120. Sindhu K, Joseph K, Joseph JM, et al. (2016) Degradation Studies of Coir Fibre / Polyester and glass fibre/polyester composites under different conditions. 26:1571-1585.
121. Tang SW, Yao Y andrade C, et al. (2015) Cement and Concrete Research Recent durability studies on concrete structure. 78: 143–154.
122. Gkikas G, Douka D, Barkoula N, et al. (2015) Nano-enhanced composite materials under thermal shock and environmental degradation : A durability study. *Composites Part B, Elsevier Ltd* 70: 206–214.
123. Jones FR, Rock JW and Wheatley AR (1983) Stress corrosion cracking and its implications for the long-term durability of E-glass fibre composites. 14(3): 262–269.

124. Griffith R and Ball A (2000) An assessment of the properties and degradation behaviour of glass-fibre reinforced polyester polymer concrete. 60: 2747–2753.
125. Kawada H and Srivastava VK (2001) The effect of an acidic stress environment on the stress-intensity factor for GRP laminates. 61: 1109–1114.
126. Saccani A and Magnaghi V (1999) Durability of epoxy resin-based materials for the repair of damaged cementitious composites. 29: 95–98.
127. Maslehuddin M and Ibrahim M (2003) Mechanical properties and durability characteristics of polymer- and cement-based repair materials. 25: 527–537.
128. Barbero Ever J, (1999), Introduction to Composite Materials Design, Taylor & Francis, Philadelphia, PA.
129. Barbero Ever J, (1999), Introduction to Composite Materials Design, Taylor & Francis, Philadelphia, PA
130. Satapathy, A. Patnaik, M.K. Pradhan, (2009) A study on processing, characterization and erosion behaviour of fish (Labeo-rohita) scale filled epoxy matrix composites, Mater. Des. 30, 2359–2371,
131. S.A. Alidokht, A. Abdollah-Zadeh, H. Assadi, (2013) Effect of applied load on the dry sliding wear behaviour and the subsurface deformation on hybrid metal matrix composite, Wear 305, 291–298.
132. J.K. Lancaster, (1972) Polymer base bearing materials: the role of fillers and fibre reinforcement, Tribology, 249–255 Ministry of Defence.
133. R. Kumar, S. Dhiman, (2013) A study of sliding wear behaviours of Al-7075 alloy and Al-7075 hybrid composite by response surface methodology analysis, Mater. Des. 50 351–359,
134. Sivapragash, M. et al., (2016) Taguchi based genetic approach for optimising the PVD process parameter for coating ZrN on AZ91D magnesium alloy. Materials & Design, 90, pp.713–722.
135. S.S. Mahapatra, A. Patnaik, A. Satapathy, (2008) Taguchi method applied to parametric appraisal of erosion behaviour of GF-reinforced polyester composites, Wear 265, 214–222.
136. Ross, P.J., (1996) "Taguchi Techniques for Quality Engineering: Loss Function, Orthogonal Experiments, Parameter and Tolerance Design - 2nd ed.", New York, NY: McGraw-Hill. Montgomery, Design and Analysis of Experiments. Singapore: Wiley.
137. Phadke M.S. (1989) —Quality Engineering Using Robust Design, Prentice Hall, Englewood Cliffs, New Jersey.

138. Taguchi, G. (1987) —System of Experimental Design|| Unipub/Kraus, International Publication
139. Taguchi, G. (1993) —Taguchi on Robust Technology Development - Bringing Quality Engineering Upstream||, ASME Press, New York.
140. Ealey Lance A. (1994) —Quality by design Taguchi methods and US industry.|| 2nd ed. Sidney: Irwin Professional publishing And ASI Press; pp. 189–207
141. Roy, R.K., (1990) A Primer on the Taguchi Method, (Van Nostrand Reinhold: New York).
142. J.P. Dumas, S. Gibout, L. Zalewski, K. Johannes, E. Franquet, S. Lassue, J.P Bédécarrats, P. Tittlein, F.C. Kuznik, (2014) Interpretation of calorimetric experiments to characterize phase change materials, Int. J. Therm. Sci. 78, 48–55.
143. Xing Jin a,b,Huoyan Hu cXingShi ,Xiaosong Zhang c, (2015) Energy asymmetry in melting and solidifying processes of PCM, Energy Conversion and Management 106, 608–614
144. Blythe T and Bloor D, (2005) Electrical Properties of Polymers, 2nd Ed. and Cambridge University Press.
145. Patel D, Banarjee S (A comparative study of effects on characteristic properties of FRP composites when exposed to distilled water , NaCl- water solution and sea water separately a comparative study of effects on characteristic properties of FRP composites when exposed to distilled water , NaCl- water.
146. Kulkarni SM, Kishore. (2003) Effect of Filler-Fibre Interactions on Compressive Strength of Fly-ash & Short Fibre Epoxy Composites. J. Appl. Polymer. Sci.; 87: 836–841p.
147. Gao, X. et al., (2015). Effect of thermomechanical treatment on sliding wear of high-Cr cast iron with large plastic deformation. Tribology International, 92, pp.117–125.
148. Mukhopadhyay, A. et al., (2015) Tribological Performance Optimisation of Electro less Ni–B Coating under Lubricated Condition using Hybrid Grey Fuzzy Logic. Journal of the Institution of Engineers (India): Series D.
149. Biswas, S. & Satapathy, A., (2009) Tribo-performance analysis of red mud filled glass-epoxy composites using Taguchi experimental design. Materials and Design, 30(8), pp.2841–2853.
150. Montgomery, (1991) Design and Analysis of Experiments. Singapore: Wiley.
151. Zhang K, Park BJ, Fang FF, et al. (2009) Sono-chemical preparation of polymer Nano composites. *Molecules* 14(6): 2095–2110.

152. Pattanaik A, Mohanty MK and Sathpathy MP (2015) Effect of Mixing Time on Mechanical Properties of epoxy-fly ash composite. *Journal of Materials & Metallurgical Engineering* 5(2): 11–17.
153. Ray BC (2004) Thermal shock on interfacial adhesion of thermally conditioned glass fibre/epoxy composites. *Materials Letters* 58(16): 2175–2177.
154. Hardis R, Jessop JLP, Peters FE, et al. (2013) Cure kinetics characterization and monitoring of an epoxy resin using DSC, Raman spectroscopy, and DEA. *Composites Part A: Applied Science and Manufacturing*, Elsevier Ltd 49: 100–108.
155. Komorowska-Durka M, Dimitrakis G, Bogdał D, et al. (2015) A concise review on microwave-assisted poly condensation reactions and curing of poly condensation polymers with focus on the effect of process conditions. *Chemical Engineering Journal*, Elsevier B.V. 264: 633–644.
156. Al-Shammari B, Al-Fariss T, Al-Sewailm F, et al. (2011) The effect of polymer concentration and temperature on the rheological behaviour of metallocene linear low density polyethylene (mLLDPE) solutions. *Journal of King Saud University - Engineering Sciences*, King Saud University 23(1): 9–14.
157. Haller PD, Bradley LC and Gupta M (2013) Effect of surface tension, viscosity, and process conditions on polymer morphology deposited at the liquid-vapor interface. *Langmuir* 29(37): 11640–11645.
158. Li N, Li Y, Jelonnek J, et al. (2017) A new process control method for microwave curing of carbon fibre reinforced composites in aerospace applications. *Composites Part B: Engineering*, Elsevier Ltd 122: 61–70.
159. Hassan A, Yahya R, Rafiq MIM, et al. (2011) Interfacial shear strength and tensile properties of injection-moulded, short- and long-glass fibre-reinforced polyamide 6,6 composites. *Journal of Reinforced Plastics and Composites* 30(14): 1233–1242.
160. Liu H and Webster TJ (2010) Mechanical properties of dispersed ceramic nanoparticles in polymer composites for orthopaedic applications. *International Journal of Nano medicine* 5(1): 299–313.
161. Mital K, Murthy LN and Goldberg K (August 1996). Micromechanics Reinforced for Particulate Composites.
162. Ye J, Chu C, Zhai Z, et al. (2017) The Interphase Influences on the Particle-Reinforced Composites with Periodic Particle Configuration. *Applied Sciences* 7(1): 102.

Annexure-I

Load Transfer Mechanism in Fibre-Reinforced Polymer Matrix Composite

There are two reasons why fibre length and the fibre /matrix interface have such a strong effect on the properties; (a) the fibre length and the interface control how effective the fibre is in carrying load (b) the number of fibre ends and the interface effect the fibre/fibre interaction and the average strain enhancement the fibres will experience as a consequence of the strain concentration from fibre ends [159].

According to shear lag approach, the tensile stress in the fibre is build up from zero at the fibre ends to a maximum value in the middle portion of the fibre. The distance along the fibre to go from zero load to the applied load is called stress transfer length. The strength of the interface will determine the stress-transfer length. Stronger, tougher interfaces will lead to a shorter stress transfer length and will lead to a shorter stress transfer length and thus more of the fibre will carry the applied load leading to higher modulus and strength at a given volume fraction. A weaker or more brittle interface will have a longer stress transfer length and less of the fibre will carry the applied load leading to lower modulus and strength [160].

Load Transfer Mechanism in Particle-Reinforced Polymer Matrix Composite

Many factors contribute to the mechanical properties of Nano ceramic/polymer composites, including size and shape of ceramic nanoparticles, ceramic/polymer phase composition and dispersion of nanoparticles, physical or chemical interactions between the ceramic and polymer phase and inherent properties of the polymer matrix. It is intriguing to speculate why well-dispersed Nano ceramics in polymer composites improved the mechanical properties of the composites and how the fracture behavior of Nano composites could be modified through controlling the dispersion. The interfacial PLGA (PLGA, poly-lactic-co-glycolic acid)-ceramic structure played a critical role in determining the mechanical properties of the composites. For example, it was reported that a better bonding between the polymer matrix and the reinforcing phase resulted in a higher elastic modulus and a higher strength. Since the predominant feature of the nanoparticles lies in their ultra-fine dimension, a large fraction of filler atoms can reside at the PLGA-ceramic interface which can lead to a stronger interfacial interaction, but only if the nanoparticles are well-dispersed at the Nano scale in the surrounding polymer matrix. Nano composites with a greater number of smaller interfaces could be expected to provide unusual properties and the shortcomings induced by the

heterogeneity of conventional (or micron) particle filled composites would also be decreased or even eliminated [161].

Scientifically, it is a great challenge to transfer the desirable mechanical properties (such as Young's modulus (E), compressive strength and hardness) of Nano scale ceramics into macro scale ceramic/polymer Nano composites, although single-phase Nano ceramics possess exceptional compressive strength, stiffness and hardness. Mechanical properties of nanoparticle-filled polymer composites have been significantly improved compared with conventional larger particle-filled polymer composites, but they are still far below the predicted theoretical values which were determined based on the assumption that Nano scale building blocks were individually dispersed in the matrix, except in the case of very low volume fractions of the reinforcing phase. Non-ideal mechanical properties of ceramic/polymer Nano composites are largely related to the difficulties in dispersing large volume fractions of the reinforcing Nano ceramics in polymer composites. As mentioned, nanoparticles have a strong tendency to agglomerate in the composites, especially when they take up more than 2 wt. % of the composites. In addition, it is important to control an effective load transfer from the polymeric matrix to the Nano scale ceramic components (that is, particle/matrix bonding) and understand the respective mechanical properties of the particles and matrix as well as the interactions of the two constituents at the Nano scale [162].

Annexure-II

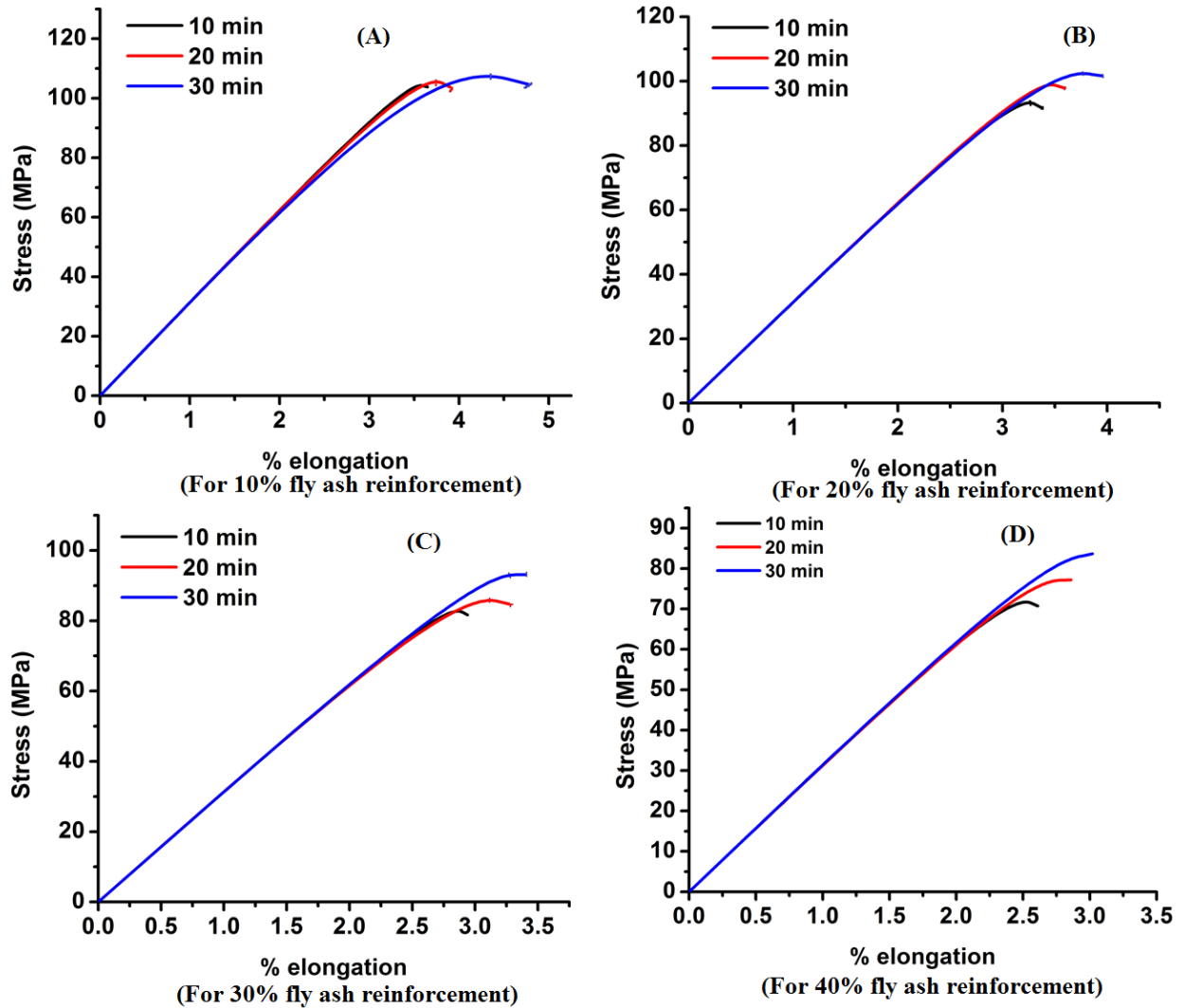


Figure: A typical set of (mixing time dependent) stress-strain curve for [(A) 10% (B) 20% (C) 30% (D) 40%] fly ash reinforcement in case of microwave treated samples.

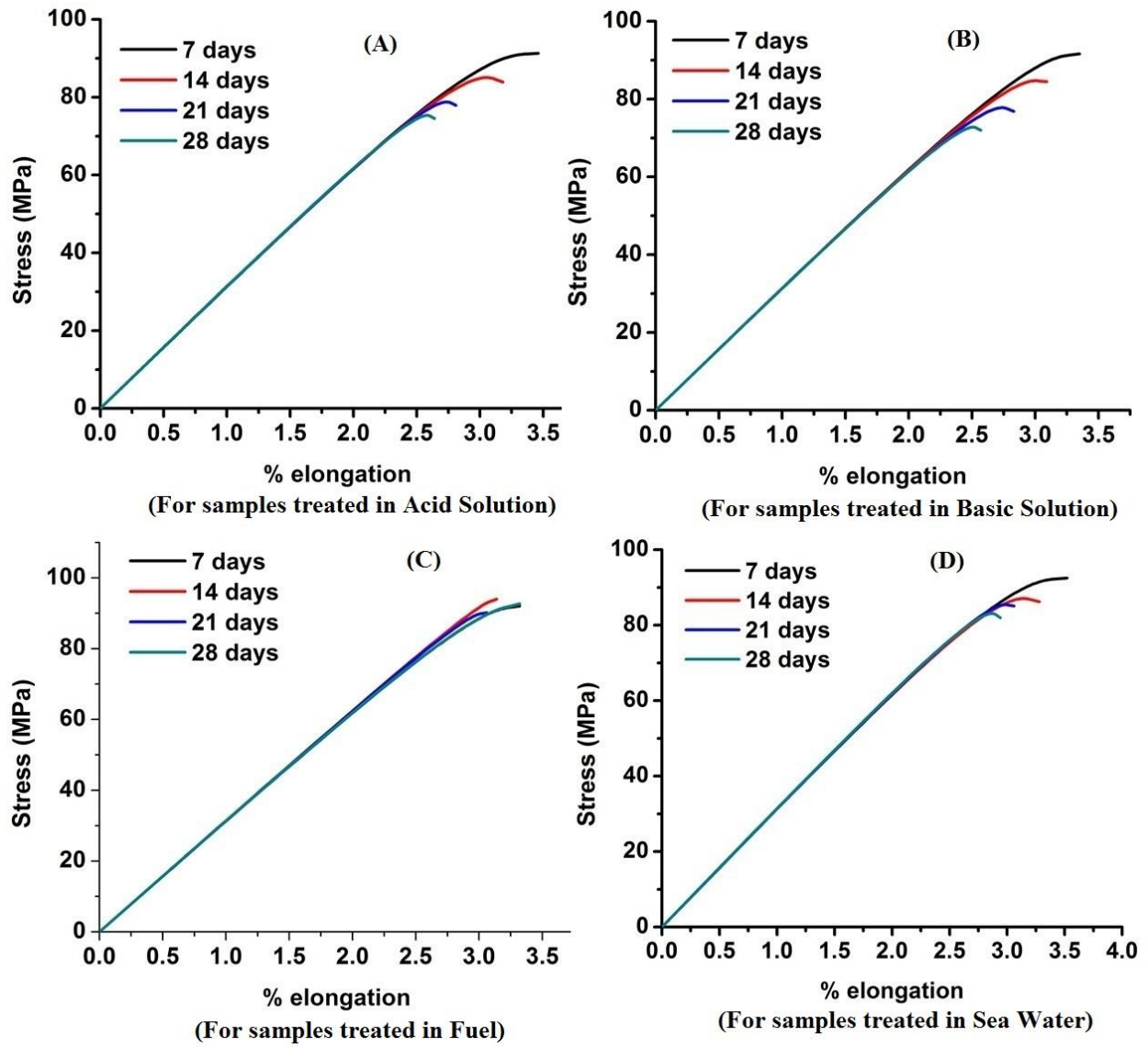


Figure: A typical set of curing time dependent stress-strain curve for samples treated in (A) Acid Solution (B) Basic Solution (C) Fuel (D) Sea Water for 10% fly ash reinforcement samples.

Table: The maximum tensile strength obtained for the samples prepared and treated in various conditions.

| Serial Number | Weight Percentage of Fly ash Reinforcement | Mixing Time (in Minutes) | Treatment Condition | Maximum Tensile Stress (MPa) |
|---------------|--|--------------------------|---------------------|------------------------------|
| 1 | 10 | 10 | NORMAL | 85.76 |
| 2 | 10 | 10 | OVEN | 95.48 |
| 3 | 10 | 10 | MICRO | 106.05 |
| | | | | |
| 4 | 10 | 20 | NORMAL | 88.24 |
| 5 | 10 | 20 | OVEN | 99.34 |
| 6 | 10 | 20 | MICRO | 109.98 |
| | | | | |
| 7 | 10 | 30 | NORMAL | 90.07 |
| 8 | 10 | 30 | OVEN | 101.32 |
| 9 | 10 | 30 | MICRO | 113.57 |
| | | | | |
| 10 | 20 | 10 | NORMAL | 79.37 |
| 11 | 20 | 10 | OVEN | 90.35 |
| 12 | 20 | 10 | MICRO | 96.92 |
| | | | | |
| 13 | 20 | 20 | NORMAL | 81.17 |
| 14 | 20 | 20 | OVEN | 90.93 |
| 15 | 20 | 20 | MICRO | 101.47 |
| | | | | |
| 16 | 20 | 30 | NORMAL | 82.57 |
| 17 | 20 | 30 | OVEN | 94.21 |
| 18 | 20 | 30 | MICRO | 104.58 |
| | | | | |
| 19 | 30 | 10 | NORMAL | 67.23 |
| 20 | 30 | 10 | OVEN | 78.2 |
| 21 | 30 | 10 | MICRO | 85.72 |
| | | | | |
| 22 | 30 | 20 | NORMAL | 70.71 |
| 23 | 30 | 20 | OVEN | 79.23 |
| 24 | 30 | 20 | MICRO | 88.67 |
| | | | | |
| 25 | 30 | 30 | NORMAL | 73.27 |

| | | | | |
|----|----|----|--------|-------|
| 26 | 30 | 30 | OVEN | 83.32 |
| 27 | 30 | 30 | MICRO | 92.88 |
| | | | | |
| 28 | 40 | 10 | NORMAL | 54.51 |
| 29 | 40 | 10 | OVEN | 63.07 |
| 30 | 40 | 10 | MICRO | 74.32 |
| | | | | |
| 31 | 40 | 20 | NORMAL | 58.67 |
| 32 | 40 | 20 | OVEN | 68.28 |
| 33 | 40 | 20 | MICRO | 76.84 |
| | | | | |
| 34 | 40 | 30 | NORMAL | 61.77 |
| 35 | 40 | 30 | OVEN | 72.01 |
| 36 | 40 | 30 | MICRO | 80.53 |

Dissemination

Internationally indexed journals

- **A Pattanaik, S C Mishra, “Microstructural Analysis of Fly Ash & Clay Compacts”,** Journal of Materials & Metallurgical Engineering, STM Journal, JOMME (2013) pp 1-10
ISSN: 2231 - 3818
- **A Pattanaik, M K Mohanty, M P Satpathy & S C Mishra, “Effect of mixing time on Mechanical Properties of Fly ash Epoxy Composite”,** Journal of Materials & Metallurgical Engineering, STM Journal (2015), Vol 5 and Issue 2, ISSN: 22313818(online), ISSN: 2321-4236(print)
- **S Kumar, A Pattanaik & S C Mishra, “Characterization of Fly ash & Cold setting Resin Powder Compacts”,** Journal of Thin Films, Coating Science Technology and Application, STM Journal (2015), Vol 2, Issue 2, pp 17-24
- **A Pattanaik, M P Satpathy & S C Mishra, “Dry sliding wear behaviour of Fly ash epoxy composite”,** Engineering Science and Technology, an International Journal, Elsevier 19 (2016) 710-716

Other Journals

- **A Pattanaik, S C Mishra, “Study of Fly ash & Clay Compacts”,** Odisha Journal of Physics Aug (2013), Vol 20, No-2, pp 225-230, ISSN: 0974-8202

Conferences

- **M Salim, A Pattanik, R Behera, S C Mishra, “Adhesive wear Behaviour of Heat Treated Spheroidal Graphite Cast Iron”,** 4th National Conference on Processing & Characterization of Materials, IOP conference Series, Material Science & Engineering 75 (2015) 01/2003
- **V K Jha, A Pattanaik, R Behera, S C Mishra, “Dry sliding wear system response of ferritic and tempered martensitic ductile Iron”,** 4th National Conference on Processing & Characterization of Materials, IOP conference Series, Material Science & Engineering 75 (2015) 012009
- **A Pattanaik & S C Mishra, “Dielectric properties of Fly ash Epoxy composite”,** 5th National Conference on Processing & Characterization of Materials, IOP conference Series, Material Science & Engineering 115 (2016) 012003

- R. Saxena, A. Patra, S. K. Karak, **A. Pattanaik** & S. C. Mishra, **“Fabrication and Characterization of novel $W_{80}Ni_{10}Nb_{10}$ alloy produced by mechanical alloying”**, 5th National Conference on Processing & Characterization of Materials, IOP conference Series, Material Science & Engineering 115 (2016) 012003
- **A Pattanaik**, S K Bhyan, S C Mishra, S. S. Patro & Ajit Behera, **“Dry Sliding Wear Behaviour of Micro oven Treated Fly Ash Reinforced Epoxy Composite using Extended Taguchi Approach Optimization”**, 6th National Conference on Processing & Characterization of Materials, IOP conference Series, Material Science & Engineering 178 (2017) 012004

Article under preparation

- **A Pattanaik**, S C Mishra, **Dry Sliding Wear Behaviour of Oven Treated Fly Ash Reinforced Epoxy Composite**, Tribology International (Communicated).
- **A Pattanaik**, S C Mishra, **“Environmental Conditioning of fly ash epoxy composite”** (Communicated)
- **A Pattanaik**, S C Mishra, **“Effect of Curing Condition on Mechanical & Thermal Properties of Fly Ash Reinforced Epoxy Composite”** (Communicated).